**Department of Chemical Engineering**

# Optimal Process Design and Sensitivity Analysis of Shell and Tube Heat Exchanger Operated with Nanofluids

**Emmanuel Yahaya**

**This thesis is presented for the Degree of**
**Master of Philosophy (Chemical Engineering)**
**of**
**Curtin University**

**August 2017**

Declaration

To the very best of my knowledge and trust, this thesis contains no materials previously published by any other person or research group except due acknowledgement has been made.

This Thesis contains no material which has been accepted for the award of any other degree or diploma in any university.

Signature : 

Date : 17/08/2017

cut, type of pitch, head type and ratio of baffle spacing to shell for optimizations (multivariable heat exchanger design) for both cases. Optimal design studies involving more deciding variables resulted in further cost reductions to 38% and 55%, respectively, as compared to the original design.

Hence, the studies involving nanofluid in the shell-and-tube heat exchanger design showed that the reduction of annual operating cost and total capital cost could be further achieved. The total annual capital cost was reduced to 40.97% and 55.77%, respectively, as compared to the original design for both case studies. These highlight the effect of nanofluid as a heat transfer fluid. The last stage of this study was to perform sensitivity analyses of heat exchanger operated with $Al_2O_3$ / water based nanofluid. These analyses were carried out by varying the two main operating conditions (mass flow rate and nanofluid concentration) and investigating the effects of those changes on the heat transfer rate, pressure drop and cost. These operating condition changes were set to be $\pm$5% and 10% from the optimal conditions obtained from the optimal design studies. From the conducted sensitivity analysis, the outcome showed that an increase in nanofluids concentration gave a negative effect on the objective function (total capital cost) in both cases. The total cost was raised with about 2.7% and 3.6% when nanofluids concentration was increased from 0 to +10. This is due to increase annual operating cost which was increased by 21% and 36% for the two cases, respectively. Therefore, the efficiency and effectiveness of the present design will be of significant importance in this area of study. In view of all the examined cases presented by the proposed model, it was observed that a minimized annual total cost was obtained. Nevertheless, it is recommended further optimal design studies should be extended to include different types and sizes of nanoparticles as deciding variables.

**Keywords**: Optimal design, sensitivity analysis, shell and tube heat exchanger, nanofluids.

**Acknowledgement**

First and foremost, I would like to express my sincere gratitude to my supervisors, Dr. Agus Saptoro and A/Prof. Perumal Kumar who offered their invaluable time, energy, expertise, experiences and patience to the success of my study. They have always been there for me with their full support in every step taken in this study since the very beginning. They have not only provided me with valuable and constructive comments, but most importantly, the wisdom and the knowledge that I've learned from them which will be beacons that enlighten my undertakings in my future career.

My special appreciation goes to all my research committee members for their guidance, advice and support throughout my studies; my heartfelt gratitude goes to A/Prof. Chua Han Bing and all the research students.

I would like to thank my friends Bamaiyi, Isaac, Eleazer, Tanimu and Ismail for their warm words of encouragement throughout the period of my studies.

Finally, I would like to dedicate this thesis to my parents and my fiancée for their love, kindness, assist, and encouragement; they have indeed always been there, till the very end.

Thank you all!

Emmanuel Yahaya

**TABLE OF CONTENTS**

**LIST OF TABLES**

**LIST OF FIGURES**

**NOMENCLATURES**

$a_1$ Numerical constant (-)

$a_2$ Numerical constant (-)

$a_3$ Numerical constant (-)

$S$ Surface area ($m^2$)

$As$ Cross sectional area ($m^2$)

$B$ Baffle spacing (m)

Bc Baffle cut (-)

$C_{aop}$ Annual operating cost (Euro/Year)

$CE$ Energy cost (Euro/kWh)

$C_i$ Capital investment (Euro)

$C_l$ Clearance (m)

$C_{od}$ Total discounted operating cost (Euro)

$C_p$ Specific heat capacity in tube side (J/kg K)

$C_{tot}$ Total annual cost (Euro)

$d_i$ Tube inner diameter (m)

$d_o$ Tube outer diameter (m)

$D_e$ Shell hydraulic diameter (m)

$D_s$ Shell diameter (m)

f Darcy frictional factor (-)

F Correction factor

$h$ Convective coefficient tube side ($W/m^2K$)

$H$ Annual operating time (h/Year)

$i$ Annual discount rate (-)

$k_1$ Numerical constant (-)

$k$ Thermal conductivity (W/m k)

$L$ Tube length (m)

$m$ Mass flow rate (kg/s)

$n$ Number of tube pass (-)

$ny$ Equipment life (Year)

$N_t$ Total number of tubes

$Nu$ Nusselt number

$P$ Pumping power (W)

$Pr$ Prandtl number (-)

$P_t$ Tube pitch (m)

$P_{type}$ Pitch type

$Q$ Heat duty (W)

$R$ Fouling coefficient (W/m/k)

$R_b$ Baffle spacing/shell diameter ratio

Re Reynold's number

$T$ Temperature (K)

$U$ Over all heat transfer ($W/m^2k$)

$v$ Velocity (m/s)

***Greek symbols***

$\Delta T_{ml}$ Mean log temperature difference ($^0C$)

$\Delta P$ Pressure drop in tube side (kPa)

ϕ Volume concentration (%)

μ Dynamic viscosity (m Pa.s)

ρ Density (kg/m$^3$)

η Pump efficiency (-)

***Subscript*** $b_f$ Base fluids

$c_n$ Nanofluids concentration (vol. fraction)

$d_n$ Particle diameter (nm)

*i* Inlet

*o* Outlet

*s* Shell

***Abbreviations*** GA Genetic algorithm

*STHE* Shell and tube heat exchanger

*DEACO* Differential evolutionary anti-colony optimization

*I-ITHS* Improved intelligent turned harmony search algorithm

*BBO* Biogeography-based algorithm

*FFA* Fire fly algorithm

*GSA* Gravitational search algorithm

*PSO* Particle swarm optimization

*PSACO Particle* swarm and anti-colony optimization

# CHAPTER 1

# INTRODUCTION

## 1.1 Background

Shell and tube heat exchanger (STHE) is one of the most commonly used heat exchangers in the petroleum refineries, power plants and allied chemical industries. Declining energy resources, increasing energy price and stringent environmental regulations are propelling industries to increase thermal efficiency, lower capital and operating costs of heat exchangers. Hence, optimization of STHE in industrial processes has always been a major goal for engineers and designers due to restriction in energy resources, increase in cost of energy and aggravation of environmental issues. Such goals are the driving force that aims to achieve thermal efficiency and reduce the operating and manufacturing cost of the heat exchanger as heat transfer is significantly and widely used in the petroleum refineries, thermal plant, food industries and chemical industries.

Owing to these wide applications, shell and tube heat exchangers contribute to a significant portion of investment in new projects. Moreover, because of the large number of exchangers employed in any processing plants, small improvements in the design of shell and tube heat exchangers offer big saving opportunities. In fact, most issues that occur concerning design, operation, and analysis of manufacturing plants are commonly associated with the reduction of annual total cost. As such, this work considers the application of nanofluids in the optimal design of shell and tube heat exchanger to be able to tap the advantages of nanofluids thermal properties. This could be very much significant in the improving heat transfer performance of the system as well as reducing the cost.

Consequently, efforts to optimally design a shell and tube heat exchanger to maximize its heat transfer performance and minimizing cost have attracted much attention from both designers and users.

Heat exchanger design software such as the ones marketed by Heat Transfer Research Inc. (HTRI) and Heat Transfer and Fluid Flow Service (HTFS) has been employed in designing industrial scale heat exchangers (Lahiri et al., 2012, 2014, and 2015). Nevertheless, the use of this software is time consuming (Lahiri et al., 2014) and in most cases leads to cost-ineffective

design due to rigorous trial-and-error methods and non-inclusion of the cost criteria. Therefore, the research to optimize the heat exchanger which complies with TEMA (turbulence exchanger manufacturers association) standards is still evolving. In literature, attempts to automate and optimize the heat exchanger design have been reported by many researchers (Yang et al., 2014; Lahiri et al., 2015). However, all these attempts were only directed towards the design of heat exchangers operated with traditional heat transfer fluids such as water, oil, kerosene and ethylene glycol. Recent studies (Chavda 2015; Vajjha and Das 2012) have indicated that nanofluids are promising heat transfer fluids due to their higher thermal properties than that of the conventional fluids. Meanwhile, its effectiveness on operating constraints such as pressure drop and the velocity is believed to enable the changes in the dimensions of the existing conventional shell and tube heat exchangers in which optimizations has to be conducted to optimize certain variables under the limit of these constraints set by (TEMA). Despite its promising applications in enhancing the thermal performance of heat transfer systems, current research works on nanofluids are mostly directed toward lab-scale experiments related to studies on the thermal and physical properties (such as conductivity, viscosity, density etc.), heat transfer coefficients and friction factors (Chavda 2015; Vajjha and Das 2012). Few studies have also been carried out to study the performance of nanofluids in lab-scale exchangers (Lee et al., 2015; Sundar et al., 2014).

However, studies on optimal design and sensitivity analysis of shell and tube heat exchangers operated with nanofluids are still limited in literature, despite its promising characters in terms of heat transfer. For this reason, these studies will be of paramount importance in accelerating the heat transfer systems through the employment of nanofluids in shell and tube heat exchanger. The findings from this project could further led to the advancement of scientific literature and also to provide a platform for accelerating industrial application by tapping into the benefits of their (nanofluids) thermal properties (high thermal conductivity) to improve the techno-economic performances of heat exchangers. However, sensitivity analysis of the designed heat exchanger should also be conducted to identify and address some practical issues related to nanofluids such as high pressure drop.

## 1.2 AIMS AND OBJECTIVES

This research project aims to address the research gap where studies on the design and operation of a shell and tube heat exchanger (STHE) operated with nanofluids have not been found in the literature. This aim will be achieved via the following objectives:

1. To optimally design a shell and tube heat exchanger operated with nanofluids in compliance with TEMA industrial standard.
2. To perform a sensitivity analysis on designed shell and tube heat exchanger operated with nanofluids.
3. To propose optimum framework and guidelines for the design and operation of STHE operated with nanofluids.

## 1.3 SIGNIFICANCE

Significances of this research can be outlined as follows:

1. Scientific contributions: the findings from this study will give further advancement and additional scientific literature to area of nanofluids heat transfer system.
2. Practical implementations:
    - ❖ It will provide a platform for accelerating and materializing the industrial applications of nanofluids technology in heat transfer system.
    - ❖ It can provide optimum framework and guidelines in designing and operating nanofluids STHE.

## 1.4 Scope

From an extensive literature review, it is observed that studies on optimal process design and sensitivity analysis of shell and tube heat exchangers operated with nanofluids are still limited in the literature. The existing studies in the literature mostly focus on optimal design of STHE using conventional fluid. However, for nanofluids only theoretical and experimental investigation has been conducted on STHE by numerous researchers. Therefore, this research aims to investigate the application of nanofluids in heat exchanger by conducting an optimal design of shell and tube heat exchanger using automated (the augmentation of) Kern's method to obtain the optimal conditions and high performance STHE with the aids $Al_2O_3$/water based nanofluids with concentration ranging from 1-6% and the particle diameter of 13nm. This design will be applied to two case studies adopted from Kern (1950) and Sinott et al. (2005), in this work $Al_2O_3$/water based will be used in the tube side of the heat exchanger in both cases, while the process fluid (methanol and distilled water) will be used in shell side of the heat exchanger in two cases as proposed by the original design of Kern (1950) and Sinott et al. (2005).

However, the model validation is conducted on three different nanoparticles $Al_2O_3$/water $SiO_2$ and CNT/water based nanofluids with experimental work by Shahrul et al. (2016) and Hosseini et al. (2016). The heat exchanger adopted in this model validation is the shell and tube heat exchanger made up of a system where $Al_2O_3$/water based nanofluids flows in the tube side of the heat exchanger with a volume concentration of 0.5vol% and particle diameter of 13nm, while for $SiO_2$, a shell and tube heat exchanger with a system where $SiO_2$/water based nanofluids flows in the tube side of the heat exchanger with a volume concentration of 0.5vol% and particle diameter of 10-20nm is used. For CNT/water based nanofluids, the simulation of exchanger adopted in this model validation is shell and tube heat exchanger with a system where CNT/water based nanofluids flows in the tube side of the heat exchanger with mass flow rate of 25kg/s and the volume concentration ranging from 0.0055 and 0.0278vol%, while in the shell side of the heat exchanger is liquefied petroleum gas with mass flow rate of 95kg/s. The inlet temperature considered is 25 and 47 $^oC$ in cold and hot stream respectively.

## 1.5 LAYOUT OF THE THESIS

This thesis is divided into seven chapters. The first chapter provides a background knowledge on the existing shell and tube heat exchanger design operated with conventional fluids such as water, ethylene glycol, methanol and oil. This report also discusses the significance of shell and tube heat exchanger and essential reasons of its optimal design in enhancing performance in process industries.

Chapter two deals with the review of similar works in this area which are mainly related to optimal design of shell and tube heat exchanger using conventional fluids. This chapter also comprehensively covers the experimental work and theoretical knowledge contributed in this arena. The findings in this chapter also cover the breakthrough of the present research gap and the future research area.

Chapter three describes the present research methodology including data collection, simulation on thermal and physical properties of nanofluids. This chapter also covers the hydraulic, thermal and economic modelling of the entire heat exchanger operating with nanofluids to arrive at the objective function (total cost).

Chapter four explains with the validations of the present research model with water and some experimental analysis that have been conducted in this field. This chapter also covers all the comparative figures to show the accuracy and the validity of the present model.

Chapter five discusses the optimization studies in shell and tube heat exchanger operated with $Al_2O_3$/water based nanofluids using automated (computationally) Kern's method. This chapter also presents the results on optimized variables and discussions on it. At this point, this chapter describes the optimally designed shell and tube heat exchanger operating with nanofluids.

Chapter six deals with sensitivity analysis, guidelines of designed shell and tube heat exchanger. This chapter also covers the effects and influences of certain input parameters such as the concentration and mass flow rate on some output parameters, which are the heat transfer and pressure drop. Presentation of result and discussion based on these information is also done in this chapter.

Chapter seven covers conclusions in addition with future work and recommendations

# CHAPTER 2

# LITERATURE REVIEW

## 2.1 Optimal process design of shell and tube heat exchanger (STHE)

Many efforts have been dedicated in having optimal design and operation of a shell and tube heat exchanger (STHE) since even a small improvement in these areas offers attractive economic benefits. Earlier works on optimal design of a shell and tube heat exchanger are summarized in Table 2.1. From this table, it is apparent that most of the existing works involve optimizations of cost criteria to meet the technical specifications by satisfying operating and geometrical constraints.

In particular, the works reported by Lahiri et al. (2012, 2014 and 2015) and Yang et al. (2014) are excellent examples for optimization of shell-and-tube heat exchanger (STHE) in compliance with TEMA standards and the industrial requirements of geometric, pressure drop and velocity constraints. Optimal design of shell and tube heat exchanger (STHE) to enhance the rate of heat transfer and to minimize the total cost was carried out by Mohsen and Bazargan (2014). This study indicated that in the design of heat exchanger some design parameters have contradictory effects to the heat transfer rate and total annual cost. Optimization on shell and tube heat exchanger (STHE) using cuckoo search algorithm was done by Asadi et al. (2014) to reduce the total annual cost and heat exchanger area. They discovered that the reduction of flow velocity both in shell and tube side of the heat exchanger enable savings on the operating expenses. Earlier, Sanaye and Hassan (2010) conducted a study on multi-objective optimal design of STHE to minimize the total cost and improve the exchanger effectiveness. They reported that geometrical parameters such as baffle spacing, tube pitch and tube arrangement are found to be influential in causing a trade-off between effectiveness and total cost.

Monhanty (2016) optimally designed a STHE using firefly and gravitational search algorithm, with the purpose of reducing the annual total cost from an economic point of view. In comparison with other optimization methods, this result showed the reduction of total cost by 22.30%. Comparative studies on the optimization of shell and tube heat exchanger were conducted by Hassan et al. (2016). Their research aimed to reduce the total cost of the system, which includes the operating cost and capital from economic point of view. In their result, they

observed a 35% improvement in the total cost in the case of shell and tube exchanger with results presented in literature. However, 13% improvement of the total cost was further observed with comparison to an optimal result in the case of gasket –plate heat exchanger in the total cost to that of STHE with the same operating conditions. Optimal design of shell and tube heat exchanger to reduce the total annual cost which includes investment and operating cost was performed by Dillip Kumar Mohanty (2016) with the application of fire flight algorithm. In comparison with other designs, he noted that the developed firefly algorithm method of optimization has reduced the operating cost by 77%, while the total cost could be reduced by 29% compared to the original.

Meanwhile, the comparison of Kern, Bell and Bell Delaware method of optimizing STHE was investigated by Kulkarni, et al. (2014). It was found that a shell side coefficient of heat transfer increases with increasing mass flow rate. Bell-Delaware method was predicted to have high coefficient of heat transfer but with respect to high pressure drop compared to that of Kern and Bell method. Design of STHE using Global Sensitivity Analysis (GSA) and Harmony Search Algorithm (HAS) was conducted by Fesanghary et al. (2009) where they attempted to account for the most influential and sensitive geometrical parameters that affect the total cost of heat exchanger. They observed that sealing trip and baffle cut were less sensitive, while shell diameter and number of tube pass were highly influential.

Caputo et al. (2009) designed a STHE using particle swarm optimization (PSO) to explore the effectiveness of their method and reduce the total annual cost from economic point of view. Their findings showed that high velocity can help to prevent fouling but at the cost of high pressure drop. Serna and Jimenez (2005) used genetic algorithm for the design of segmental baffled STHE. In their study, they developed a compact relationships (equation) based on Bell-Delaware method for pressure drop, heat transfer coefficient and heat exchanger for the shell side, taking into account the effects baffle leakage and bypass. They observed that the usage of compact formulations for pressure drop estimation provided a simple algorithm with remarkable convergence properties.

Lahiri et al. (2012) optimally designed a STHE with the total cost as an objective function and they pointed out that an increase in velocity can help in preventing fouling propensity at the expense of higher pressure drop. Jie and Wei (2015) numerically investigated a plate baffled

novel shell and tube heat exchanger and verified it with experimental approach. They observed that the pressure drop for the plate baffle heat exchanger was around 128-139% of that for the rod baffles. They also noted that the novel plate baffles heat exchanger evidently illustrated higher comprehensive performance (112-122%) than that of the rod baffles. Research on optimal design of a STHE to optimize both heat exchanger area and pumping power was conducted by Fettaka et al. (2013). Other studies by Lahiri et al. (2014), Lahiri et al. (2015), Yang et al. (2014a), Yang et al. (2014b), Ponce et al. (2009) and Mohsen and Bazargan (2014) have also indicated the same phenomena (the design and optimization of STHE) and these encourage further studies on the optimal design of a STHE to meet the technical specifications by satisfying operating and geometrical constraints and complying with TEMA standards.

**Table 2.1** Summary of the previous works on optimal design STHE (TEMA standard compliance)

| HT fluids | Objective function | Optimising variables | Constraints | Optimisation method | Reference |
|---|---|---|---|---|---|
| Shell: methanol<br>Tube: sea water | Optimal design of STHE to reduce the total cost | Tube diameter, tube length, ratio of baffle spacing, Npass, Ptype, Head type, baffle cut, t, tube pitch | Velocity, pressure drop | FFA | Dillip K.M (2016) |
| Water | Comparative studies on the optimization of STHE to reduce annual cost | Tube diameter, tube length, ratio of baffle spacing, Npass, Ptype, Head type, baffle cut, t, tube pitch | Velocity, pressure drop | GA | Hassan et al. (2016) |
| Shell: Kerosene<br>Tube: Crude oil | Economic optimization of STHE to reduce the total cost | Tube diameter, tube length, ratio of baffle spacing, Npass, Ptype, Head type, baffle cut, t, tube pitch | Velocity, pressure drop | GSA | Dillip K. M (2016) |
| Shell: Kerosene<br>Tube: | To optimize heat exchanger in comply with TEMA | Tube diameter, tube length, ratio of baffle spacing, Npass, Ptype, Head type, baffle cut, t, | Velocity, pressure drop, baffle spacing shell | PSACO | Lahiri et al. (2015) |

| | | | | | |
|---|---|---|---|---|---|
| Crude oil | standard | tube pitch | diameter | | |
| Shell: Methanol Tube: Sea water | To optimize the total cost, including investment cost | Tube layout, tube diameter, length, Npass, tube wall thickness | Pressure drop | GA | Yang et al. (2014) |
| Shell: Water Tube: Oil | To optimize the heat exchanger by increasing the rate of heat transfer and decrement of total cost. | Tube and shell diameters, baffle spacing ratio, number of sealing trips, lay out angle, length, total number of tubes and pass | Baffle spacing ratio, tube pitch ratio, tube length | GA | Mohsen and Bazargan, (2014) |
| Shell: Methanol Tube : Sea water | To optimize the total cost which includes manufacturing and operating cost | Tube lay out, tube diameter, length, Npass, tube wall thickness | Pressure drop | GA | Yang et al. (2014) |
| Shell: Kerosene Tube: Crude oil | To optimize shell and tube heat exchanger from economic point of view | Ratio of baffle spacing, length, tube diameter, t, Npass, Ptype, baffle cut, head type, tube pitch | Pressure drop, velocity, baffle spacing/ shell diameter | DEACO | Lahiri et al. (2014) |
| Shell: Water Tube: Water | To design and optimize heat transfer area and pumping power | Tube lay out, number of tube pass, baffle cut and spacing, clearance, | pressure drop, heat exchanger area | GA | Fettaka et al. (2013) |
| Shell: Water Tube: Cooling water | To minimize the total annual cost from economic point of view | Tube diameter, tube length, ratio of baffle spacing, Npass, Ptype, Head type, baffle cut, t, tube pitch | Velocity, pressure drop, baffle spacing, tube length and shell diameter | PSO | Lahiri et al. (2012) |
| Shell: Water Tube: Oil | To minimize the total cost which includes capital investment for equipment and | Baffle cut ratio, tube pitch ratio, Lbc ratio, tube diameters, number of tube pass, and tube arrangement | Pressure drop | GA | Sanaye and Hassan, (2010) |

| | | | | | |
|---|---|---|---|---|---|
| | operational cost | | | | |
| Shell: Water<br><br>Tube: Water | To design and optimize the equipment and maintenance policy for cost reduction | Shell and tube diameters, sealing trips, length, baffle spacing, number of baffles, baffle cut. | Fouling resistance and velocity | GA | Caputo et al. (2009) |
| Shell: Water<br><br>Tube: Water | To minimize the total annual cost by optimally designing a STHE | Tube diameter, Ntube, tube layout and pitch, type of head, fluids allocation, number of sealing trips, inlet and outlet baffles | Tube length, velocity shell diameter, pressure, ratio of baffle | GA | Ponce et al. (2009) |

## 2.2 Nanofluids heat transfer system

Past studies revealed that water, oil, ethylene glycol and methanol have been widely used as heat transfer fluids. Therefore, there have been efforts to enhance the thermal performance of traditional fluids by adding nano-sized particles (generally less than 100nm) into them. These new type of fluids are called nanofluids. Applications of nanofluids as working fluids in heat transfer systems are expected to be popular in the near future due to their improved thermal performance. Nanofluids have attracted a great deal of attention from researchers due to their superior thermal properties. Eastman et al. (1997) measured thermal conductivity of CuO and Cu nanoparticles with water and oil as based fluids. In their study, they observed that the thermal conductivity of the nanofluids was increased by 60% compared to the corresponding base fluids, after adding up to 5% volume concentration of the nanofluids. Lee et al. (1999) suspended CuO and $Al_2O_3$ (18.6nm and 23.6nm, 24.40nm and 38.40nm) into water and ethylene glycol as based fluids respectively. The result they obtained showed that nanofluids have substantially higher thermal conductivities compared to than the base fluids. Hwang et al. (2007) carried out an experimental analysis to quantify the thermal character of nanofluids, where the thermal conductivity of nanofluids was observed to be dramatically increased as a result of increase in volume fraction of nanoparticles.

An experimental analysis was conducted by Vasu et al. (2009) and Pantzali et al. (2009) to compare heat transfer performance of nanofluids and the base fluids, where the case study observed that the heat transfer rate of nanofluids was almost twice that of base fluids. An experimental analysis was conducted by Anoop et al. (2009) using a mixture of $Al_2O_3$ / water nanoparticles in the developing region of pipe flow. They observed that the nanofluids with 45nm particle size showed better heat transfer coefficient than that by 150nm particles. It was concluded that the observed increase in heat transfer with nanofluids was not only due to intensification in thermal conductivity, but also because of the effects of particle migration and thermal dispersion. A laboratory scale experiment was conducted by Mintsa et al. (2009) to investigate the effectiveness of nano size particle in base fluids and noted that the smaller size of nanoparticles has greater effectiveness on thermal conductivity of nanofluids at the same volume fraction. Mansour et al. (2009) investigated the problem of thermally developing laminar mixed convective flow inside an inclined tube. They discovered that by increasing the particle volume concentration, the heat transfer was observed to be increasing. Numerical analysis of turbulent flow and heat transfer of three different nanofluids (CuO, $Al_2O_3$ and $SiO_2$) were studied by Nanburu et al. (2009) using water and ethylene glycol as base fluids in circular tube under constant heat flux. They observed that nanofluids with smaller diameter nanoparticle have higher viscosity and Nusselt number. Xie and Chen (2009) produced homogeneous and stable nanofluids using suspended and well dispersible multi-walled carbon nanotubes (WCNTs) into ethylene glycol base fluids. They noted that CNT nanofluids improved the thermal conductivity and the enhancement ratios increased with increasing nanotube loading and temperature.

Farajollahi et al. (2010) conducted an experimental analysis to evaluate the heat transfer characteristics of $Al_2O_3$-water (particle diameter 25nm and volume concentration up to 2%) and $TiO_2$-water (particle diameter 10nm and volume concentration up to 0.75%) nanofluids in shell and tube exchanger under turbulent flow condition. Their result showed that the coefficient of heat transfers in both the two nanofluids appear to be higher than that of base fluids. From their study, they discovered that the particle volume concentration of nanofluids has reached an extent, beyond which the convective heat transfer began to decrease at constant Peclet number. Duangthongsuk and Wongwise (2010) reported an experimental analysis on heat transfer coefficient and friction factor of $TiO_2$/water based nanofluids flowing in a horizontal double pipe counter-flow heat exchanger under turbulent flow conditions. The particle diameter was 21nm

dispersed in water with a volume concentration of 0.2-2.0%. The result showed that the heat transfer coefficient increased with an increase in Reynold number and particle volume concentration. The heat transfer coefficient was found to increase by 26%, greater than that of base fluid. Vajjha et al. (2010) on their investigation of measuring convective heat transfer of three different nanofluids (CuO, $Al_2O_3$ and $SiO_2$) attempted to compare the experimental specific heat capacity value with that of literature correlation as a function of temperature. They discovered that the specific heat capacity of all the three nanofluids at 2% volume concentration increases with increase in temperature.

Studies on convective heat transfer performance of water base alumina nanofluids in a circular tube under constant temperature was done by Heris et al. (2010). Their findings showed that there was augmentation of the nanofluids convective heat transfer coefficient with the increase of nanoparticle volume concentration. Vajjha et al. (2010) measured convective heat transfer rate and the viscosity of nanofluids. They noted that the use of nanofluids in heat exchanger decreased the volumetric and mass flow rate which resulted in overall saving pumping power. They discovered that the viscosity of the nanofluids increases with increase in the volume concentration at a specific temperature, meanwhile the rate of heat transfer increases with the increase in Reynold number. Hayat et al. (2012) studied convective heat transfer characteristic for $Al_2O_3$/water nanofluids in fully developed turbulent regime. Their results showed that the heat transfer coefficient of nanofluids was higher than that of base fluids and they also noted that there was an increase in the rate of heat transfer with increase in particle concentrations. Vajjha et al. (2012) experimentally analyzed the influence of temperature and concentration on viscosity and thermal conductivity of ($Al_2O_3$ and CuO) nanoparticles dispersed in an ethylene glycol and water mixture as base fluids. The result showed that the viscosity of the nanofluids decreased with increase in temperature and increased with increase in particle volume concentration; it was noticed that the viscosity of $Al_2O_3$ nanofluids of 6% volume concentration at 323K is 2.18 times that of base fluid. They further discovered that the thermal conductivity increased significantly with increase in particle volume concentration. Meanwhile, with increase in temperature, the thermal conductivity of CuO at 323K and 6% particle volume concentration was enhanced about 40% over the base fluids as shown in Figure 2.1 respectively.

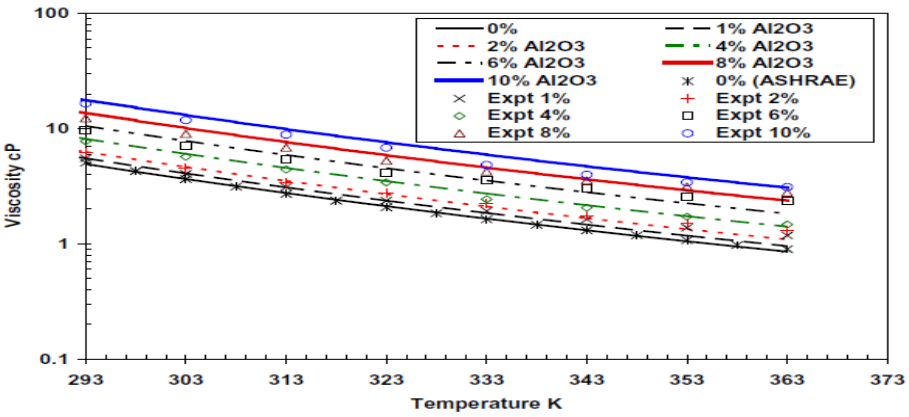


(a)

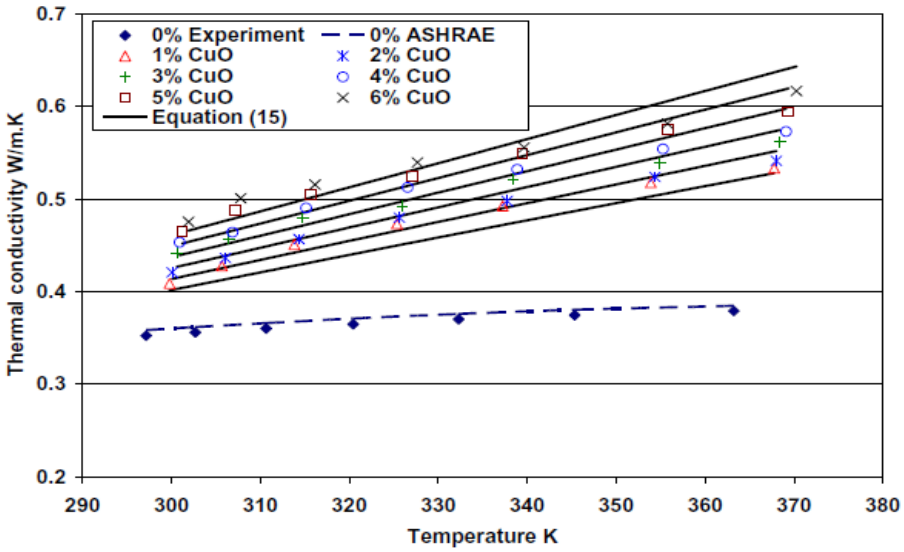


(b)

**Fig 2.1** Viscosity and thermal conductivity variation with particle volumetric concentration as a function of temperature (Vajjha et al, 2012)

Esmaeilzadeh et al. (2013) considered hydrodynamic and heat transfer characteristics of $Al_2O_3$ nanoparticles (15nm) with distilled water as base fluid inside a circular tube. They observed that increasing the volume fraction of the nanofluids leads to the enhancement of convective heat transfer coefficient. Their result showed that the average heat transfer coefficient increased by 6.8% with 0.5% volume concentration, while at 1% volume concentration, the heat transfer upgraded to 19.10% in comparison with water. Munish et al. (2014) carried out an experimental investigation on forced convective heat transfer characteristics of various nanofluids. They

observed that nanofluids enhanced the coefficient of heat transfer compared to the base fluids. Their conclusion was that heat transfer coefficient increases significantly with increase in volume concentration of the nanofluids. Elias et al. (2014) investigated the effect of different shape of nanoparticles in shell and tube heat exchanger, using different baffle angles at different temperature ranging from 20 to 50$^{o}$C. They noted that the cylindrical nanoparticles showed best performance with regards to the overall heat transfer coefficient and heat transfer rate in both segmental and baffle angles at 20$^{o}$C compared to bricks, blades and platelets shapes. Their study further discovered that the overall heat transfer coefficient and the overall heat transfer rate at 1% concentration of nanofluids with cylindrical shape have increased by 2.5% at 20$^{o}$C

Few studies have also been carried out to study the performance of nanofluids in lab-scale exchangers (Lee et al., 2015; Sundar et al., 2014) despite its promising applications in enhancing the thermal performance of heat transfer systems. Current research works on nanofluids are mostly directed toward lab-scale experiments related to studies on the thermal and physical properties (such as conductivity, viscosity, density etc.), heat transfer coefficients and friction factors. Chavda (2015). Meibo et al. (2015) experimentally studied the thermo physical properties of water-base single-walled carbon nanotube (SWCNT) nanofluids. The investigation was done at 0.1-1wt% volume concentration with temperature ranging from 10-60$^{o}$C. Their result showed that the density, viscosity and thermal conductivity of single-walled carbon nanotube nanofluids increased with increase in nanotubes concentration. Arun (2015) investigated the thermal performance of shell and tube heat exchanger using 0.5-3% $Al_2O_3$-water base nanofluids. He noted that the thermal conductivity, viscosity and density increased while specific heat capacity decreased with increase in nanoparticle concentration, and hence forth both Reynolds number and Prandtl number decreased for the same operating mass flow rate as illustrated in Figure 2.2.

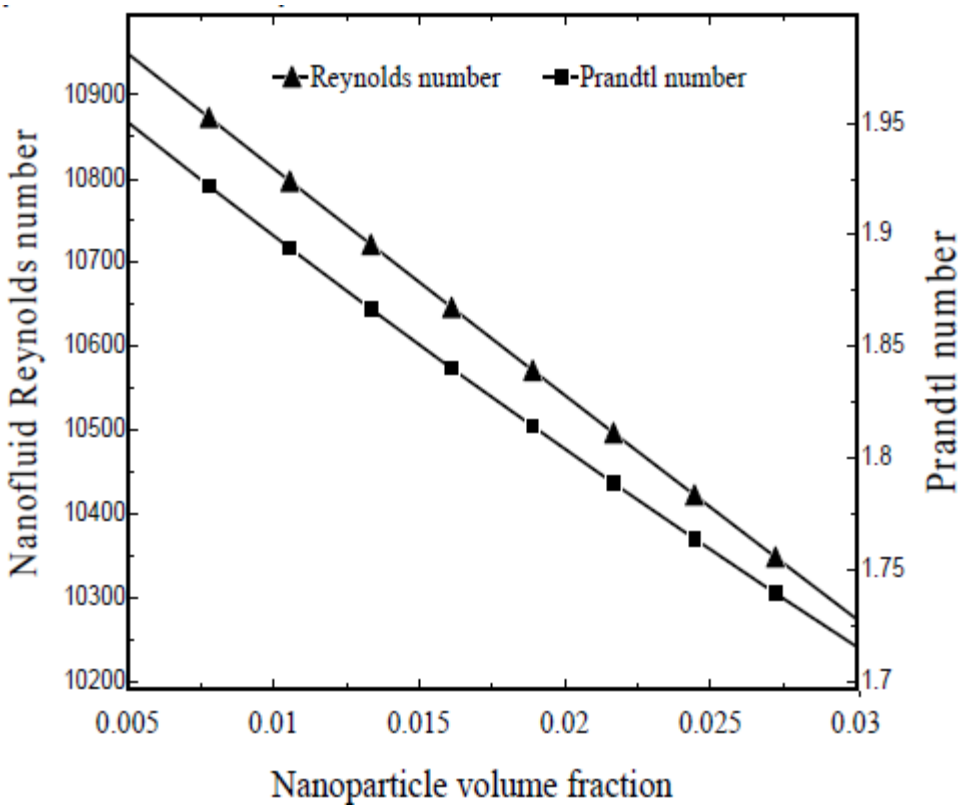


**Fig 2.2** Variation of nanofluids Reynold and Prandtl number with volume concentration. (Arun 2015)

Arun (2015) investigated the thermal performance of shell and tube heat exchanger using 0.5-3% $Al_2O_3$-water based nanofluids. The result showed that there was an increase in pressure drop, while volumetric flow rate decreased with increase in the volume concentration of the nanoparticles, hence the pumping power slightly decreased. They further discovered that there was increase in overall heat transfer with increase in thermal conductivity of the nanofluids in variation with flow rate.

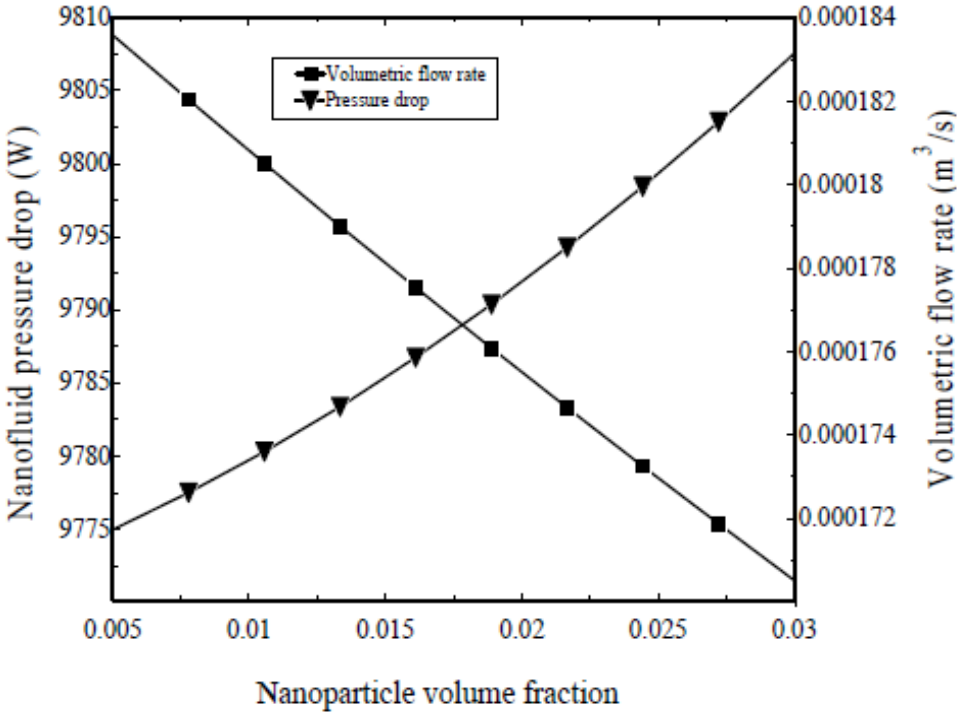


(a)

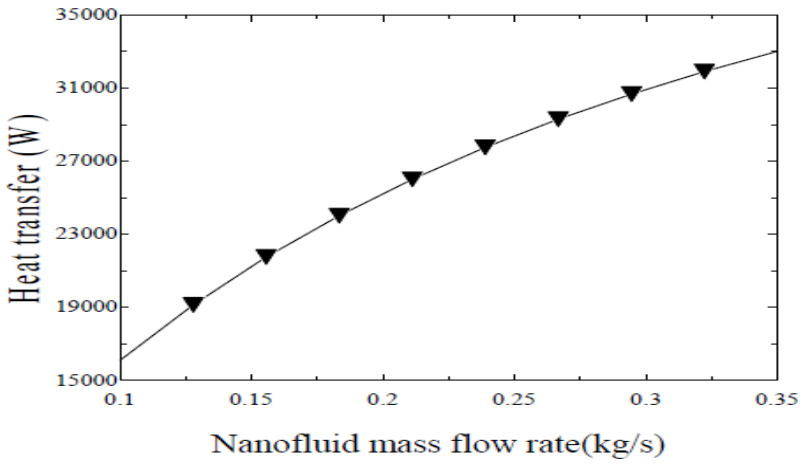


(b)

**Fig 2.3** Pressure drop and mass flow rate variation with volume concentration and variation of nanofluids mass flow rate with heat transfer. (Arun 2015)

Recently, an experimental investigation on the enhancement of heat transfer was done by Durga et al. (2016) using $Al_2O_3$/ water based nanofluids. As they compared their findings of 0.03vol.% nanofluids within a tube with twisted ratio of H/D =5 to water, they found out that the Nusselt

number increased by 18.18% at the lowest Reynold number of 3000, while the friction factor of 0.03vol.% nanofluids volume concentration increased by 1.3 times, at the same Reynold number as shown in (Figure 2.4).

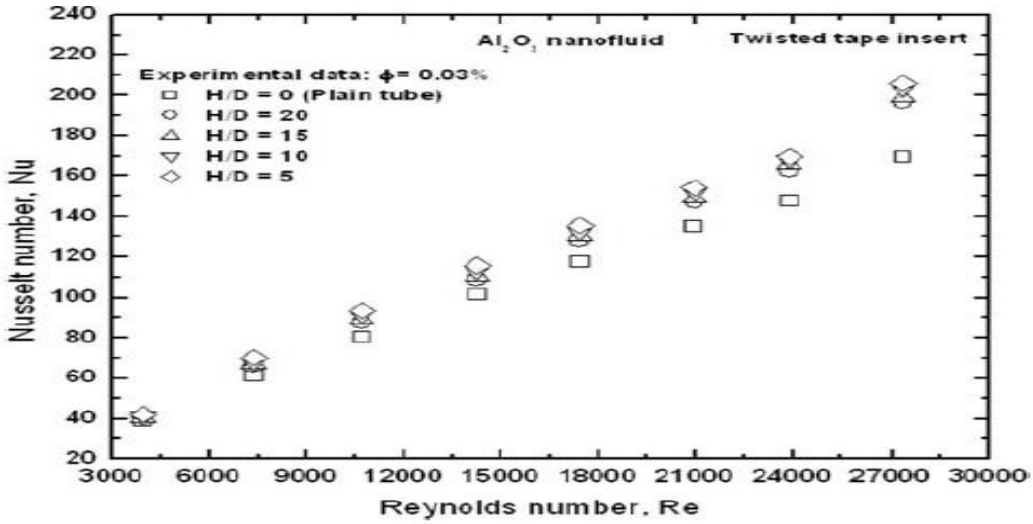


(a)

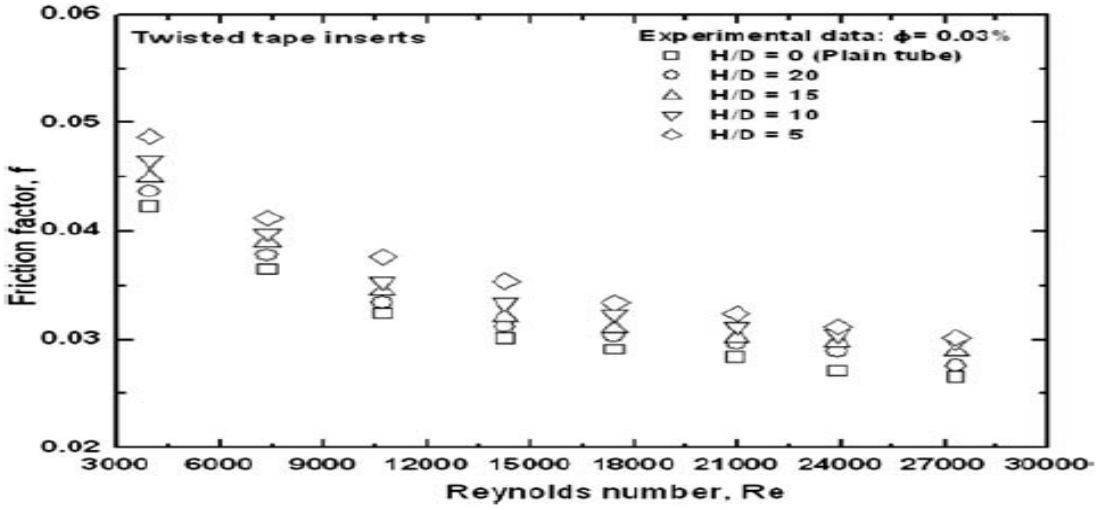


(b)

**Fig 2.4** Experimental Nusselt number of 0.03vol. % concentration flowing in twisted tube tape inserts with Reynold number and Friction factor of 0.03vol. % volume concentration flowing in twisted tube tape inserts with Reynold number (Durga et al, 2016).

Durga et al. (2016) in their conclusions highlighted that the maximum heat transfer performance and friction factor were found with the usage of $Al_2O_3$/water nanofluids at 0.03% volume concentration with twisted tape insert of ratio 5 and Reynold number of 28,000.

Mamourian et al. (2016) investigated the sensitivity analysis of a combined mixed convection heat transfer on solar heat exchanger. They noted that the positive value of sensitivity reveals an increase in the objective function due to the enhancement of input parameters. However, they further discovered that by increasing the particle diameter, the pressure drop increases. Azad et al. (2016) investigated the application $Al_2O_3$ /water based nanofluids in shell and tube heat exchanger to increase the overall efficiency of the heat exchanger and reduce the cost. They found that $Al_2O_3$ /water based nanofluids increased the Nusselt number and thereby increases the heat transfer coefficient of the heat exchanger. They further discovered that by increasing the number of tube passes, the velocity of the nanofluids decreases, and the reduction of velocity is effective in reducing the pressure drop of the heat exchanger. Numerical investigation of $Al_2O_3$ /water based nanofluids on heat transfer and pressure drop was done by Shah Mohammade et al. (2016) in shell and tube heat exchanger. Their findings revealed that heat transfer, pressure drop increased with the increase in mass flow rate.

Sarafraz and Hormozi (2016) recently performed comparative experimental studies on the boiling thermal performance of metal oxide and multi-walled carbon nanotube (MWCNT) nanofluids. They indicated that multi-walled carbon nanotube/water nanofluids had higher boiling thermal performance, higher thermal conductivity and lower thermal fouling resistance value compared to other nanofluids. They further discovered that the boiling performance of MWCNT/nanofluids was found to be intensified, when heat flux, mass flux and concentration of nanofluids were increased. Many experimental works as well as theoretical contributions have been performed to investigate the change in thermal conductivity and the effect of nanofluids concentration. Some of their report showed that the thermal conductivity of nanofluids is higher as compared to conventional fluids (Yousefi et al. 2017), and that Nanofluids concentration affects the design structure of the heat exchanger as observed by Abdolbaqi et al. (2017). Experimental work from Manetti et al. (2017) also attested to the scenario that, internal friction rising with increase in nanofluids volume fraction while the specific heat capacity reduces.

From the extensive publications in the literature, it is evident that the applications of nanofluids may enhance the value of thermal conductivity up to 49% depending on the concentration, type of nanoparticles and base fluid employed. However, it has also been observed that the most common used nanoparticle is $Al_2O_3$, which has been proved experimentally to improve heat transfer rate and also found to be stable using ultrasonic without surfactant Elias et al. (2014) and Shahrul et al. (2016). Therefore, $Al_2O_3$ is considered in this study. Table 2.2 shows samples of recent research works on different types of nanofluids.

**Table 2.2** Summary of recent studies on nanofluids heat transfer systems

| Type of nanoparticles | Base fluids | Concentration (Vol %) | Particle size (nm) | Temp (ºC) | Enhancement (K) | Reference |
|---|---|---|---|---|---|---|
| CuO | Water | 2 | 55-66 | - | 24 | Agarwal et al. (2016) |
| CNT | Water | 0.48 | <100 | - | 8-16 | Xing et al. (2016) |
| $TiO_2$ | Ethylene Glycol | 5 | 7 | - | 19.52 | Khedkar et al. (2016) |
| $Al_2O_3$ | Ethylene Glycol | 1.5 | 13 | _ | 5.0 | Serebraykova et al. (2015) |
| ZnO | Ethylene Glycol | 7.0 | 30 | _ | 9.13 | Lee et al. (2015) |
| $SiO_2$ | Water | 4 | <100 | | 9 | Anyayarkanni et al. (2014) |
| $Al_2O_3$ | Ethylene glycol | 1.5 | 36 | 60 | 32.26 | Sundar et al. (2014) |
| $TiO_2$ | Water | 4 | <100 | | 15 | Anyayarkanni et al. (2014) |
| $TiO_2$ | water | 0-3.0 | 0.22 | 30 | 7 | Azmi et al. (2014) |
| CuO | Water | 0.01 | >50 | - | 27 | Ponmani et al. (2014) |
| $TiO_2$ | Water | 1.00 | 13 | - | 8 | Anyayarkanni et al. (2014) |
| $Al_2O_3$ | Kerosene | 0.5 | 13 | - | 22 | Agarwal et al. (2013) |

It can also be observed from the Table 2.1 above that metaheuristic optimizations such as genetic algorithm (GA), differential evolution (DE), particle swarm optimization (PSO), ant colony optimization (ACO), and cuckoo search algorithm (CSA) have been popularly implemented as optimization approaches where GA is the most frequently used algorithm. However, these advanced optimization algorithms have their own merits, but they also required tuning off their specific parameters. For example, GA requires cross over probability, mutation, selection and other operators for effective implementation specific parameters need to be controlled in addition to common control parameters of population size and number of generation (Rao and Saroj 2017). Furthermore, these parameters are highly sensitive to geometric parameters of the heat exchanger. Therefore, automated Kern's method is applied in this work due to its simplicity and has no specific parameters to be turned off, thus making it easier for implementation in design optimization where complex problems and multiple variables are involved. This aspect also reduces designer's effort to arrive at the optimum value of the objective function.

However, the entire model of this project was proposed from Kern's method. This method was try and error design that was manually conducted by Kern in 1950, based on experimental work on commercial exchangers. Thus, the bottom line was to estimate the overall heat transfer. Nonetheless, this present work modified this method named (automated Kern's method) by conducting the optimal design of shell and tube heat exchanger with the aids of nanofluids as a process fluids flowing in the tube side of the exchanger for cooling application computationally (specifically using MATLAB codes) rather than manually as done by Kern. The codes will be simulated to determine thermal, hydraulic and economic modelling. The objective function of this project is the economic evaluation of cost, total annual cost to be precise (including capital investment and annual operating cost). Fig 3.1 simplified the steps involved in this proposed method.

## 2.3 Research gaps

Shell and tube heat exchanger is the workhorse of the process industries due to its wide range of applications in industries. As a result, its design gives significant amount of capital cost, even a small improvement in design and operation of shell and tube heat exchanger offers an attractive benefit economically. A thorough literature survey shows that a lot of work has been dedicated for the optimal design of shell and tube heat exchanger, but most of the studies focus on the optimal process design of shell and tube heat exchanger operated with conventional fluids. Nevertheless, to date, studies on optimal design and operation of shell and tube heat exchangers operated with nanofluids are still limited in literature. On the other hand, these studies are of paramount importance in accelerating the applications of nanofluids in heat transfer systems and tapping the benefits from their thermal properties most especially the thermal conductivity and others such as specific heat capacity, density, and viscosity to improve the techno-economic performances of heat exchangers. Specifically, sensitivity analysis should also be carried out to identify and minimize the effects of nanofluids on the pressure drop and some other possible practical issues.

In view of the aforementioned, the main objective of this research project is, therefore, to conduct an optimal process design and sensitivity analysis of heat exchangers using nanofluids. During the process design and simulation of the heat exchangers, a popular nanofluid such as $Al_2O_3$ will be put into consideration as working fluids. Thermal and transport properties will be obtained from the literature. Optimal design and sensitivity analysis of the exchangers will be carried out using MATLAB. Optimization covering technical and economic aspects will be performed using Kern's automated method. It is expected that the results and findings from this project will provide a solid foundation to accelerate industrial scale applications of nanofluids as working fluids in heat transfer systems especially in the heat exchangers. Therefore, this research aims to address the research gap by optimizing STHE operated with nanofluids through the application of automated Kern's method.

## 2.4 Summary

The reviews of similar work conducted in this area are basically on optimal design of shell and tube heat exchanger using conventional fluids. This chapter also comprehensively covers the experimental work and theoretical knowledge of nanofluids contributed in this field of studies. The findings in this chapter also cover the breakthrough of the present research gap and the future research area.

# CHAPTER 3

# RESEARCH METHODOLOGY

This research was carried in four main stages: heat exchanger model development and validation, optimal design studies of heat exchangers operated with traditional fluids, optimal design studies of heat exchangers operated with nanofluids and sensitivity analysis.

## 3.1 Model development and validation

The models in this research were validated against experimental data obtained from the literature. These models include hydraulic models, thermal and economic models. The original models and heat exchanger design were adopted from Kern's method. This method was a trial and error design that was manually conducted by Kern in 1950 based on experimental work on commercial exchangers. Its main objectives were to estimate the overall heat transfer coefficient and heat exchanger area. This present work modified Kern's method by conducting the optimal design of shell and tube heat exchanger with the aids of nanofluids as a process fluids flowing in the tube side of the exchanger for cooling application computationally using an engineering software (MATLAB) rather than manually as carried out by Kern. Thus, this modified method is named automated Kern's method. The models will be simulated to determine the thermal, hydraulic and economic performances. The economic models used to evaluate total annual cost (consisting of capital investment and annual operating cost) were employed as the objective functions of the heat exchanger design. Fig 3.1 summarizes and presents the steps involved in this proposed method.

Meanwhile, the first part of the modeling work is to conduct simulations on physical and thermal properties of nanofluids (density, specific heat capacity viscosity, thermal conductivity), these properties are estimated with the aids of given correlations as listed in equation 1-4 respectively. After that, the simulation on thermal, hydraulic and economic modeling of shell and tube heat exchanger will be carried out. The dimensions and specifications of shell and tube heat exchanger to be designed are presented in Table 3.0. The input data regarding physical and thermal properties of operating fluids are presented in the Table 3.1. The methodology of this work is to arrive at the formulated objective function for the optimal design which is the total cost.

Model design structure (with variables sourced from Lahiri et al. 2012, 2014 and 2015)

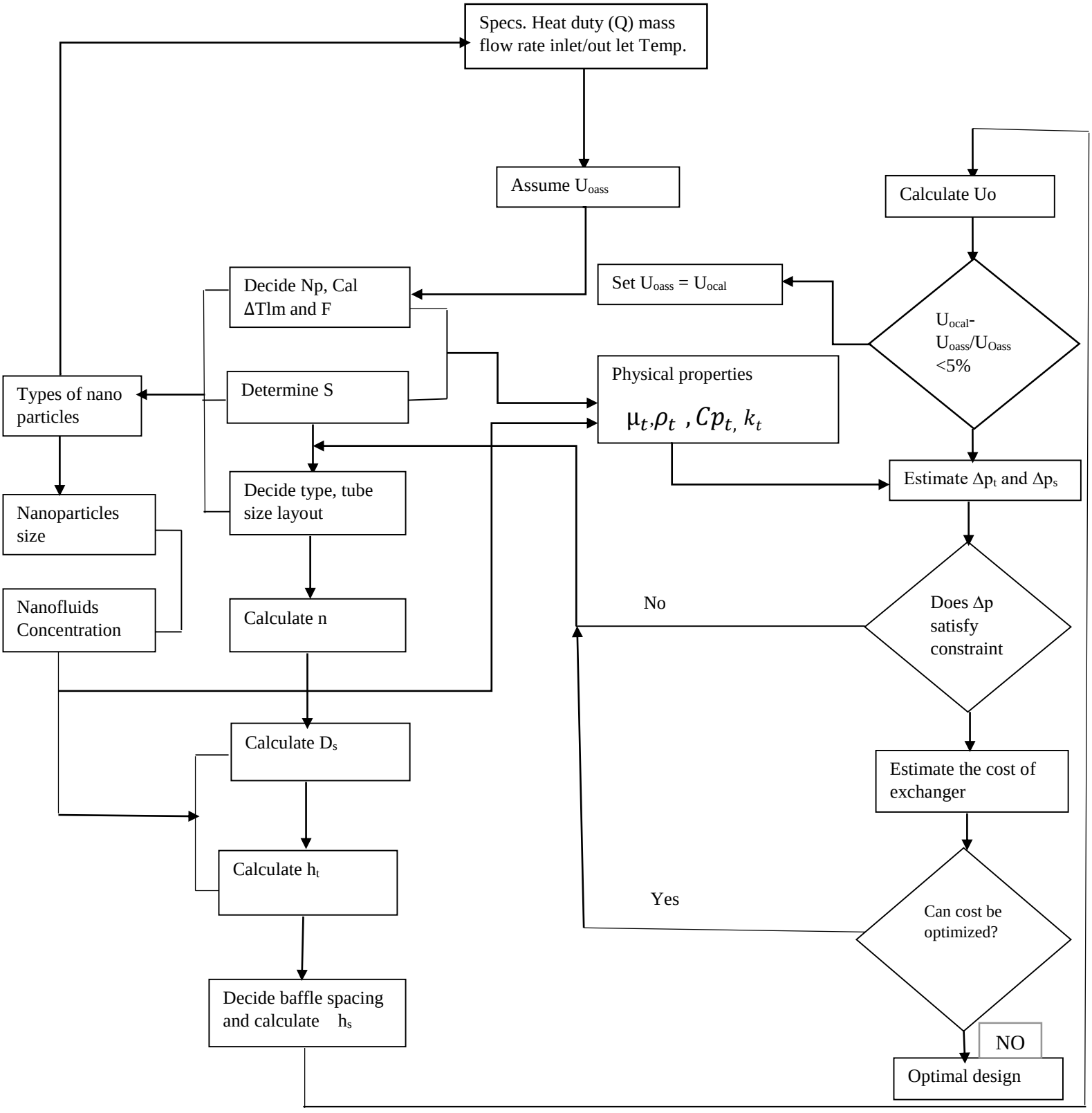


**Fig 3.1** Flow chart for heat exchanger design

**Table 3.0** Process input and properties of operating fluids

| **Operating parameters** | **Case study1** | | **Case study 2** | |
|---|---|---|---|---|
| | **Shell: methanol** | **tube: sea water** | **Shell: Distilled water** | **tube: raw water** |
| Mass flow rate (kg/s) | 27.80 | 68.90 | 22.07 | 35.31 |
| Inlet temperature $Tt_i$ and $Ts_i$ (°C) | 95 | 25 | 33.9 | 23.9 |
| Outlet temperature $Tt_o$ and $Ts_o$ (°C) | 40 | 40 | 29.4 | 26.7 |
| Density $\rho$ (kg/m$^3$) | 750 | 995 | 995 | 999 |
| Specific heat capacity $Cp$ (J/kgK) | 2840 | 4200 | 4180 | 4180 |
| Viscosity μ (m.pas) | 0.00034 | 0.00080 | 0.00080 | 0.00092 |
| Thermal conductivity $K$ (W/mK) | 0.19 | 0.59 | 0.62 | 0.62 |
| Rfouling(m$^2$K/W) | 0.00033 | 0.00033 | 0.00017 | 0.00017 |

**Table 3.1** Process input and properties of nanoparticles ($Al_2O_3$ /water based)

| **Operating parameters** | **Case study1** | | **Case study 2** | |
|---|---|---|---|---|
| | **Shell: methanol** | **tube: nanoparticle** | **Shell: Distilled water** | **tube: nanoparticle** |
| Mass flow rate (kg/s) | 27.80 | 68.90 | 22.07 | 35.31 |
| Inlet temperature $Tt_i$ and Tsi (°C) | 95 | 25 | 33.9 | 23.9 |
| Outlet temperature $Tt_o$ and $Ts_o$ (°C) | 40 | 40 | 29.4 | 26.7 |
| Density $\rho$ (kg/m$^3$) | 750 | 3700 | 995 | 3700 |
| Specific heat capacity $Cp$ (J/kgK) | 2840 | 880 | 4180 | 880 |
| Viscosity μ (m.pas) | 0.00034 | 0.00080 | 0.00080 | 0.00092 |
| Thermal conductivity $K$ (W/mK) | 0.19 | 40 | 0.62 | 40 |
| Rfouling(m$^2$K/W) | 0.00033 | 0.00033 | 0.00017 | 0.00017 |

### 3.1.1 Model validations

The validation of this model is accounted for four different systems, meanwhile, the physical and thermal properties data and correlations of nanofluids are obtained from literature. These include data and correlations for density, viscosity, thermal conductivity and heat capacity for different types of nanofluids. Range of nanofluids concentrations and nanoparticle size are determined by observing typical ranges usually used by researchers. Other design data are obtained from TEMA standard and Perry's Chemical Engineering handbooks (latest editions). For the first system, the validation is performed for the same heat exchanger specification found in experimental manual for heat exchanger SOLTEQ (2014). The system of heat exchanger adopted in this model validation is with water flowing in both pipes as process fluids, while all the properties of the fluids are held constant. The validation of the second system was performed under the same experimental condition as Shahrul et al. (2016). The heat exchanger adopted in this model validation is shell and tube heat exchanger with a system where $Al_2O_3$/water based nanofluids flows in the tube side of the heat exchanger with a volume concentration of 0.5vol. % and particle diameter of 13nm while in the shell side of the heat exchanger was water. The inlet temperature considered is 70 and 20$^oC$ respectively. The properties and the data for heat exchanger specifications are found Table 3.2 and 3.3 respectively.

**Table 3.2** Heat exchanger design specifications for $Al_2O_3$ Shahrul et al. (2016)

| Description | Specification |
|---|---|
| Type of heat exchanger | 1 tube pass and shell |
| Tube outside diameter $d_o$ | 0.007m |
| Tube inside diameter $d_i$ | 0.0064m |
| Number of tube pass $N_t$ | 20 |
| Tube length L | 1.220m |
| Tube arrangement | Rotated square |
| Shell inside diameter $D_i$ | 0.1150m |
| Shell outside diameter $D_o$ | 0.0890m |
| Baffle cut | 25% |
| Baffle spacing | 0.05545m |
| Tube pitch $P_t$ | 0.0088m |

**Table 3.3** Process input and properties of operating fluids for $Al_2O_3$ Shahrul et al. (2016)

| **Operating parameters** | **Tube side nanofluids** | **Shell side water** |
|---|---|---|
| Mass flow rate (L/min) | 2-8 | 4 |
| Inlet temperature $Tt_i$ and $Ts_i$ ($^oC$) | 20 | 70 |
| Outlet temperature $Tt_o$ and $Ts_o$ ($^oC$) | 40.10 | 41.40 |
| Density $\rho$ ($kg/m^3$) | 3700 | 985.12 |
| Specific heat capacity $Cp$ (J/kgK) | 880 | 4065.8 |
| Viscosity μ (m.pas) | - | 0.0007733 |
| Thermal conductivity $K$ (W/mK) | - | 0.59 |
| Nanofluids concentration ϕ (%) | 0.5 | - |
| Nanoparticle diameter $d_n$ (nm) | 13 | - |

The simulations for the third system were performed under the same experimental heat exchanger configuration according to Hosseini et al. (2016). This is done to verify the accuracy of this model. The simulation of heat exchanger adopted in this model validation is shell and tube heat exchanger with a system where CNT/water based nanofluids flows in the tube side of the heat exchanger with mass flow rate of 25kg/s and the volume concentration ranging from 0.0055 and 0.0278vol. %, while in the shell side of the heat exchanger was liquefied petroleum gas with mass flow rate of 94.8075kg/s. The inlet temperature considered was 25 and 47$^o$C in cold and hot stream respectively. The properties and the data for heat exchanger specifications are shown in Table 3.4 and 3.5 respectively.

**Table 3.4** Process input and properties of operating fluids for CNT Hosseini et al. (2016).

| Description | Specification |
|---|---|
| Type of heat exchanger | 1 tube pass and shell |
| Tube outside diameter $d_o$ | 0.0191m |
| Tube inside diameter $d_i$ | 0.0153m |
| Number of tube pass $N_t$ | 1040 |
| Tube length L | 6.1000 |
| Tube arrangement | Rotated square |
| Shell inside diameter $D_i$ | 1.0700m |
| Shell outside diameter $D_o$ | 1.0960m |
| Baffle cut | 16.5% |
| Baffle spacing | 0.05800m |
| Tube pitch $P_t$ | 0.0250m |

**Table 3.5** Process input and properties of operating fluids for CNT Hosseini et al. (2016).

| Operating parameters | Tube side nanofluids | Shell side water |
|---|---|---|
| Mass flow rate (kg/s) | 25-45 | 94 |
| Inlet temperature $Tt_i$ and $Ts_i$ ($^oC$) | 25 | 47 |
| Outlet temperature $Tt_o$ and $Ts_o$ ($^oC$) | 40.80 | 30.50 |
| Density $\rho$ (kg/m$^3$) | 2600 | 995.18 |
| Specific heat capacity $Cp$ (J/kgK) | 600 | 4070.20 |
| Viscosity μ (m.pas) | - | 0.00121 |
| Thermal conductivity $K$ (W/mK) | - | 0.59 |
| Nanofluids concentration ϕ (%) | 00550,0.055,0.111,0.275 | - |

The validation of the last system was performed under the same experimental condition as (Shahrul et al. 2016). The heat exchanger adopted in this model validation is shell and tube heat exchanger with a system where $SiO_2$/water based nanofluids flows in the tube side of the heat exchanger with a volume concentration of 0.5% and particle diameter of 10-20nm, while in the

shell side of the heat exchanger was water. The inlet temperature considered is 70 and 20ºC respectively. The properties and the data for heat exchanger specifications are found Table 3.6 and 3.7 respectively.

**Table 3.6** Heat exchanger design specifications for $SiO_2$ Shahrul et al. (2016)

| **Description** | **Specification** |
|---|---|
| Type of heat exchanger | 1 tube pass and shell |
| Tube outside diameter $d_o$ | 0.007m |
| Tube inside diameter $d_i$ | 0.0064m |
| Number of tube pass $N_t$ | 20 |
| Tube length L | 1.220m |
| Tube arrangement | Rotated square |
| Shell inside diameter $D_i$ | 0.1150m |
| Shell outside diameter $D_o$ | 0.0890m |
| Baffle cut | 25% |
| Baffle spacing | 0.05545m |
| Tube pitch $P_t$ | 0.0088m |

**Table 3.7** Process input and properties of operating fluids for $SiO_2$ Shahrul et al. (2016)

| **Operating parameters** | **Tube side nanofluids** | **Shell side water** |
|---|---|---|
| Mass flow rate (L/min) | 2-8 | 4 |
| Inlet temperature $Tt_i$ and $Ts_i$ (ºC) | 20 | 70 |
| Outlet temperature $Tt_o$ and $Ts_o$ (ºC) | 40.10 | 41.40 |
| Density $\rho$ (kg/m$^3$) | 2200 | 985.12 |
| Specific heat capacity $Cp$ (J/kgK) | 703 | 4070.2 |
| Viscosity μ (m.pas) | - | 0.0007733 |
| Thermal conductivity $K$ (W/mK) | - | 0.59 |
| Nanofluids concentration ϕ (%) | 0.5 | - |
| Nanoparticle diameter dn (nm) | 10-20 | - |

### 3.1.2 Specific correlations used for estimating the thermo physical properties of nanofluids

Equation (1-3), correlation for density, heat capacity and viscosity were obtained from Azad (2016)

$$\rho_{t=}(1-\phi)\rho_{bf+}\rho_p\,\phi_p \quad (1)$$

$$Cp_t = \frac{\phi_p Cp_p+(1-\phi)\rho_{bf}\,Cp_p}{\rho_t} \quad (2)$$

$$\mu_t=((1+39.11\phi)+(533.9\,\phi^2))\mu_{bf} \quad (3)$$

Equation (4), correlation for thermal conductivity are obtained from Alina (2016)

$$k_t = k_p+2k_{bf}+2C_n(k_p-k_{bf})/k_p+2k_{bf}-C_n(k_p-k_{bf}) \quad (4)$$

### 3.2 Optimal design studies of STHE with conventional fluids

The methodology of this work has been applied to determine the minimum total cost for shell and tube heat exchangers operated with nanofluids. However, this research considered to perform an optimal design of heat exchanger with conventional fluids such as (ethylene glycol, water and oil) used in the system same as that of Kern (1950) and Sinnott et al. (2005) before introducing the $Al_2O_3$/water based nanofluids into the system and lastly the sensitivity analysis was carried out for the two case studies adopted as explained in details below

The optimization codes have been developed in MATLAB and the simulations are performed using a desktop. The upper and lower bound of these design optimization variables were adopted exactly as that of Kern (1950). The parameters for estimating the capital investment cost and the annual operating cost were obtained from Sinnott et al. (2005), with ny=10Years, energy cost=0.12Euro/KW, i=10 annual discount rate, H=7000h/yr annual amount of work per hour. Nevertheless, to make this design optimization more effective, the research methodology grouped the optimal design into three major stages with two cases studies adopted from Kern (1950) and Sinnott et al. (2005).

Case 1. Case study was taken from Kern (1950) where methanol and sea water were used in shell and tube side respectively as the original designed heat exchanger with heat duty 4.34MW. The original designed heat exchanger is a two tube pass and a single shell heat exchanger. The

process parameters and the physical properties of both shell and tube side operating fluids are summarized in Table 3.0

Case 2. The case study 2 was taken from Sinnott et al. (2005). In this case, distilled water and raw water were considered as heat exchanger operating fluids, with a heat duty 0.46MW. The original design is a single shell pass and two tube pass heat exchanger. The physical properties are summarized in Table 3.0

**Table 3.8** Heat exchanger design specifications for Kern (1950) and Sinnott et al. (2005)

| **Description** | Kern (1950) Specification | Sinnott et al. (2005) Specification |
|---|---|---|
| Type of heat exchanger | 2 tube pass and a single shell | 2 tube pass and a single shell |
| Tube outside diameter $d_o$ | 0.02m | 0.019m |
| Tube inside diameter $d_i$ | - | - |
| Number of tube pass $N_t$ | 918 | 160 |
| Tube length L | 4.83m | 4.88m |
| Tube arrangement | Triangular | Triangular |
| Shell inside diameter $D_i$ | 0.894m | 0.387 |
| Shell outside diameter $D_o$ | - | - |
| Baffle cut | 0.356m | 25% |
| Baffle spacing | 25% | 0.305m |
| Tube pitch $P_t$ | 0.025m | 0.023m |

In stage one, the proposed model conducted a design optimization with same number of variables and the system of heat exchanger were considered as that suggested by Kern (1950) and Sinnott et al. (2005) for case 1 and case 2 respectively. In stage two, more variables were included, such as tube diameter, tube length, number of tube pass, baffle cut, type of pitch, head type and ratio of baffle spacing to shell diameter for optimizations (multivariable heat exchanger design) for both cases.

**Table 3.9** Optimization variables for stage one and two.

| Optimisation variables | Symbol | Variable name Stage 1 | Stage 2 |
|---|---|---|---|
| $X_1$ | do | Tube diameter m | Tube diameter m |
| $X_2$ | L | Tube length | Tube length |
| $X_3$ | $R_{b= B/Ds}$ | Ratio of baffle spacing to shell diameter | Ratio of baffle spacing to shell diameter |
| $X_4$ | Np | - | Number of pass |
| $X_5$ | Ptype | - | Type of pitch /Tube layout |
| $X_6$ | Head type | - | Head type |

However, the method adopted in this research is automated Kern's method. Even though, the design of shell and tube heat exchanger involves a large number of geometric and operating variables as a part of search that meets the heat duty requirement on a given set of constraint. Values of the design variables are defined based on the design specifications and the assumption of several mechanical and thermodynamic parameters in order to have a satisfactory heat transfer coefficient leading to a suitable utilization of heat exchanger surface area. In this design optimization, thermal, hydraulic and economic modeling of the shell and tube heat exchanger was carried out to arrive at the optimal design as illustrated in Fig 3.1. The objective function in this case will be the annual total cost involved. Two case studies were adopted in this design originally conducted by Kern (1950) and Sinnott et al. (2005) as discussed above in the stages of this optimal design. During the process of simulation of this design method, the bottom line is the estimation of the overall heat transfer ($U_o$), and the operating and geometric constraint must be met to arrive at the objective function. The overall heat transfer coefficient is assumed based on the design optimization variables, while the design routine determines the overall heat exchanger area satisfying the assigned thermal duties specification. The overall actual heat transfer coefficient is then calculated and compared with that of assumed overall heat transfer coefficient. If the difference between the two falls within the range of 5%, then the optimization process moves to the next step, or else it assigns new $U_{assumed} = U_{cal}$ and iterates the previous step until the criteria is met.

### 3.2.1 Brief description of advanced search algorithm using the cost as objective function

The metahuristics (advanced search GA PSO, FFA GFA, etc.) algorithm functions in the same way to arrive at same target point (objective function). It starts by creating initial population randomly of design candidate that represent parent to generate young ones with shared characters from the parent. A new generation is formed from the young ones that are fits, and this process is repeated, as a result complex combination in design space arise and this continues until the best design is obtain. For the design optimization of STHEs the operational and geometric variables, are subjected to chromosomes, fitness values and individual

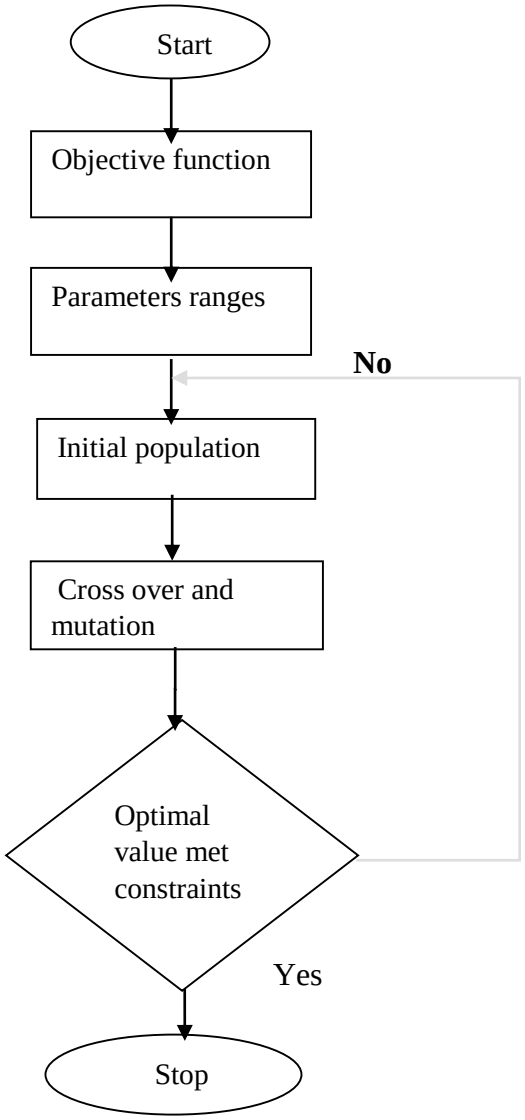


**Fig 3.2:** flow chart of algorithm using total cost objective function

### 3.1.2 Model correlations

**THERMAL MODELING**

Equation (5-14) is obtained from Lahiri et al. (2014, 2015)

Actual heat transfer

$$Q = m_t Cp_t(T_{to} - T_{ti}) = m_s Cp_s(T_{si} - T_{so}) \quad (5)$$

Logarithm mean temperature difference

$$\Delta T_{ml} = \frac{(T_{si} - T_{to}) - (T_{so} - T_{ti})}{\ln[\frac{T_{si} - T_{to}}{T_{so} - T_{ti}}]} \quad (6)$$

Correction factor is computed as

$$F = \{\frac{\sqrt{R^2+1}}{R-1} \cdot \frac{\ln(1-\frac{P}{1-PR})}{\ln[\frac{2-P\left(R+1-\sqrt{R^2+1}\right)}{2-P(R+1+\sqrt{R^2+1})]}} \quad (7)$$

Where

$$R = \frac{(Ts,i - Ts,o)}{(Tt,o - Tt,i)} \quad (8)$$

$$P = \frac{(Tt,o - Tt,i)}{(Ts,i - Tt,i)} \quad (9)$$

**TUBE SIDE CORRELATIONS**

The tube pitch

$$P_t = 1.25 d_o \quad (10)$$

Where $d_o$ = outer tube diameter

The tube inner diameter

$$d_i = 0.8 d_o \quad (11)$$

Where $d_i$ = inner tube diameter

Surface area is computed as

$$S = \frac{Q}{U_o \Delta T_{ml} F} \quad (12)$$

The total of tubes (n) = $\frac{S}{\pi doL}$ (13)

Where L is the length of tube, n is the total number of tube

Tube side velocity

$$v_t = \frac{N_p}{n} \frac{m_t}{(\pi {d_i}^2/4)\rho_t} \quad (14)$$

$m_t$ Is the mass flow rate

Reynold number is given as

$$Re_t = \frac{\rho_t v_t d_i}{\mu_t} \quad (15)$$

Prandtl number

$$Pr_t = \frac{Cp_t \mu_t}{k_t} \quad (16)$$

Coefficient of heat transfer

$$h_t = 0.027 \frac{\lambda t}{di} Re_t^{0.8} Pr_t^{1/3} \left(\frac{\mu s}{\mu sw}\right)^{0.14} \quad (17)$$

Over all heat transfer

$$Uo = \left[\frac{1}{ht}\left(\frac{do}{di}\right) + Rt\left(\frac{do}{di}\right) + \frac{do \ln(\frac{do}{di})}{2.\lambda w} + Rs + \frac{1}{hs}\right]^{-1} \quad (18)$$

Viscosity at the outer wall temperature and wall temperature is estimated as

$$T_{tw} = U_o \frac{Tb_s - Tb_t}{h_t} + T_{bt} \quad (19)$$

**SHELL SIDE CORRELATIONS**

Cross sectional area

$$A_s = \frac{D_s B\,(P_t - d_o)}{P_t} \quad (20)$$

Shell side velocity is given as

$$v_s = \frac{m_s}{\rho_t A_s} \quad (21)$$

Shell side diameter is given as

$$Ds = \left(\frac{n}{k_1}\right)^{1/n_1} d_o \quad (22)$$

Shell side Reynold number

$$Re_s = \frac{m_s D_e}{\mu_s A_s} \quad (23)$$

$D_e$ Is the hydraulic shell diameter

Shell side Prandtl number

$$Pr_s = \frac{Cp_s \mu_s}{k_s} \quad (24)$$

Baffle spacing

$$B = R_b D_s \quad (25)$$

Where $R_b$ is the ratio of baffle spacing to shell diameter

For rotated square $30^0$

$$D_e = \frac{\frac{P_t^2}{2} - \left(\frac{\pi d_o^2}{4}\right)}{\pi d_o} \quad (26)$$

For triangular $90^0$

Hydraulic diameter

$$D_e = 4\left(\frac{\frac{P_t^2}{2} X\ 0.87P_t - \left(\frac{0.5\pi d_o^2}{4}\right)}{\pi d_o}\right) \quad (27)$$

$h_s = 0.36 \frac{\lambda_s}{D_e} Re_s^{0.55} p_{rs}^{1/3} (\frac{\mu_s}{\mu_{sw}})^{0.14}$ shell side coefficient of heat transfer from Yang et al. (2014) (28)

Viscosity at the outer wall temperature is estimated as

$$T_{tw} = T_{bs} - U_o \frac{T_{bs} - T_{bt}}{h_s} \quad (29)$$

Equations (17-30) were obtained from Lahiri et al. (2014), Lahiri et al. (2015) and Yang et al. (2014)

## HYDRAULIC MODELING

Pressure drop on tube side is computed as

$$\Delta p_t = N_p (4 f_t \frac{L}{d_i} + 2.5) \frac{\rho_t v_t^2}{2} \quad (30)$$

Tube side frictional factor

$$f_t = (1.82 \log Re_t - 1.64)^{-2} \quad (31)$$

Shell side pressure drop

$$\Delta p_s = f_s (\frac{\rho_s v_s^3}{2}) (\frac{L}{B}) (\frac{D_s}{D_e}) \quad (32)$$

Where $f_s$ is the shell side frictional factor obtain as

$$f_s = 2_{bo}. Re_s^{-0.15} \quad (33)$$

$b_o = 0.72$ for $Re_s < 40000$

Pumping power $P = \frac{1}{\eta} (\frac{m_t}{\rho_t} \Delta p_t + \frac{m_s}{\rho_s} \Delta p_s)$ (34)

$\eta$ =Pump efficiency

## ECONOMIC MODELING

Capital investment $C_{inv} = a_{1+} a_2 S^{a3}$ (35)

Where $a_1$= 8000, =$a_2$ 259.2, $a_3$=0.93 (for exchanger made with stainless steel for both shell and tube)

Operating cost $C_o = P.C_E.H$ (36)

Where P = Pump Power Consumption

$C_E$= Energy (Electricity) Cost

*H* = amount of working hours per Year

Annual operating cost $C_{aop}$

$$C_{aop} = \sum_{k=1}^{ny} \frac{C_o}{(1+i)^k} \quad (37)$$

Where *i* = the fractional interest rate (annual discount rate)

*ny* = equipment life (10Years)

The total cost of STHEs $C_{tot}=C_{inv} + C_{aop}$ (38)

However, the dimensional and constructive details of heat exchanger structure, which also include the thermo physical properties of the nanofluids applied, the operating parameters such as pressure drop and velocity (which are considered as constraint in this design are then computed to evaluate the objective function (total cost), while the optimal design trial variables are then subjected to iterations to develop a new structure of shell and tube heat exchanger and this will be done repeatedly until the cost (objective function) criteria is met . The schematic flow chart of the design optimization is illustrated in Fig 3.1.

**Operating Constraints**

Both operating and geometry constraint were obtained from Lahiri et al. (2015), Yang et al. (2014)

Tube = $\Delta p_t < \Delta p_t^{max} p_t \quad dp_t \leq 35kPa$ (39)

Shell = $\Delta p_s < \Delta p_t^{max}\ dp_s \leq 35kPa$ (40)

$v_t = 1.0 \leq v_t \leq 2.00\ m/s$ (41)

$v_s = 0.4 \leq v_s \leq 1.0\ m/s$ (42)

**Geometry constraint**

Ratio of tube length to shell diameter = $3 \leq \frac{tube\ length}{shell\ diameter} \leq 5\text{m}$ (43)

Ratio of baffle spacing to shell diameter = $0.050 \leq \frac{L_{bs}}{D_s} \leq \text{B} \leq 0.5^{\max} L_{bs}/D_s$ (44)

Equations (31-44) were also obtained from Lahiri et al. (2014), Lahiri et al. (2015) and Yang et al. (2014)

### 3.3.1 Optimal design studies on nanofluids design heat exchanger

However, in stage three, the optimal design of heat exchanger system was considered to be different. For case 1, the system was operated with nanofluids in the tube side of the heat exchanger, while methanol was still on the shell side of the exchanger with the same thermal duty 4.34MW as proposed by Kern (1950). For case 2, the system was operated with nanofluids in the tube side of the heat exchanger, while distilled water was still on the shell side of the exchanger with same thermal duty 0.64MW as proposed by Sinnott et al. (2005).

The optimizations for this section were performed using $Al_2O_3$ / water based nanofluids in the tube side of heat exchanger. Hence, more variables were considered for this optimization which includes nanofluids volume concentration, tube diameter, tube length, number of tube pass, baffle cut, type of pitch, head type and ratio of baffle spacing to shell diameter

The design parameters and properties for both case studies involved in this design including that of $Al_2O_3$ /water based nanofluids are listed in Table 3.0 and 3.1 respectively, followed by the presentation of models correlations.

In this project, eight deciding (optimization) variables will be optimized and they include nanofluids concentration, tube diameter, tube length, number of tube pass, baffle cut, type of pitch, head type, ratio of baffle spacing to shell diameter and tube wall thickness. This will be done during the process of evaluating the objective function ($C_{tot}$) while geometric and operating constraints (pressure drop and velocity) are being satisfied in compliance with TEMA standards. Thus, tube pitch and type of base fluids are constant. These variables and thsseir corresponding options are summarized in Table 3.10

**Table 3.10** Optimization variables and their corresponding options.

| Optimisation variables | Symbol | Variable name | Corresponding options | Available options |
|---|---|---|---|---|
| $X_1$ | Do | Tube diameter m | 0.00635, 0.009525, 0.0127, 0.022225, 0.0254, 0.03175, 0.0381, 0.044445, 0.05715, 0.05715, 0.0635 | 12 |
| $X_2$ | L | Tube length | 1.2192, 1.8288, 2.4384, 3.048, 3.6576, 4.8768, 6.096, 6.7056, 7.3152 | 8 |
| $X_3$ | $R_{b= B/Ds}$ | Ratio of baffle spacing to shell diameter | 0.2, 0.25, 0.30, 0.35, 0.40, 0.45, 0.50, 0.55, 0.60, 0.65, 0.70, 0.75, 0.80, 0.85, 0.90, 0.95, 1.00 | 17 |
| $X_4$ | Np | Number of pass | 1-1, 1-2, 1-4, 1-6, 1-8 | 5 |
| $X_5$ | Ptype | Type of pitch /Tube layout | Triangular (30°) and (square 90°) | 2 |
| $X_6$ | Head type | Head type | Fixed tube sheet or U tube; outside packed split ring floating head, pull through floating head | 4 |
| $X_7$ | Bc | Baffle cut (%) | 20, 25, 35, 45 | 4 |
| $X_8$ | Pt | Tube pitch | 1.25do | 1 |
| $X_9$ | Cn | Nanoconcentration (vol %) | 1- 6 (with an interval of 0.1%) | 60 |
| $X_{10}$ | Bf | Base fluids | Water | 1 |

Note: Data for $X_1$- $X_8$ adopted were obtained from Lahiri et al. (2012), Lahiri et al. (2014), and Lahiri et al. (2015). Data for $X_9$ was obtained from Vjjha and Das (2012), and Ray and Das (2014).

### 3.4 Additional correlations used

Nusselt number is obtained from Boungiorno (2005) as follows

$$Nu_t = 0.021\, Re_t^{0.8}\, Pr_t^{0.5} \quad (45)$$

Coefficient of heat transfer in the tube side is therefore defined as (Azad (2016))

$$h_t = \frac{Nu_t k_t}{d_i} \quad (46)$$

The tube side frictional factor ($f_t$ ) is adopted from Sajedi et al (2016) for laminar and transient flow regimes and from Vajjha and Das (2012) for turbulent flow region

$$f_t = \frac{64}{Re_t} \quad (47)$$

$$f_t = \quad 1.82 \ (\log \ Re_t - 1.64)^{-2} \tag{48}$$

$$f_t = 0.316 \ Re_t^{-0.25} \tag{49}$$

However, the Reynold number was considered in both laminar, transient and turbulent regime (>2300, >=10000 and <10000) in regards to equation 47, 48 and 49 respectively.

**3.5 Sensitivity analysis**.

One of the important parts of computational and simulation model is the sensitivity analyses. The developed method will therefore, further perform a sensitivity analysis which marks the second objective of this research. To accomplish this objective, some of the input parameters will be monitored and observed on the effects they have on the output results, most importantly the total cost. In this research, a sensitivity analysis was performed to examine the effect of nanofluids volume concentration and mass flow rate on heat transfer rate, total cost and pressure drop. This can be achieved by varying the values of input variables (including the optimum values from the optimal design in stage 3). The optimum values will be employed as base case and other cases will be studied and evaluated by varying the values of the input variables up to $\pm$10%. Analysis and recommendations then will be outlined to assist an optimal operation of a shell and tube heat exchanger operated with nanofluids.

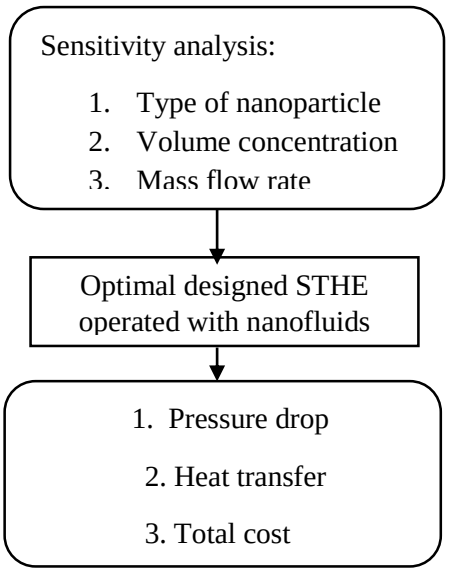


**Fig 3.3** Showing the scheme of sensitivity analysis

### 3.6 Computational facilities

The modeling and simulation are performed using MATLAB R2014b software and a computer with the following specifications:

1. Processor: Intel(R) Core(TM) i3-4160 CPU @ 3.60 GHz
2. Installed memory: 4.00 GB
3. System type: 32-bit Operating System

### 3.7 Summary of research methodology

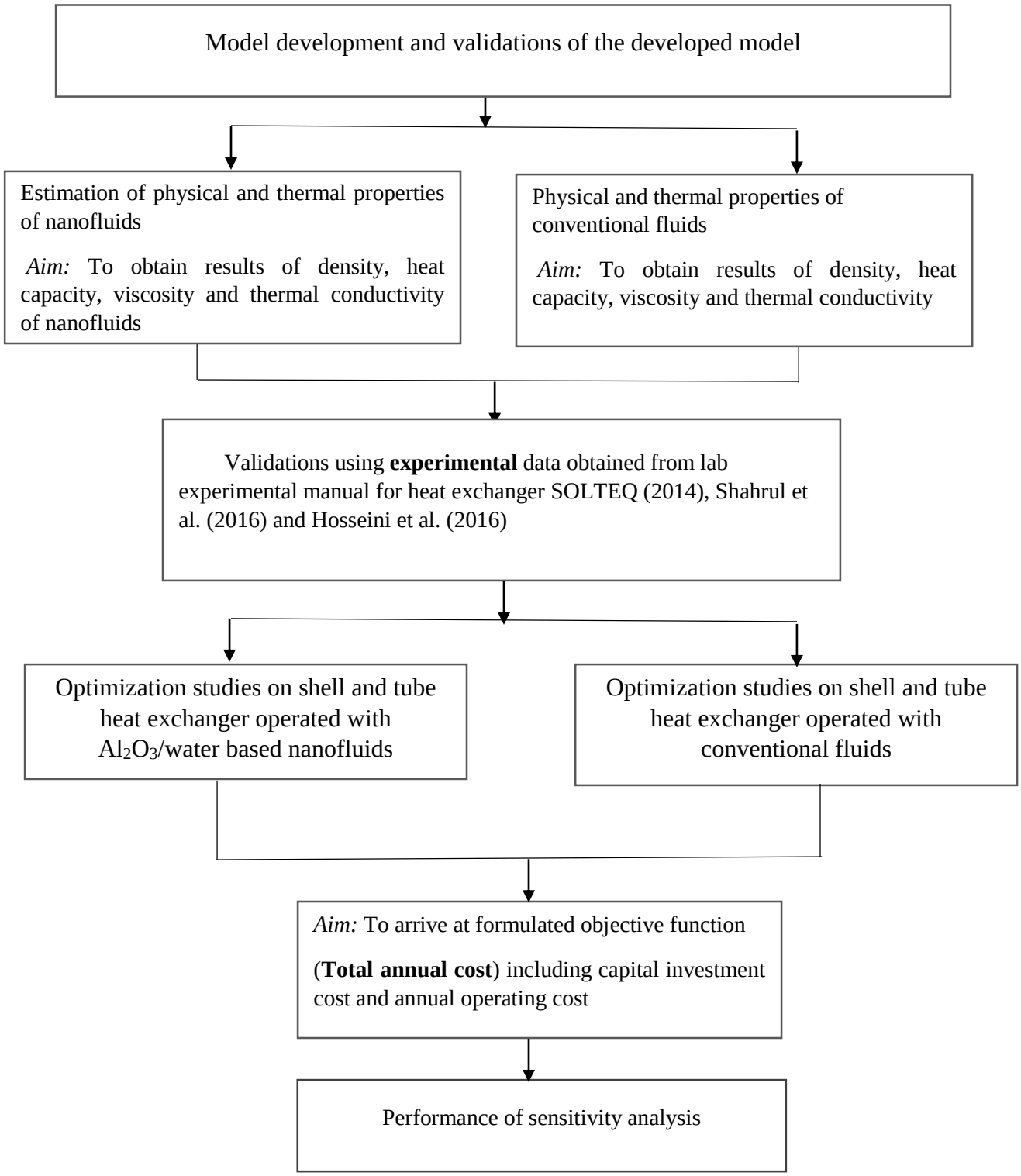


**Fig 3.3** Flow chart showing the research methodology

# CHAPTER 4

# MODEL VALIDATION

## 4.1 Model validation for water

The present model was validated for water using experimental data obtained from manual for heat exchanger training of shell and tube heat exchanger. The comparison between overall heat transfer coefficients ($U_o$) with varying volumetric flow rate is shown. It is observed that the simulated data are in good agreement with the experimental data.

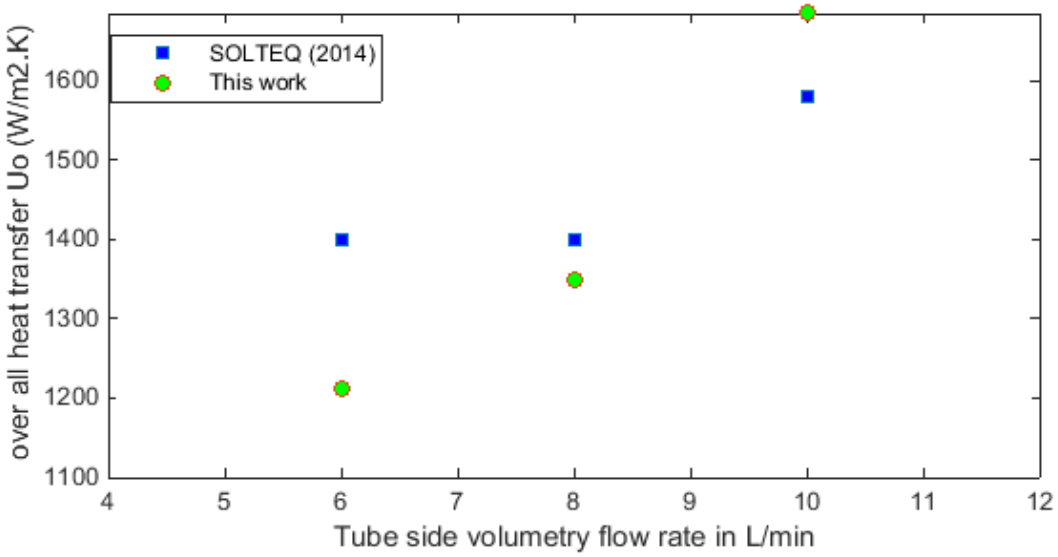


**Fig 4.1** Comparison of overall heat transfer coefficient with experimental values obtained from manual for heat exchanger training as a function of volumetric flow rate

The validation of the model was performed for the same heat exchanger specification found in experimental manual heat exchanger. The heat exchanger adopted in this model validation is a double pipe heat exchanger with water flowing in both pipes as process fluids. This validation was done to attest the efficiency of the present model in varying the mass flow rate. To monitor that, the shell side volumetric flow rate was held constant at 5 L/min, while the tube side volumetric flow rate was varied from 2-10L/min. The overall heat transfer coefficient vs volumetric flow rate is presented in Fig 4.1. It shows that the overall heat transfer increases with

increase in volumetric flow rate in the heat exchanger. This is because heat transfer is proportional to the mass flow rate and thermal conductivity, in other words, the rate of heat transfer does not depend solely on the flow rate, but it is also affected positively by the influence of the Reynolds number and the thermal conductivity of the process fluids. Hence, the movement of molecules becomes faster with increase in mass flow rate of the fluids. This contributes the increment of heat transfer but at the expense of higher pressure drop. It is also observed that the model values at the volumetric flow rate of 6 and 8 L/min were less than that of the experimental values, while at 10 L/min, the value became higher at constant shell volumetric mass flow rate. However, the compatibility of the present model with experimental studies was also confirmed by computing the percentage error, which was found to approximately 8.5% which signified the validity and the compatibility of this model in comparison to the experimental findings. Table 4.1 shows the percentage error of this work and the data obtained from experimental analysis.

**Table 4.1** Percentage error for this work and experimental data on overall heat transfer ($U_o$)

| Experimental | This work | Percentage error (%) |
|---|---|---|
| 1400 | 1220 | 14.8 |
| 1410 | 1350 | 4.4 |
| 1700 | 1600 | 6.24 |
| Average (%) | | 8.5 |

### 4.2 Model validation for $Al_2O_3$/water based nanofluids

To validate the present model, simulations were performed under the same experimental condition as mentioned by Shahrul et al. (2016), this is done to verify the accuracy of this model. The heat exchanger adopted in this model validation is shell and tube heat exchanger with a system where $Al_2O_3$/water based nanofluids flows in the tube side of the heat exchanger with a volume concentration of 0.5vol. % and particle diameter of 13nm, while in the shell side of the heat exchanger was water. The volumetric flow rate was taken from 2-10L/min in both the streams (hot and cold) while the inlet temperature considered was 70 and 20$^o$C respectively. The comparison of the data obtained from the model on convective coefficient of heat transfer ($h_t$) in

tube side of the STHE, the rate of heat transfer (Q) and the overall heat transfer were in good agreement with that of the experimental data.

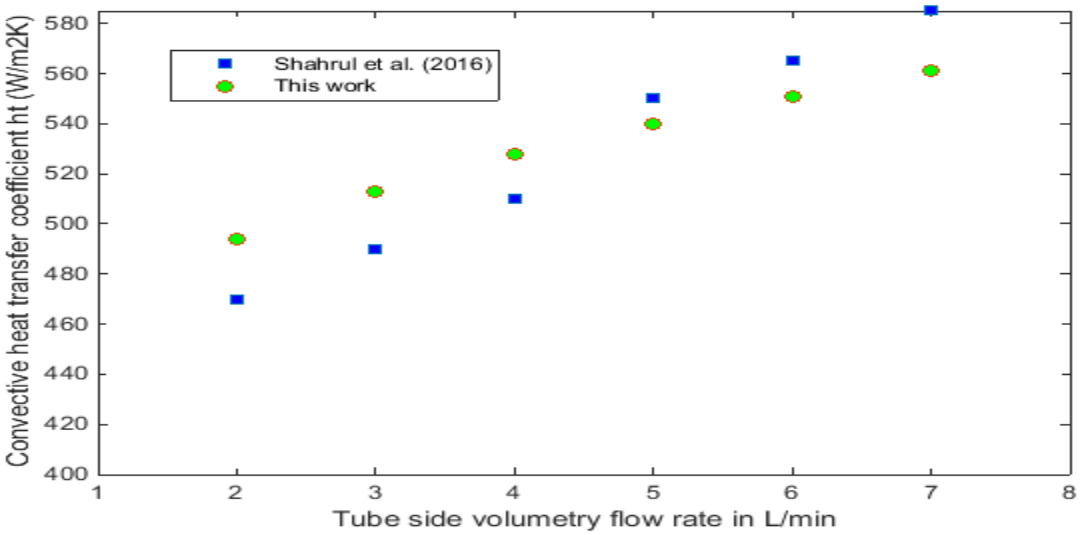


**Fig 4.2** Comparison of convective heat transfer ($h_t$) with experimental values adopted from Shahrul et al. (2016) on $Al_2O_3$/water based nanofluids with 0.5%vol. concentration and 13nm particle diameter

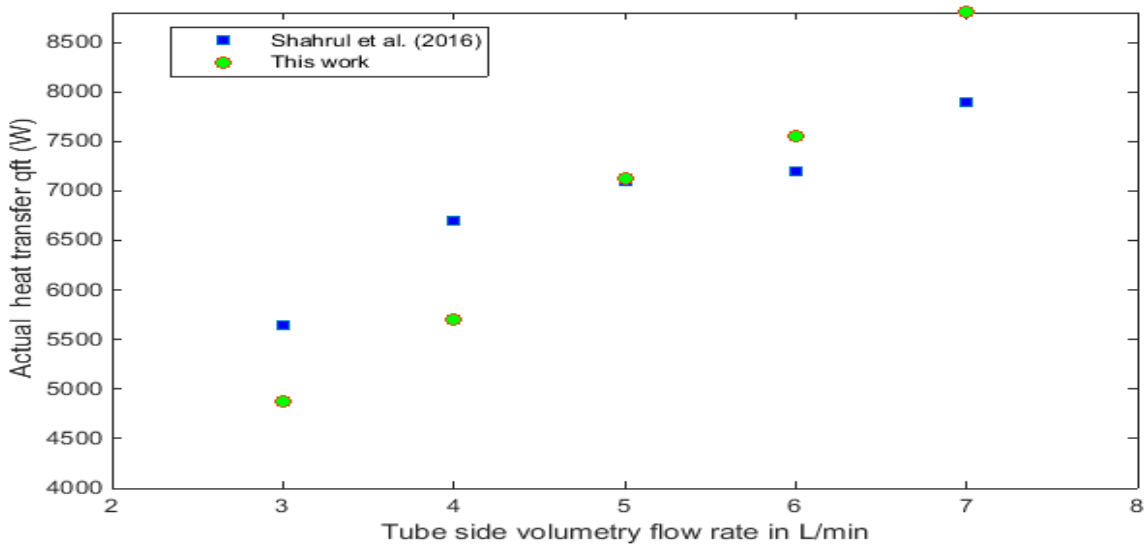


**Fig 4.3** Comparison of actual rate of heat transfer (Q) with experimental values adopted from Shahrul et al. (2016) on $Al_2O_3$/water based nanofluids with 0.5%vol. concentration and 13nm particle diameter.

**Table 4.2** Illustration of the percentage error between this work and experimental data for convective heat transfer, actual heat transfer and overall heat transfer for $Al_2O_3$/water based nanofluids respectively.

| $h_t$ (W/m$^2$.K) | | | Q (W) | | | $U_o$ (W/m$^2$.K) | | |
|---|---|---|---|---|---|---|---|---|
| Shahrul et al. (2016) | This work | % Error | Shahrul et al. (2016) | This work | % Error | Shahrul et al. (2016) | This work | % Error |
| 470 | 494 | 4.9 | 5650 | 4877 | 13.7 | 300 | 260 | 13.13 |
| 490 | 513 | 4.15 | 6700 | 5702 | 14.8 | 370 | 330 | 12.12 |
| 510 | 528 | 3.4 | 7100 | 7128 | 0.4 | 390 | 370 | 5.4 |
| 550 | 540 | 1.9 | 7200 | 8550 | 4.6 | 460 | 450 | 2.2 |
| 565 | 551 | 2.5 | 7900 | 8800 | 11.2 | 455 | 520 | 12.5 |
| 585 | 561 | 4.3 | - | - | | - | - | - |
| Average (%) | | 3.6 | | | 8.94 | | | 9.07 |

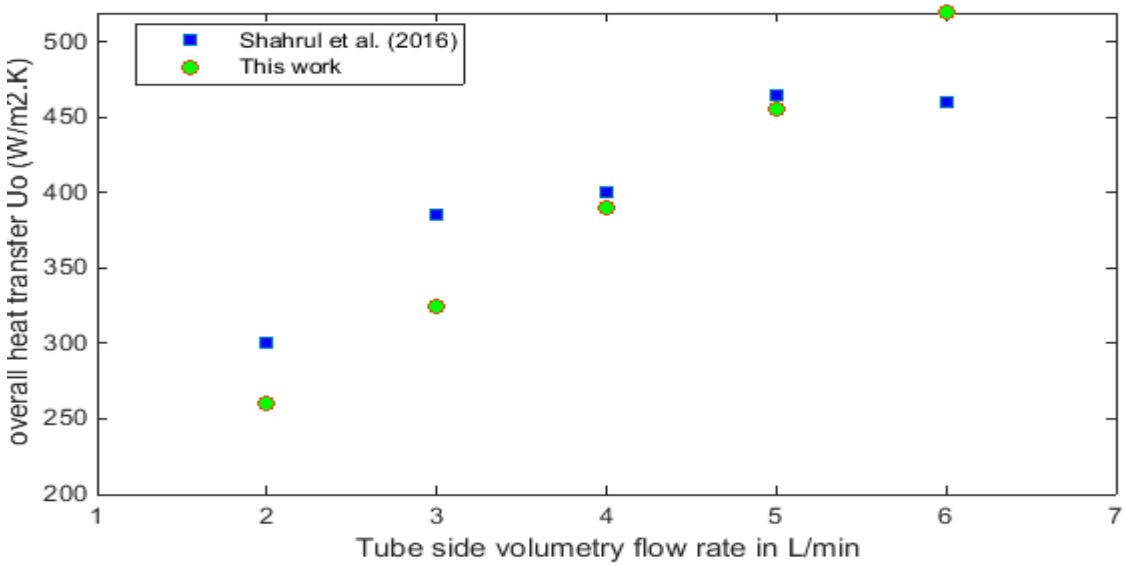


**Fig 4.4** Comparison of overall heat transfer ($U_o$) with experimental values adopted from Shahrul et al. (2016) on $Al_2O_3$/water based nanofluids with 0.5%vol. concentration and 13nm particle diameter

The validation of this model was conducted for $Al_2O_3$/water based nanofluids flowing through the cold stream and water is used in hot stream as process fluid which is flowing in the shell side of shell and tube heat exchanger under counter current flow arrangement. The simulation was performed under the same heat exchanger design configuration as shown in Table 3.1, with the volume concentration and particle diameter of $Al_2O_3$/water based nanofluids constant at 0.5%vol and 13nm respectively.

The volumetric flow rate in the tube side was varied from 2-8L/min at different outlet temperature in the tube side. The outlet temperature is varied due to the fact that as the volumetric flow rate varies (increases), more heat is being consumed by the flowing material and this results in a linear decrease of outlet temperature in the tube side of the shell and tube heat exchanger of this model. The volumetric flow rate on shell side is at a constant of 4 L/min. Based on Fig 4.2 which shows convective heat transfer vs volumetric flow rate, it can be observed that the present model and the experimental data are in excellent agreement, where both increase as the volumetric flow rate increases. It can also be seen that at the volumetric flow rate of 2-4L/min, the values of the model are slightly higher than that of the experimental data, while from 5-7L/min, the experimental data are less compared to the model.

Fig 4.3 shows the rate of heat transfer vs volumetric flow rate for the heat exchanger. It can be observed that the rate of heat transfer increases with the increase in volumetric flow rate at constant shell side volumetric flow rate of the heat exchanger. The overall heat transfers of $Al_2O_3$/water based nanofluids against volumetric flow rate is presented in Fig 4.4. It is clear that the overall heat transfer is a function of volumetric flow rate, because as the volumetric flow rate increases, heat transfer increases as well. It can be seen from the figures listed above that the variation trends of flow characteristics for the present model are in good agreement with the trends for (convective heat transfer ($h_t$), rate of heat transfer (Q) and the overall transfer) as compared with that of experimental data. Generally, the present model showed increase in heat transfer as volumetric flow rate increases, in which both factors are in good agreement as ascribed in many theoretical reports and some experimental analysis contributed in the literature. However, the presentation of the results and figures for this validation ascertains the efficiency of this model, but for further evidence and convictions, this work proceeds in standardizing this model by accounting for the percentage error as illustrated in Table 4.2 which is found to be

approximately ranging from 3.6%, 8.94%, and 9.07% respectively and were in good agreement with the experimental result reported.

### 4.3 Model validation for CNT/water nanofluids

To validate the present model, the simulations were performed under the same experimental condition as suggested by Hosseini et al. (2016), this is done to verify the accuracy of this model. The simulation of exchanger adopted in this model validation was shell and tube heat exchanger with a system where CNT/water based nanofluids flowed in the tube side of the heat exchanger with mass flow rate of 25kg/s and the volume concentration ranging from 0.0055 and 0.0278vol. %, while in the shell side of the heat exchanger was liquefied petroleum gas with mass flow rate of 94.8075kg/s. The inlet temperature considered was 25 and 47$^{o}$C in cold and hot stream respectively The comparison of the data obtained from the model on convective coefficient of heat transfer, in tube side of the shell and tube heat exchanger (STHE), the rate of heat transfer, the overall heat transfer, and the Reynold number were in good correlation with that of the experimental findings.

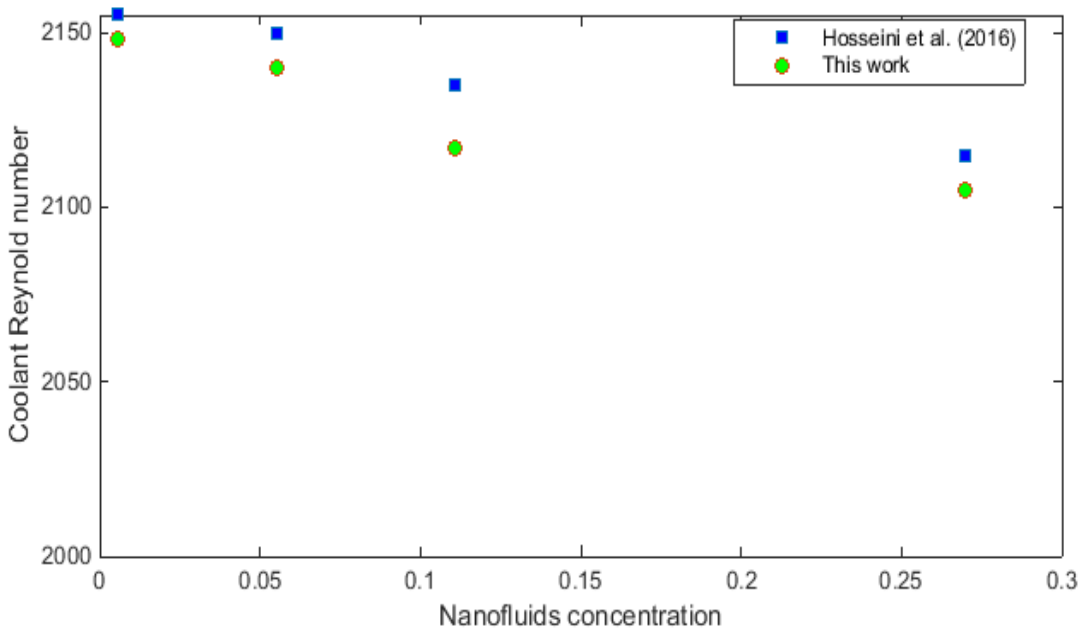


**Fig 4.5:** Comparison of Reynold number (Re) with experimental values of Hosseini et al. (2016) on CNT/water based nanofluids with 0.0055, 0.055, 0.111 and 0.278%vol. concentration.

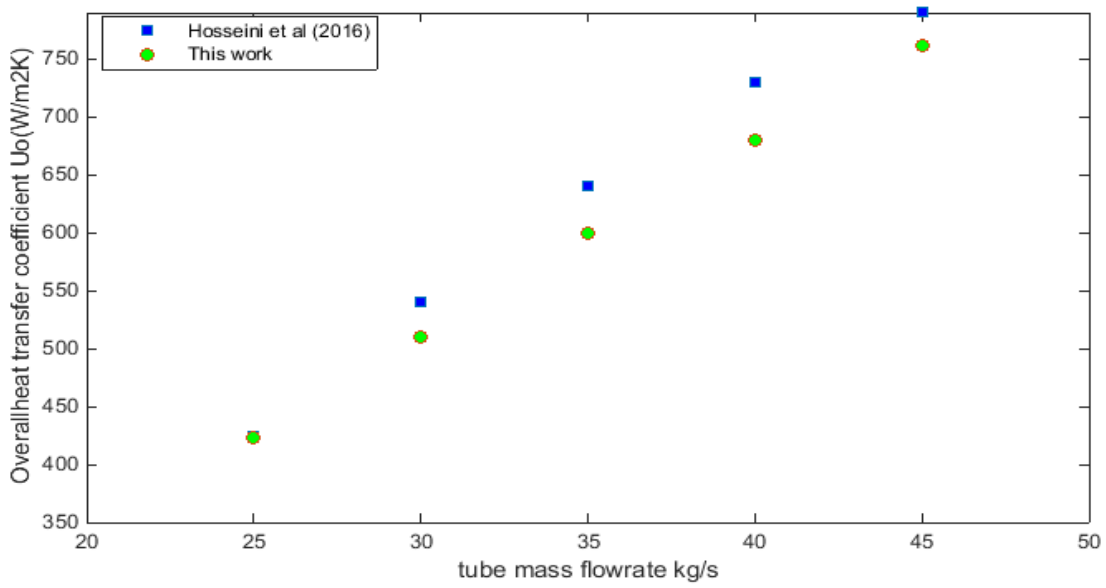


**Fig 4.6** Comparison of overall heat transfer ($U_o$) against mass flow rate with experimental values of Hosseini et al. (2016) on CNT/water based nanofluids with 0.278%vol. concentration.

**Table 4.3** Illustration of the percentage errors between this work and experimental data for Reynold number and overall heat transfer for CNT /water based nanofluids respectively

| (Re) | | | $U_o$ (W/m$^2$.K) | | |
|---|---|---|---|---|---|
| Hosseini et al. (2016) | This work | % Error | Hosseini et al. (2016) | This work | % Error |
| 2155 | 2148 | 0.32 | 424 | 423 | 0.24 |
| 2150 | 2140 | 0.5 | 540 | 510 | 5.6 |
| 2135 | 2117 | 0.8 | 640 | 600 | 6.25 |
| 2115 | 2105 | 0.5 | 730 | 6800 | 6.8 |
| - | - | - | 790 | 762 | 3.5 |
| Average (%) | | 0.53 | | | 0.5 |

The validation of this model was conducted for CNT/water based nanofluids flowing through the cold stream in the tube side of shell and tube heat exchanger under counter current flow

arrangement. The simulation was performed under the same heat exchanger design specification as shown in Table 3.3, with the volume concentration of CNT/water based nanofluids ranging from 0.0055, 0.055, 0.1111 and 0.278%vol. Fig 4.5 illustrates the effects of nanofluids particle volume concentration against the Reynold number which was used as a coolant in the tube side of heat exchanger at constant mass flow rate 25kg/s. It can be seen that with the increase of nanofluids volume concentration to a certain level, the Reynold number began to drop gradually, and this may likely also affect the heat transfer system. However, it can be said that, the gradual dropping of the Reynold number could be as a result of increment of nanofluids viscosity due to increase in volume concentration of the CNT/water based nanofluids. It is also noted that addition of nanoparticles is related with the increase in share stress of the nanofluids which is associated with a high viscosity. Fig 4.6, shows the result of the validated model with experimental data of the overall coefficient of heat transfer against the mass flow rate in the tube side of heat exchanger at constant volume concentration of CNT/water based nanofluids. It can be seen that the change of mass flow rate has a tremendous effect in changing the rate of heat transfer, while the concentration of the nanofluids is held constant at 0.278%vol. However, the rate of heat transfer does not rely only on the mass flow rate, but it is also affected positively by the influence of the Reynold number and the thermal conductivity of the CNT/water based nanofluids.

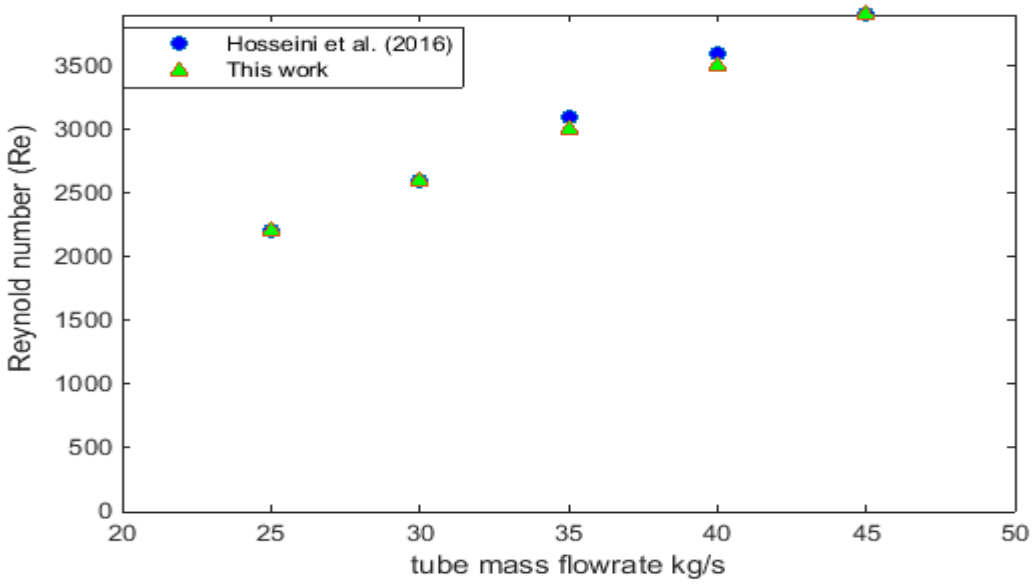


(a)

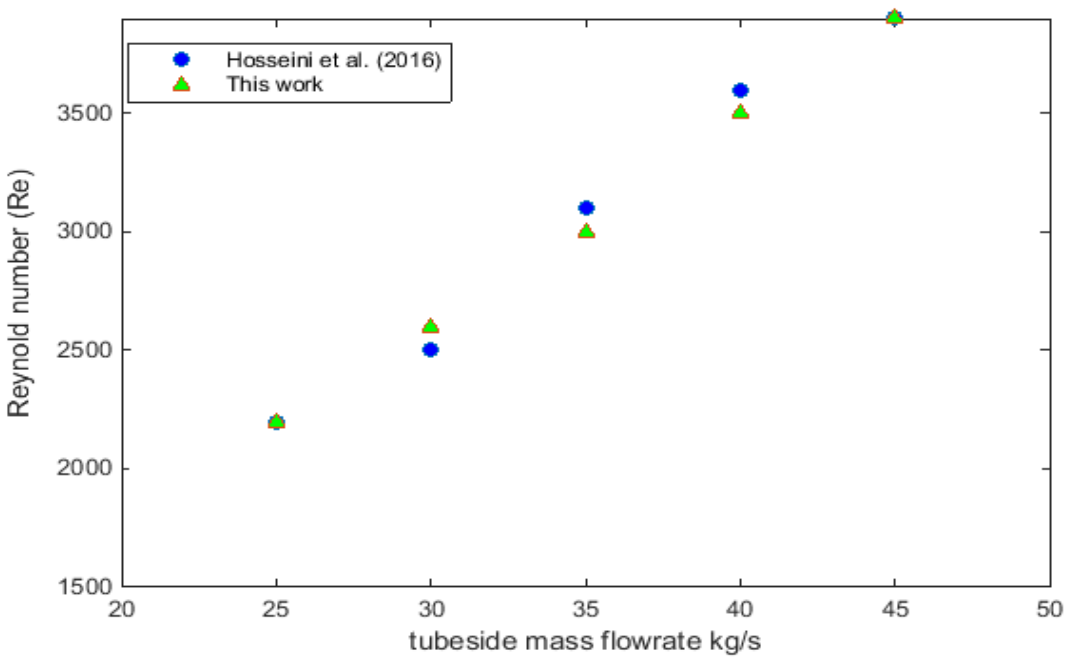


(b)

**Fig 4.7** (a) and (b) shows the comparison of Reynold number (Re) against mass flow rate with experimental values of Hosseini et al. (2016) on CNT/water based nanofluids with 0.0550%vol. and 0.1110%vol. concentration respectively

Fig 4.7 (a) and (b) show the validation of the present model with the experimental data obtained from Hosseini et al. (2016), under the experimental condition as illustrated in Table 3.3., and the properties of CNT are found in Table 3.4. This verification was done to comprehensively test the validity of the present model. It is apparent that the variation of mass flow rate does not only affect the rate of heat transfer but also the Reynold number. At various volume concentration of CNT/water base nanofluids being held constant at 0.0550 and 0.1110%vol, as shown above, the Reynold number increased with the increase in mass flow rate. This occurred as a result of influence in the thermal conductivity of the nanofluids, in that case, the temperature of the hot fluids found in shell side of heat exchanger was also found to be decreasing in the simulations and this was because, with the increase of nanofluids, the mass flow rate in the tube side of heat exchanger which is associated with thermal conductivity has led to more absorptivity of heat in shell side (hot fluids) by the nanofluids in the flowing in the tube side. On the other hand, it increases the heat transfer rate from the hot fluids to the nanofluids. Generally, the description of

the results and figures for this validation ascertained the efficiency of this model, but for further evidence and convictions, this work proceeded in accounting for the percentage error as presented in Table 4.3 and 4.4. The average error was found to be approximately ranging from 0.53%, 0.5%, 1.5% and 2.04% respectively, which are in good agreement as compared to the experimental data obtained from the literature.

**Table 4.4** Illustration of the percentage error between this work and experimental data for Reynold numbers at different concentrations for CNT /water based nanofluids respectively.

| Re (0.0550 %vol.) | | | Re (0.1110 %vol.) | | |
|---|---|---|---|---|---|
| Hosseini et al. (2016) | This work | % Error | Hosseini et al. (2016) | This work | % Error |
| 2197 | 2200 | 1.5 | 2200 | 2200 | 0.0 |
| 2600 | 2600 | 0.0 | 2500 | 2600 | 4.00 |
| 3100 | 3000 | 3.2 | 3100 | 3000 | 3.2 |
| 3600 | 3600 | 2.7 | 3600 | 3500 | 2.7 |
| 3900 | 3900 | 0.0 | 3886 | 3900 | 0.3 |
| Average (%) | | 1.5 | | | 2.04 |

### 4.4 Model validation for $SiO_2$/water nanofluids

The validation of this model was carried out for $SiO_2$/water based nanofluids flowing through the cold stream and water is used in hot stream in the shell side of shell and tube heat exchanger. The simulations of heat exchanger adopted in this model validation is shell and tube heat exchanger with a system of $SiO_2$/water based nanofluids flowing in the tube side of the heat exchanger with a volume concentration of 0.5% and particle diameter of 10-20 nm, while in the shell side of the heat exchanger was water. The volumetric flow rate was taken from 2-10L/min in both the streams (hot and cold) while the inlet temperature considered was 70 and 20$^{o}$C respectively. The simulation was performed under the same heat exchanger design specification as shown in Table 3.5. The properties of the operating fluids considered in this validation are found in Table 3.6.

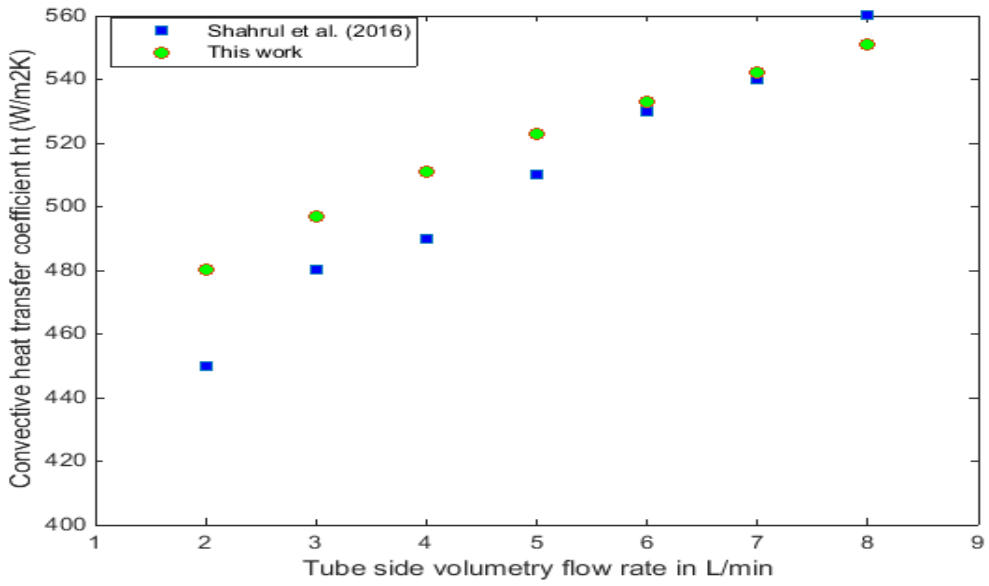


**Fig 4.8** Comparison of Reynolds number (Re) against mass flow rate with experimental values of Shahrul et al. (2016) on $SiO_2$/water based nanofluids with 0.5% vol. concentration and 10-20nm particle diameter.

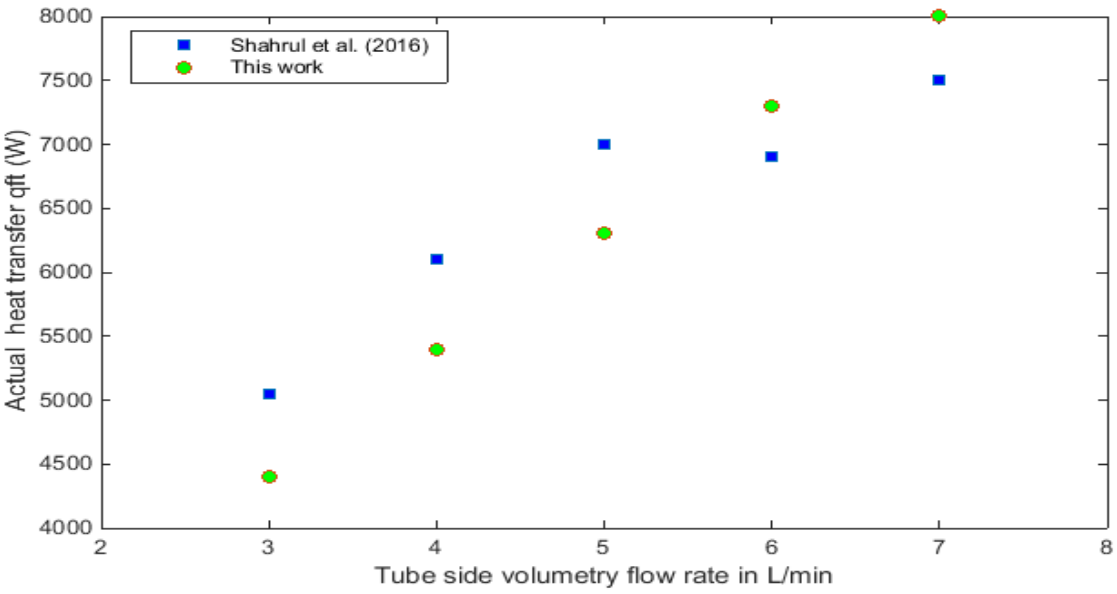

**Fig 4.9** Comparison of actual heat transfer ($h_t$) against mass flow rate with experimental values of Shahrul et al. (2016) on $SiO_2$/water based nanofluids with 0.5%vol. concentration and 10-20nm particle diameter.

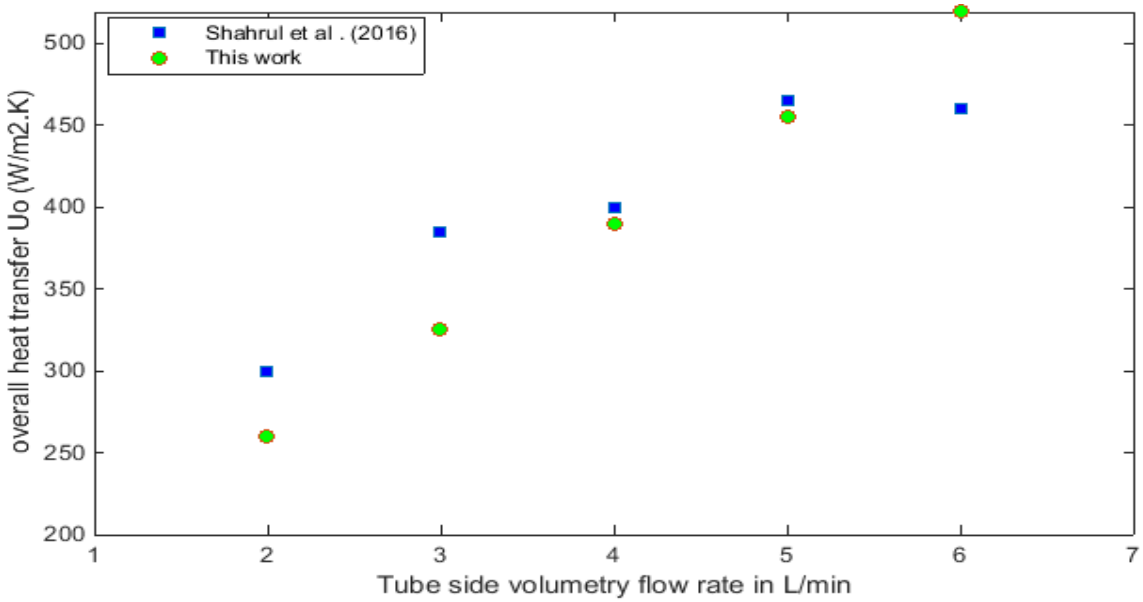


**Fig 4.1.0** Comparison overall heat transfer ($U_o$) against volumetric flow rate with experimental values of Shahrul et al. (2016) on $SiO_2$/water base nanofluids with 0.5%vol. concentration and 10-20nm particle diameter.

The volumetric flow rate in the tube side was varied from 2-8L/min at different outlet temperature in the tube side. The outlet temperature is varied due to the fact that as the volumetric flow rate varies (increases), more heat is being absorbed by the flowing material in the tube side (more heat is being transferred or consumed due to high movement of molecules) and this result in linear decrease of outlet temperature in the tube side of the shell and tube heat exchanger of this model. The volumetric flow rate on shell side was held constant at 4 L/min. From Fig 4.8, it can be seen that the actual rate of heat transfer is plotted against volumetric flow rate for the tube side of the heat exchanger. The illustrations depicted that the rate of heat transfer increase with increase in volumetric flow while the shell side volumetric flow rate of the heat exchanger is kept constant. This is due to the increase in the thermal conductivity of the nanofluids (coolant) flowing in the tube side of the exchanger. The overall heat transfers of $SiO_2$/water based nanofluids against volumetric flow rate is presented in Fig 4.9. It is clear that the overall heat transfer is a function of volumetric flow rate, this due to the fact that at a varying

volumetric flow rate, there is significant effect on the enhancement of overall heat transfer. The influence of the overall heat transfer occurs as a result of the positive impact and effect of Reynold and Prandtl number in the heat transfer system.

**Table 4.5** Illustration of the percentage error between this work and experimental data for convective heat transfer, actual heat transfer and overall heat transfer for $SiO_2$ /water based nanofluids respectively

| $h_t$ (W/m$^2$.K) | | | Q (W) | | | $U_o$ (W/m$^2$.K) | | |
|---|---|---|---|---|---|---|---|---|
| Shahrul et al. (2016) | This work | % Error | Shahrul et al. (2016) | This work | % Error | Shahrul et al. (2016) | This work | % Error |
| 450 | 480 | 4.9 | 5050 | 4200 | 12.9 | 300 | 260 | 13.13 |
| 480 | 497 | 4.15 | 6100 | 5400 | 11.5 | 385 | 325 | 15.6 |
| 490 | 511 | 3.4 | 7000 | 6300 | 10 | 400 | 390 | 2.5 |
| 510 | 523 | 1.9 | 6900 | 7300 | 5.8 | 465 | 455 | 2.2 |
| 530 | 533 | 2.5 | 7500 | 8000 | 6.6 | 460 | 519 | 12.5 |
| 540 | 542 | 4.3 | - | - | | - | - | - |
| Average (%) | | 2.9 | | | 9.36 | | | 9.2 |

Fig 4.1.0. Is an illustration of effect of flow rate flow rate on convective coefficient of heat transfer? It shows that the change of volumetric flow rate has a tremendous effect in changing the rate of convective heat transfer, while the concentration of the nanofluids is held constant at 0.5%vol. It is clear that the rate of heat transfer increases in regards with the increase of flow rate. However, the rate of heat transfer does not depend only on the flow rate, but it is also affected positively by the influence of the Reynold number and the thermal conductivity of the $SiO_2$/water based nanofluids.

Table 4.5, shows the error to be ranging approximately from 2.9%, 9.36% and 9.2% respectively. Hence, this further reveals the validity and suitability of this model. However, from the figures above, it shows that the variation trends of flow characteristics for the present model are in good agreement with the trends for rate of heat transfers, as well as the Reynold number in comparison with that of experimental data.

## 4.5 Summary

The present model has been validated with experimental data found in literature for water, $Al_2O_3$, CNT and $SiO_2$/water. The comparison was done on actual heat transfer, convective heat transfer, overall heat transfers and Reynold number. As demonstrated above, it is apparent in all figures that the present model is in excellent agreement with the experimental findings reported in the literature which offered confident for further research, noticing the validity of the model and couple with the fact that the error was also evaluated and found to be less than 10%.

Therefore, it is decided that the whole model approach is valid for further optimization on predicting the thermal and heat transfer performance of water, $Al_2O_3$, CNT and $SiO_2$/water based nanofluids.

# CHAPTER 5

# OPTIMAL DESIGN OF SHELL AND TUBE HEAT EXCHANGER (STHE)

The design and optimization in this research was done using automated Kern's method to find out the optimal design of shell and tube heat exchanger operated with nanofluids from an economic point of view. The main target of this work is to arrive at the minimum of the objective function which is the capital cost.

In order to estimate the suitability of the proposed methodology, two case studies were considered, which were previously analyzed by Kern (1950) and Sinnott et al. (2005) using GA, Petal ant Rao (2010) using PSO, Yang et al. (2014)-PSO, Turget et al. (2014), using I-ITHS, Hadidi and Nazari (2013) using BBO, Lahiri et al. (2014) using DEACO, Dillip Kumar (2016) using FFA and GSA, and Azad et al. (2016) using GA. However, from different combinations assessed in this study, the findings from this project as presented in the Tables below showed that the proposed model proved to be the best in terms of training effectiveness and efficiency as well as the generalization capabilities.

Case 1. Case study was taken from Kern (1950), where methanol and sea water were used in shell and tube side respectively, with the original designed heat exchanger with heat duty of 4.34MW. The original designed heat exchanger is a two tube pass and a single shell heat exchanger. The process parameters and the physical properties of both shell and tube side operating fluids are summarized in Table 3.0.

Case 2. The case study 2 was taken from Sinnott et al. (2005). In this case, distilled water and raw water were considered as heat exchanger operating fluids, with a heat duty of 0.46MW. The original design is a single shell pass and two tube pass heat exchanger. The physical properties are summarized in Table 3.0.

## 5.1 Analysis of optimal design stages

To evaluate the performance and efficiency of the proposed model, the design optimization was conducted in three different stages. In stage one, the same number of variables and the system of heat exchanger as proposed by Kern (1950) and Sinnott et al. (2005) were considered for case 1 and case 2 respectively. In stage two, more variables were included such as tube diameter, tube

length, number of tube pass, baffle cut, type of pitch, tube pitch, head type, ratio of baffle spacing to shell.

Diameter and tube wall thickness for optimizations (multivariable heat exchanger design) are considered for both cases. However, in stage three, the optimal design of heat exchanger system was considered to be operated with nanofluids flowing in the tube side. For case 1, the system was induced to be operated with nanofluids in the tube side of the heat exchanger while methanol was still on the shell side of the exchanger with same thermal duty of 4.34MW as proposed by Kern (1950). For case 2, the system was induced to be operated with $Al_2O_3$ -water nanofluids in the tube side of the heat while distilled water was still on the shell side of the exchanger with same thermal duty 0.64MW as proposed by Sinnott et al. (2005). The optimizations for this section were performed using $Al_2O_3$ / water nanofluids in the tube side of heat exchanger. The variables considered for optimization were nanofluids concentration, tube diameter, tube length, number of tube pass, baffle cut, type of pitch, tube pitch, head type, ratio of baffle spacing to shell diameter and tube wall thickness which can be found in Table 3.10. The physical properties of both operating fluids are summarized in Table 3.0 and 3.1 respectively. An important factor to be considered in this optimization by the proposed model is the number of multiple variables included and the introduction of nanofluids in the system which were important in order to establish and visualize the precision of this method. Relative knowledge with regard to the type of fluids and the dimension of shell and tube heat exchanger which are of critical importance in heat exchanger design have been proven by this project and the various result obtained were evaluated for ease of understanding. Nonetheless, another significant importance of this project is that, this research was conducted in compliance with TEMA standard, where all the geometric and operating constraints such as pressure drop and velocity are all considered and monitored. Hence, the heat exchanger design dimensions accounted for in this work such as tube diameter, tube length, baffle cut, head type, ratio of baffle spacing, tube lay out, baffle spacing and so on were all obtained from literature in accordance with TEMA standard. Thus, this platform was considered due to its simplicity and economic benefits.

**Table 5.0:** Key criteria of TEMA standard used in this work: Reference from Lahiri et al. (2015) and Yang et al. (2014)

| Parameters | Tube side | Shell side |
|---|---|---|
| Velocity | 1.0 <= 2.00m/s | 0.4 <=1.0m/s |
| Pressure drop | <= 35KPa | <=35KPa |
| Ratio of tube length to shell diameter | $3 \leq \frac{tube\ length}{shell\ diameter} \leq 5$m | - |
| Ratio of baffle spacing to shell diameter | $0.050 \leq \frac{L_{bs}}{D_s} \leq B \leq 0.5^{\max} L_{bs}/D_s$ | - |

The criterial for the heat exchanger dimension in compliance with TEMA standard have been signified in Table 3.10.

**Table 5.1: Comparison on optimal geometry and thermal performance parameters for case1**

| Parameters | Literature (Kern, 1950) | Caputo et al. (2008) | Patel et al. (2010) PSO | Hadidi et al. (2013)-BBO | Turgut et al. (2014) I-ITHS | Lahiri et al. (2014)DEACO | Present Approach with three variables | Approach with seven variables |
|---|---|---|---|---|---|---|---|---|
| Type of pitch | Triangular | Triangular | - | - | - | Triangular | Triangular | Triangular |
| No of tube pass | 2 | - | - | 2 | 2 | 2 | 2 | 1 |
| Type of head | Ring floating head | - | - | - | - | Ring floating head | Ring floating head | pull through floating head |
| Ds (m) | 0.894 | 0.83 | 0.81 | 0.801 | 0.7635 | 0.74 | 0.7946 | 0.6282 |
| L (m) | 4.83 | 3.379 | 3.115 | 2.04 | 2.0391 | 2.438 | 1.2192 | 1.8288 |
| Rb | 0.4 | 0.6 | 0.52 | 0.62 | 0.65 | 0.8 | 0.80 | 1 |
| B (m) | 0.356 | 0.5 | 0.424 | 0.5 | 0.4955 | 0.592 | 0.6357 | 0.6282 |
| Baffle cut (%) | 25 | 25 | - | - | - | 45 | 25 | 15 |
| do (m) | 0.02 | 0.016 | 0.015 | 0.01 | 0.01 | 0.009525 | 0.00635 | 0.00635 |
| Pt (m) | 0.025 | 0.02 | 0.0187 | 0.0125 | 0.0125 | - | 0.0079 | 0.0079 |
| Cl (m) | 0.005 | 0.004 | 0.0037 | 0.0025 | 0.0025 | - | 0.0647 | 0.0910 |
| Nt | 918 | 1567 | 1658 | 3587 | 3558 | 3031 | 8785 | 4287 |
| vt (m/s) | 0.75 | 0.69 | 0.67 | 0.77 | 0.7744 | 1 | 0.7778 | 0.7970 |
| Ret | 14925 | 10936 | 10503 | 7642.49 | 7701.29 | - | 4915 | 5035 |
| Prt | 5.7 | 5.7 | 5.7 | 5.7 | 5.7 | - | 5.6949 | 5.6949 |
| ht (W/m2/K) | 3812 | 3762 | 3721 | 4314 | 4388.79 | 5428.64 | 5562 | 5669 |
| Ft | 0.028 | 0.031 | 0.0311 | 0.034 | 0.03555 | | 0.0388 | 0.0385 |
| deltaPt (Pa) | 6251 | 4298 | 4171 | 6156 | 6887.63 | 12690.22 | 7107 | 5167 |
| Sa (m2) | 0.032 | 0.0831 | 0.0687 | 0.0801 | 0.07567 | - | 0.1010 | 0.0789 |
| De (m) | 0.014 | 0.011 | 0.0107 | 0.007 | 0.00711 | - | 0.0045 | 0.0045 |
| vs (m/s) | 0.58 | 0.44 | 0.53 | 0.46 | 0.48979 | 0.42 | 0.3669 | 0.4696 |
| Res | 18.381 | 11075 | 12678 | 7254 | 7684.054 | - | 3654 | 4676 |
| Prs | 5.1 | 5.1 | 5.1 | 5.1 | 5.08215 | - | 5.0821 | 5.0821 |
| hs (W/m2/K) | 1573 | 1740 | 1950.8 | 2197 | 2230.913 | 2137.09 | 2471 | 3333 |
| Fs | 0.33 | 0.357 | 0.349 | 0.379 | 0.37621 | - | 0.4207 | 0.4054 |
| deltaPs (Pa) | 35789 | 13267 | 20551 | 13799 | 14953.91 | 11708.97 | 7169 | 13582 |
| U (W/m2/K) | 615 | 660 | 713.9 | 755 | 761.578 | 782.36 | 812.82 | 901.9 |
| S (m2) | 278.6 | 262.8 | 243.2 | 229.95 | 228.03 | 221.07 | 213.658 | 156.34 |
| Cinv (Euro) | 51507 | 49259 | 46453 | 44536 | 44259.01 | 43250.34 | 42173 | 33727 |
| Co (Euro/year) | 2111 | 947 | 1038.7 | 984 | 962.4858 | - | 909 | 1034 |
| Cod (Euro) | 12973 | 5818 | 6778.2 | 6046 | 5914.058 | 9679.63 | 5588 | 6350 |
| Ctot (Euro) | 64480 | 55077 | 53231 | 50582 | 50173 | 52929.97 | 47761 | 40077 |

The simulation codes were run for several times, this was done to evaluate the effectiveness and efficiency of the present method and also to ensure that the termination criteria for the program were accurate besides to set in relation to the design constraints. Pressure drop and velocity were the operating constraints considered in this study and the overall optimization was done in compliance with TEMA standard.

**Table 5.2 Comparison on optimal geometry and thermal performance parameters for case 2**

| Parameters | Literature (Sinnott et al. 2005) | Caputo et al. (2008) –GA | Yang et al. (2014)- GA | Present approach with three variables | Approach with seven variables |
|---|---|---|---|---|---|
| Type of pitch | Triangular | Triangular | Triangular | Triangular | Triangular |
| No of tube pass | 2 | - | - | 2 | 1 |
| Type of head | Ring floating head | Ring floating head | - | Ring floating head | Pull through floating head |
| Ds (m) | 0.387 | 0.62 | 0.5368 | 0.6771 | 0.5252 |
| L (m) | 4.88 | 1.548 | 2.438 | 1.2192 | 1.8288 |
| Rb | 0.79 | 0.71 | - | 0.75 | 1 |
| B (m) | 0.305 | 0.44 | 0.58 | 0.5078 | 0.5252 |
| Baffle cut (%) | 25 | 25 | - | 25 | 15 |
| do (m) | 0.019 | 0.016 | 0.01588 | 0.0127 | 0.009525 |
| Pt (m) | 0.023 | 0.02 | 0.01985 | 0.0159 | 0.0119 |
| Cl (m) | 0.004 | 0.004 | 0.00397 | 0.0615 | 0.0900 |
| Nt | 160 | 803 | 590 | 1306 | 989.75 |
| vt (m/s) | 1.76 | 0.68 | 0.9651 | 0.6675 | 0.7831 |
| Ret | 36400 | 9487 | 13181 | 7364 | 6479.5 |
| Prt | 6.2 | 6.2 | 6.2 | 6.2026 | 6.2026 |
| ht (W/m2/K) | 6558 | 6043 | 4852 | 4699 | 5463.5 |
| Ft | 0.023 | 0.031 | 0.006899 | 0.0343 | 0.0356 |
| deltaPt (Pa) | 62812 | 3673 | 7303 | 2945 | 3386 |
| Sa (m2) | 0.0236 | 0.0541 | 0.06227 | 0.0688 | 0.05516 |
| De (m) | 0.013 | 0.015 | 0.01128 | 0.0090 | 0.0094 |
| vs (m/s) | 0.94 | 0.41 | 0.3562 | 0.3225 | 0.4021 |
| Res | 16200 | 8039 | 4995 | 3621 | 4714 |
| Prs | 5.4 | 5.4 | 5.4 | 5.3935 | 5.3935 |
| hs (W/m2/K) | 5735 | 3476 | 3755 | 4906.27 | 5228 |
| Fs | 0.337 | 0.374 | 0.4014 | 0.4212 | 0.4049 |
| deltaPs (Pa) | 67684 | 4365 | 5071 | 3925 | 6321 |
| U (W/m2/K) | 1471 | 1121 | 966.6 | 1096 | 1214.3 |
| S (m2) | 46.6 | 62.5 | 71.71 | 63.546 | 54.1634 |
| Cinv (Euro) | 16549 | 19163 | 20653 | 19336 | 17802 |
| Co (Euro/year) | 4466 | 272 | 444.7 | 229.41 | 312 |
| Cod (Euro) | 27440 | 1671 | 2733 | 1409.61 | 1916 |
| Ctot (Euro) | 43989 | 20834 | 23386 | 20745 | 19718 |

## 5.2 Analysis of optimal design using conventional fluids

Table 5.1 presents the results of present work together with those obtained from literature, with the total cost of the heat exchanger from the present work reduced to about 25.93%, 13.3%, 10.28%, 5%, 4.81%, and 9.77% compared to the original design by Kern (1950) and other methods using GA, PSO, BBO, I-ITHS, and DEACO respectively. The reduction in total cost further increased to 37.85%, 27.23%, 24.71%, 20.77%, 20.12% and 24.28% as compared to the original design by Kern (1950) and other methods GA, PSO, BBO, I-ITHS, and DEACO respectively when more variables were induced (multivariable optimizations). Therefore, it is apparent that the multi variables design optimization is more suitable and significant in estimating the overall cost.

However, the diameter of shell for the design with lesser variables was found to be smaller by approximately 0.81% as compared to GA, PSO, BBO, I-ITHS method. Consequently, for the optimal design with multiple variables, the shell diameter was found to be approximately 11% smaller than that of the original design and also the other methods found in the literature as shown in Table 5.1. The tube length was lowered by 74% as compared to the original design and approximately 67% as compared GA, PSO, BBO, I-ITHS, and DEACO. Meanwhile, for the multivariable design, the tube length is found to be 62% lower than original design and approximately 41.29% as compared to other method found in literature.

However, several works have been previously conducted on the optimal design of shell and tube heat exchanger, where researchers considered different objective functions. Some of them considered the overall cost of the required heat transfer area and energy needed to overcome friction has induced pumping power some investment cost (Mott, Brock, and Pearson 1972) as the objective function.

Beside these cases, various variables have been considered as a degree of freedom in the optimization process by numerous research authors. Some studies used parameters such as baffle spacing (Saffar-Avval and Damangir 1995) as optimal design variable while others used different systems of heat exchanger design as considered by the present work. Thus, the method used to find the optimal points are different in various studies conducted. For example, numerical methods of optimization are useful in finding the optimum solutions of continuous and differentiable functions (Rao and Rao 2009; Koupaei, Hosseini, and Ghaini 2016). These

methods are analytical and make use of techniques of differential calculus in finding the optimal point. But, since some of the practical problems involve objective functions that are not continuous, the numerical optimal design technique has limited background in practical applications (Rao and Rao 2009). The proposed model of the present work is applicable for both continuous and discrete problems effectively.

Table 5.2 shows the results of optimization that cover stage one and stage two respectively for Case 2. It can be observed that there is a slight increase in the number of tubes as compared to the original design and the findings from other methods which are adopted from literature. On the other hand, the tube length of the optimization for the first stage was found to be reduced to 75%, 21.24%, and 49% as compared to original design according to Sinnott et al. (2005), GA and PSO respectively. However, by including more variables while considering multivariable designed heat exchanger, the tube length was found to be further lowered by 62.52%, 15%, and 24.99% as compared to the original design and other methods from literature. The optimization results from first and second stage (multi variables design) of the proposed model are tabulated in Table 5.2. It can be observed that the outer tube diameter is found to be smaller by 33.12%, 20.62%, 20.03% and when more variables were induced (multi variables design) the diameter was further lowered by 49.89%, 46%, and 45.01% in regard to the original design, GA and PSO respectively.

Taking into account both the tube length and shell diameter, it is apparent that the specification of designed heat exchanger with present methodology is much lower than that of the original design. Observing the outcome presented by the present developed method, it can be seen that for the first two stages involved in the optimizations, the tube length is smaller as compared to the methods adopted from the literature. On the other hand, the total number of tubes as compared to the original design becomes higher.

Apparently, due to decrease in heat exchanger tube length and the surface area, for the optimizations involving stage one and two, it is observed that the reduction of total capital cost, being the function of capital investment and the surface area of heat exchanger is achieved by 52.84%, 0.43% and 11.29% for stage one as compared to the original design and PSO. On the other hand, with more variables included (multivariable designed heat exchanger), the reduction of cost was further improved to 55.18%, 5.36% and 15.68% as compared to original, GA and

PSO respectively. The proposed model has been proven to be consistent with other design methods in the literature, meanwhile the results outshined all other methods when compared. It can therefore be concluded that the present methodology is more effective and efficient for further applications.

### 5.3 Analysis of optimal design using $Al_2O_3$/ water base nanofluids

The proposed model (Kern's automated method) was applied to the two case studies and the outcome was compared with other design optimization methods to test the effectiveness and suitability of the present methodology. In these case studies, the optimal design of heat exchanger system was considered to be operated with $Al_2O_3$/water base nanofluids in the tube side of the heat exchanger while methanol was still on the shell side of the exchanger with same thermal duty of 4.34MW as proposed by Kern (1950). For Case 2, the system was included to be operated with nanofluids in the tube side of the heat while distilled water was still on the shell side of the exchanger with the same thermal duty of 0.64MW as proposed by Sinnott et al. (2005).

However, since the purpose of this study is to investigate the effects of nanofluids in the reduction of the overall cost of the heat exchanger, the overall cost including investment and operational cost of the heat exchanger is minimized by Kern's automated method (proposed model). The present model also observed that to determine the optimal geometry of heat exchanger, the optimal conditions should be put into consideration among the increased heat transfer coefficient and reduced pumping power. If the thermal duty of a heat exchanger is a predefined value, then the required surface area for heat transfer will be reduced with increasing the heat transfer coefficient, as a result, the manufacturing cost is reduced. However, the pressure drop can impose additional cost for pumping power, in other words, the annual operating cost will be increased, as such the overall cost increased.

Many studies have been performed to gain a better understanding of the performance of nanofluids in the heat transfer system. However, the problem of this design system was originally formulated to quantify the significance of nanofluids in the optimal design of shell and tube heat exchanger. The objective function, which is to minimize the annual total cost, the design variables, operating constraints and the results obtained are all presented in this work. Meanwhile, to evaluate the efficiency and the outstanding performance of the present model, the

results were compared with the literature findings. It is interesting that the present model provided an outstandingly better result compared to others. Table 5.3 presents the results obtained from nanofluids operated heat exchanger for Case 1. Thus, with the same criteria as in the previous design with multivariable, even in these cases, the nanofluids volume concentration was well optimized ranging from 0.01-0.06 vol.%, as shown in Table 3.10. This range is considered as the experimental analysis was conducted by Vajjha and Das (2012) and Ray and Das (2014) up to this range of concentration. It is proven that the lower volume concentration of nanofluids happens to be more promising and significant in offering high heat transfer value in the system. Experimental analysis conducted by Anoop et al. (2013) and Azmi et al. (2017) suggested the same phenomenon as stated above. This offers the motivation and driving force in considering this range of nanofluids volume fraction for this optimization process. However, all the results obtained from this work have proven to be in good agreement with the experimental suggestion and also found to be more competent and efficient as compared to other methods of design in the literature. The optimum volume concentration was found to be 0.023 vol.% and 0.043 vol.% for both the two case studies 1 and 2, while the diameter of the nanoparticle was held constant at the range of 13nm as adopted from the references above. Meanwhile, the difference in optimum concentration could be due to the properties of the base fluids used, and perhaps the heat exchanger specification (heat duty, correction factor and others) and this can actually have effect on the operating criteria of the entire system. The operating conditions and physical properties are presented in Table 3.1 for this design. Based on table 5.3, the proposed methodology proves to be effective and significant in the optimization process based on the result obtained.

The results depicted that the total cost of the design heat exchanger operated with nanofluids is reduced by 40.97% as compared to the original design by Kern (1950). Similarly, the cost reduction was further achieved by 30.38%, 28.5%, 24.75%, 28.09, 16.86% and 24% as compared to literature findings using GA, PSO, BBO, DEACO, FFA and GSA methods respectively.

However, considering the increase in tube side coefficient of heat transfer (nanofluids stream), as the overall heat transfer coefficient becomes higher, the overall heat exchanger area is reduced. The capital investment cost is computed as a function of overall heat transfer area. Corresponding to lower tube length by the present design and high value of overall coefficient of

heat transfer achieved, the capital investment cost is reduced as a result of minimum heat exchanger area. The nanofluids operated heat exchanger area was minimized to 44%, 40.73%, 35.95%, 32.26%, 29.54%, 23% and 24.25%, as compared to the original design, and other optimization methods using GA, PSO, BBO, DEACO, FFA and GSA.

Owing to that, the reduction of capital investment being the function of heat exchanger surface area was also achieved by 34.70% 31.72%, 27.60%, 24.48%, 22.2%, 14% and 25.98% as compared to the original design and other optimization methods obtained from literature (GA, PSO, BBO, DEACO, FFA and GSA). The evaluation of the present model result showcased the superiority in terms of better values obtained, which is proven and supported by some theoretical contributions and experimental studies that have been conducted in this aspect on the thermal performance of nanofluids in the heat transfer system. This study is of paramount importance to the existing knowledge and in the future especially in the field of nanotechnology and for industrial applications. The heat exchanger, most specifically shell and tube heat exchanger, plays an important role in industrial process to recover heat between two process fluids. They are widely used because of their simple manufacturing and their adaptability to different conditions. However, the numbers of industries nowadays are in search of effective yet less time consuming alternatives in designing the shell and tube heat exchangers. As per literature and industrial survey, it is observed that there is a need of effective design options for shell and tube heat exchanger now and in the future. Thus, this means that the present work is of significance and predominant for the present situation.

**Table 5.3 Comparison on optimal geometry and thermal performance parameters for case1 with $Al_2O_3$ / water nanofluids**

| Parameters | Literature (Kern,1950) | Caputo et al. (2008) | Patel et al. (2010) PSO | Hadidi et al. (2013)-BBO | Lahiri et al. (2014)DEACO | Mohanty Dillip (2016) –FFA | Mohanty Dillip (2016) GSA | Design with Nanofluids (eight variables) |
|---|---|---|---|---|---|---|---|---|
| Type of pitch | Triangular | Triangular | - | - | Triangular | - | - | Triangular |
| No of tube pass | 2 | - | - | 2 | 2 | - | - | 1 |
| Type of head | Floating head | - | - | - | Floating head | - | - | Pull through floating head |
| Ds (m) | 0.894 | 0.83 | 0.81 | 0.801 | 0.74 | 0.858 | 0.842 | 0.6272 |
| L (m) | 4.83 | 3.379 | 3.115 | 2.04 | 2.438 | 2.416 | 2.783 | 1.8288 |
| Rb | 0.4 | 0.6 | 0.52 | 0.62 | 0.8 | - | - | 1 |
| B (m) | 0.356 | 0.5 | 0.424 | 0.5 | 0.592 | 0.402 | 0.486 | 0.6272 |
| Baffle cut (%) | 25 | 25 | - | - | 45 | - | - | 15 |
| do (m) | 0.02 | 0.016 | 0.015 | 0.01 | 0.009525 | 0.01575 | 0.015 | 0.00635 |
| Pt (m) | 0.025 | 0.02 | 0.0187 | 0.0125 | - | 0.01968 | 0.0187 | 0.00794 |
| Cl (m) | 0.005 | 0.004 | 0.0037 | 0.0025 | - | - | - | 0.9010 |
| Nt | 918 | 1567 | 1658 | 3587 | 3031 | 1692 | 1806 | 4269.6 |
| vt (m/s) | 0.75 | 0.69 | 0.67 | 0.77 | 1 | 0.656 | 0.678 | 0.7531 |
| Ret | 14925 | 10936 | 10503 | 7642.49 | - | 10286 | 10118 | 2317 |
| Prt | 5.7 | 5.7 | 5.7 | 5.7 | - | 5.7 | 5.7 | 10.8998 |
| ht (W/m2/K) | 3812 | 3762 | 3721 | 4314 | 5428.64 | 6228 | 4029 | 4229 |
| Ft | 0.028 | 0.031 | 0.0311 | 0.034 | - | 0.0311 | 0.031 | 0.00644 |
| deltaPt (Pa) | 6251 | 4298 | 4171 | 6156 | 12690.22 | 4246 | 4501 | 1445 |
| Sa (m2) | 0.032 | 0.0831 | 0.0687 | 0.0801 | - | - | - | 0.0787 |
| De (m) | 0.014 | 0.011 | 0.0107 | 0.007 | - | 0.0105 | 0.0107 | 0.0045 |
| vs (m/s) | 0.58 | 0.44 | 0.53 | 0.46 | 0.42 | 0.54 | 0.453 | 0.47115 |
| Res | 18381 | 11075 | 12678 | 7254 | - | 12625 | 10662 | 4692 |
| Prs | 5.1 | 5.1 | 5.1 | 5.1 | - | 5.1 | 5.1 | 5.1 |
| hs (W/m2/K) | 1573 | 1740 | 1950.8 | 2197 | 2137.09 | 1991 | 2060 | 3353 |
| Fs | 0.33 | 0.357 | 0.349 | 0.379 | - | 0.349 | 0.538 | 0.4052 |
| deltaPs (Pa) | 35789 | 13267 | 20551 | 13799 | 11708.97 | 18788 | 12458 | 13664 |
| U (W/m2/K) | 615 | 660 | 713.9 | 755 | 782.36 | 876.4 | 732.6 | 847.57 |
| S (m2) | 278.6 | 262.8 | 243.2 | 229.95 | 221.07 | 202.3 | 236.9 | 155.77 |
| Cinv (Euro) | 51507 | 49259 | 46453 | 44536 | 43250.34 | 39336 | 45439 | 33632 |
| Co (Euro/year) | 2111 | 947 | 1038.7 | 984 | - | 1040 | 4673 | 720.75 |
| Cod (Euro) | 12973 | 5818 | 6778.2 | 6046 | 9679.63 | 6446 | 4673 | 4429 |
| Ctot (Euro) | 64480 | 55077 | 53231 | 50582 | 52929.97 | 45782 | 50112 | 38061 |
| Conc (vol. fraction) | | | | | | | | 0.023 |
| Diameter(nm) | | | | | | | | 13 |

**Table 5.4 Comparison of optimal geometry and thermal performance parameters for case 2 with $Al_2O_3$ / water nanofluids**

| Parameters | Literature (Sinnot et al. (2005) | Caputo et al. (2008)-GA | Yang et al. (2014)-GA | Azad et al. (2016) -GA | Design with Nanofluids (eight variables ) |
|---|---|---|---|---|---|
| Type of pitch | Triangular | Triangular | Triangular | - | Square |
| No of tube pass | 2 | - | - | - | 2 |
| Type of head | Floating head | Floating head | - | - | Pull through floating head |
| Ds (m) | 0.387 | 0.62 | 0.5368 | 0.7158 | 0.6139 |
| L (m) | 4.88 | 1.548 | 2.438 | 1.21 | 1.2129 |
| Rb | 0.79 | 0.71 | - | - | 0.8 |
| B (m) | 0.305 | 0.44 | 0.58 | 0.4765 | 0.4911 |
| Baffle cut (%) | 25 | 25 | - | - | 15 |
| do (m) | 0.019 | 0.016 | 0.01588 | 0.0123 | 0.009525 |
| Pt (m) | 0.023 | 0.02 | 0.01985 | 0.0204 | 0.01191 |
| Cl (m) | 0.004 | 0.004 | 0.00397 | 0.0041 | 0.09090 |
| Nt | 160 | 803 | 590 | 909 | 1509 |
| vt (m/s) | 1.76 | 0.68 | 0.9651 | 0.6562 | 0.9204 |
| Ret | 36400 | 9487 | 13181 | 8754.1 | 2317 |
| Prt | 6.2 | 6.2 | 6.2 | 6.2323 | 17.9 |
| ht (W/m2/K) | 6558 | 6043 | 4852 | 4349.3 | 4013 |
| Ft | 0.023 | 0.031 | 0.006899 | - | 0.00644 |
| deltaPt (Pa) | 62812 | 3673 | 7303 | 2766 | 3335 |
| Sa (m2) | 0.0236 | 0.0541 | 0.06227 | - | 0.0601 |
| De (m) | 0.013 | 0.015 | 0.01128 | 0.0118 | 0.0094 |
| vs (m/s) | 0.94 | 0.41 | 0.3562 | 0.3253 | 0.3679 |
| Res | 16200 | 8039 | 4995 | 4640.7 | 4312 |
| Prs | 5.4 | 5.4 | 5.4 | 5.5548 | 5.3935 |
| hs (W/m2/K) | 5735 | 3476 | 3755 | 3510.6 | 5124 |
| Fs | 0.337 | 0.374 | 0.4014 | - | 0.4104 |
| deltaPs (Pa) | 67684 | 4365 | 5071 | 3299.7 | 4467 |
| U (W/m2/K) | 1471 | 1121 | 966.6 | 1169.9 | 1117 |
| S (m2) | 46.6 | 62.5 | 71.71 | 56.2734 | 55 |
| Cinv (Euro) | 16549 | 19163 | 20653 | - | 17947 |
| Co (Euro/year) | 4466 | 272 | 444.7 | - | 246 |
| Cod (Euro) | 27440 | 1671 | 2733 | - | 1509 |
| Ctot (Euro) | 43989 | 20834 | 23386 | 19708.9 | 19456 |
| Conc (vol. fraction) | | | | | 0.043 |
| Diameter(nm) | | | | | 13 |

The result for the nanofluids operated heat exchanger is shown in Table 5.4 for Case 2. It can be noticed that the shell diameter of the present design is smaller as compared to GA and PSO methods but became slightly higher than the original design. The tube length is reduced by 75%, 21.24% 49% as compared to the original design, GA and PSO methods. Hence, it can also be observed that the tube length of the present design is same as that of Azad et al. (2016). It is interesting to note that the total number of tubes from this method becomes higher as compared to the original design by Sinnott et al. (2005) and other methods found in literature. Corresponding to the overall heat transfer coefficient, the heat transfer coefficient in both the tube side and the shell side of the heat exchanger was found to be increased by 26.72%, and 32.16% for the shell side as compared to the design conducted by Yang et al. (2014) and Caputo et al. (2008), as a result of that, the value of overall heat transfer was increased to about 13.46%. This could be hypothesized that the change and increase in overall coefficient of heat transfer for the nanofluids as compared to the other methods would be the result of an increase in thermal property that leads to the increase in convective heat transfer at the heat exchanger. Nevertheless, the pressure drop of any successful design in the field of heat transfer is a parameter that plays a major role in estimating the total annual operating cost, eventually the total capital cost. Due to this, pressure drop is another significant factor that should be considered and monitored while applying nanofluids in heat exchanger. By applying the present model and using nanofluids as operating fluids, the optimum value of pressure drop obtained from this designed heat exchanger is lower compared to the other methods. Thus, this could be as a result of smaller number of tube pass and lower value of the friction factor obtained. On the other hand, the shell side pressure drop was found to be increased by 2.28% and 26.55% as compared to GA's methods. Whereas for the design conducted using PSO method the pressure drop on the shell side of the heat exchanger becomes higher than the present work with about 11%. However, for the tube side of the exchanger, a significant lower pressure drop is achieved through the present work in the tube side of heat exchanger but as compared to literature findings, it becomes higher than the design conducted using PSO method with about 17%. Although the increase in flow velocity of the convective fluids influenced the rate of heat transfer, it resulted in higher pressure drop of the heat exchanger fluid which required extra pumping cost of pump. As such, pressure drop was considered in this work as an operating constraint. It was also observed from this model that the convective heat transfer coefficient depends on the nature of the heat exchanger fluids flow other

than the thermal properties. However, looking at the Table 5.4 it is noticed that the Reynold number of the present work found to be slightly lower than the literature findings while as for Prandtl number it was found to be in good agreement with other methods. In view of the present results, it is envisaged that the optimization of heat exchanger cost should also be computed by acting on pressure drops, through the proper choice of fluids velocity, rather than on the surface area. While a minimization of surface area in general does not represent a cost-effective strategy, other parameters play important roles in the optimal design which need to be considered as well.

**Table 5.5 Percentage of reduction in the total cost compared to the ones from original design and other design methods**

| **Other methods of design** | **Case 1 (%)** | **Case 2 (%)** |
|---|---|---|
| Original design | 41 | 56 |
| Genetic algorithm (GA) | 30 | 7 |
| Particle swarm optimization (PSO) | 29 | 17 |
| Biogeography-based algorithm (BBO) | 25 | - |
| Deferential evolutionary ant-colony search algorithm (DEACO) | 28 | - |
| Firefly algorithm (FFA) | 17 | - |
| Gravitational search algorithm (GSA) | 24 | - |

On the other hand, the capital investment cost is computed as a function of overall heat transfer area. The heat transfer area is a function of heat transfer's coefficient; in other words, the area of an exchanger is minimized at the expense of higher heat transfer value. Presumably, the high thermal property of nanofluids used to create this platform provides the advantage of achieving a maximum value of heat transfer coefficients and this offers a minimized nanofluids designed heat exchanger area. Due to this, the capital investment is reduced by 13%, and 6.35% as compared to the result obtained from Yang et al. (2014) and Caputo et al. (2008). On other hand, the annual operating cost and hence the total discounted operating cost depends on both shell and

tube side pressure drops. Owing to the pressure drop value obtained in both tube and shell side of the heat exchanger by present work, the total discounted cost and the annual operating cost were found to be lowered as compared to other methods' outcomes as described in Table 5.4. However, when it comes to optimal design of heat exchanger for any given task, various parameters have to be put into consideration including satisfying a required heat transfer while keeping a desired objective function minimum. Changing of nanofluids volume concentration can affect all the thermo-physical properties of the fluids which could also cover some heat exchanger parameters, such as pressure drop, convective coefficient of nanofluids and eventually the overall total cost.

Nevertheless, taking into account both annual operating cost, total discounted and capital investment cost (objective function), it is observed in Table 5.4 that the total capital cost of a nanofluids designed heat exchanger is reduced by 55.77%, 6.6%, 16.80% and 1.28% as compared to the original design, GA and PSO methods with the aid of present proposed methodology. Thus, this is achieved as a result of tremendous heat transfer capacity and most importantly, a reduced surface area through a designed shell and tube heat exchanger operated with nanofluids. Numerous studies have been successfully carried out to show the superior performance of nanofluids in heat transfer and to characterize this relatively technology (Leong et al. 2012). There have been few reported studies on optimum design of nanofluids-run system based on experiment. Hence, many studies on nanofluids have been reported to be focused on the thermal performance (Garg et al. 2008). In recent decades, more attention has been directed to the study of nanotechnology, which reveals a future dream to become predominant in heat transfer system. Therefore, the efficiency and effectiveness of the present design will be of significant importance in this area of studies. The result obtained from this work further explains and presents evidence that automated Kern's method to optimize the overall structure of heat exchanger has great engineering value and can also contribute in solving complex optimization problems in the limited time in which this is an indispensable issue in the heat transfer field of engineering optimization. Basically the overall design system is applicable for cooling.

Furthermore, in all the examined cases presented by the proposed model, the total cost was drastically cut off and significant percent of annual total cost reduction were obtained. Hence, this proved and confirmed the effectiveness and the efficiency of the proposed approach.

## **5.4** Summary

This chapter concludes that the present model has shown a great improvement in terms of cost reduction, and most probably the nanofluids designed heat exchanger, as its outcomes outshine every other method as compared to the literature findings. Finally, it is noticed that the multi-variable designed heat exchanger was more effective and significant compared to designs with less variables.

# CHAPTER 6

## SENSITIVITY ANALYSIS

This section analyses the influence of design parameters on the objective function. In order to investigate the capability of automated Kern's method, computational studies are performed in this project by parametrically changing mass flow rate and nanofluids concentrations with respect to pressure drop, heat transfer and total cost.

However, the incorporation of nanoparticles in the base fluids leads to change in thermal properties such as thermal conductivity which affects the convective heat transfer. Many experimental works as well as theoretical contributions have been performed to investigate the change in thermal conductivity of nanofluids. Some of their report showed that the thermal conductivity of nanofluids is higher as compared to conventional fluids (Yousefi et al. 2017) . Nanofluids concentration is one of the most important factors that virtually affects the design structure of the heat exchanger as observed in the present work. Experimental analysis on how nanofluids concentration can affect the rate of heat transfer has been reported by Abdolbaqi et al. (2017) and their findings are in good agreement with the sensitivity analysis conducted using automated Kern's method.

This result is further elaborated in the sub-sections of this chapter. For this purpose, each input parameter is varied, keeping the others constant. Sensitivity of the varying parameters is monitored against the output parameters and this is then discussed with respect to the changes that take place. Meanwhile, for these researches that consider the operating fluids conditions (thermo physical properties) in the tube side of the exchanger, the effects of some optimized parameters and the flow rate of some operating constraints such as pressure drop, heat transfer which lead to the objective function have been investigated in this section, whereas the conditions on the shell side of the heat exchanger are considered fixed. The effect of nanofluids volume fraction on the heat transfer system is proven by the present model and supported by experimental and theoretical findings in the literature. This work therefore serves as an additional contribution through the successful sensitivity analysis conducted in this section whereby the design of nanofluids operated heat exchanger is more significant as compared to conventional fluids operating heat exchanger. This offers an interesting insight to challenges involved in optimized design of nanofluids based thermal system.

### 6.1 Effect of mass flow rate on actual rate of heat transfer

In this section, the study of mass flow rate on heat transfer system was performed on both the case studies as shown in Fig 6.1 (a) and (b). To detect that, the mass flow rate of the designed exchanger was varied from 68.90-76.90kg/s in tube side of the exchanger, while that of shell side was held constant at 35.31kg/s; for case study two, the mass flow rate was varied from 35.31-43.31kg/s, in the tube side of heat exchanger keeping shell side mass flow rate at a constant value of 22.07 kg/s. The rate heat transfer is proportional (function) to the mass flow rate of the nanofluids and its specific heat capacity. It can be observed that at constant volume fraction and particle diameter, the rate of heat transfer increases as the mass flow rate increases. This is due to an increase of tube side's temperature and that of the outlet of the shell side decreased because at constant volume concentration of the nanofluids, the increase in mass flow rate of the nanofluids increased thermal conductivity and the cold fluids (nanofluids) absorbed more heat from the shell side of the heat exchanger. An experimental work conducted by Hosseini et al. (2016) also attested to that. On the other hand, it influenced the heat transfer rate from the hot fluids and led drastic drop of the shell side outlet temperature. However, for both case studies, it is noticed that the heat transfer increased by approximately 2.9% and 5% with an increase of 2kg/s of the flow rate respectively. The present model results proved to be efficient and in excellent agreement with numerous experimental work and some theoretical knowledge contributed in this field of studies.

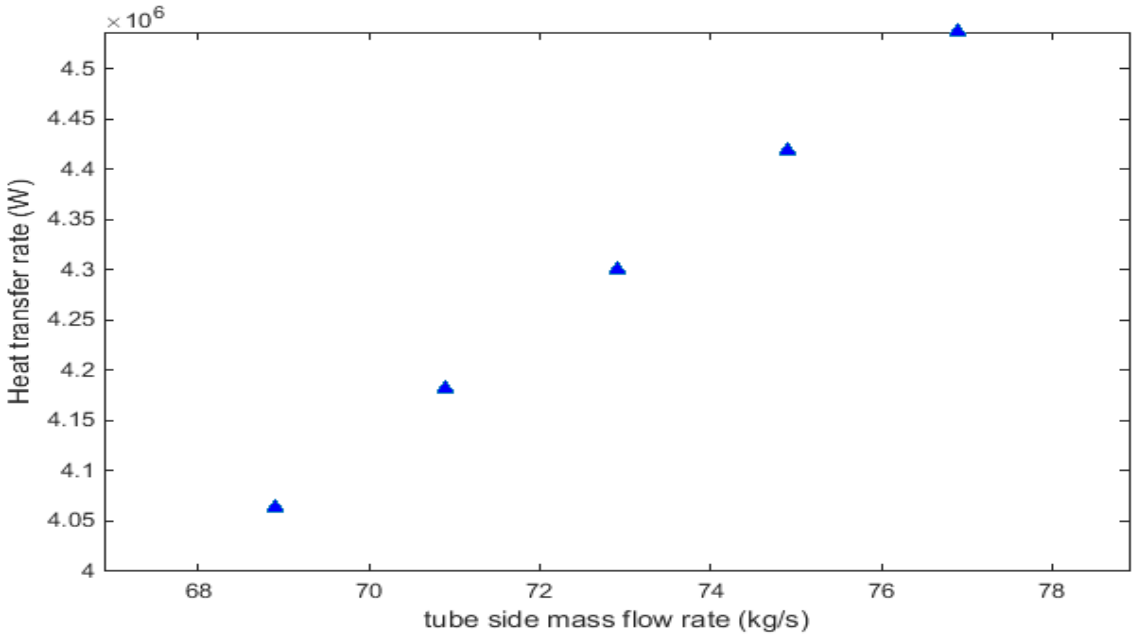


(a)

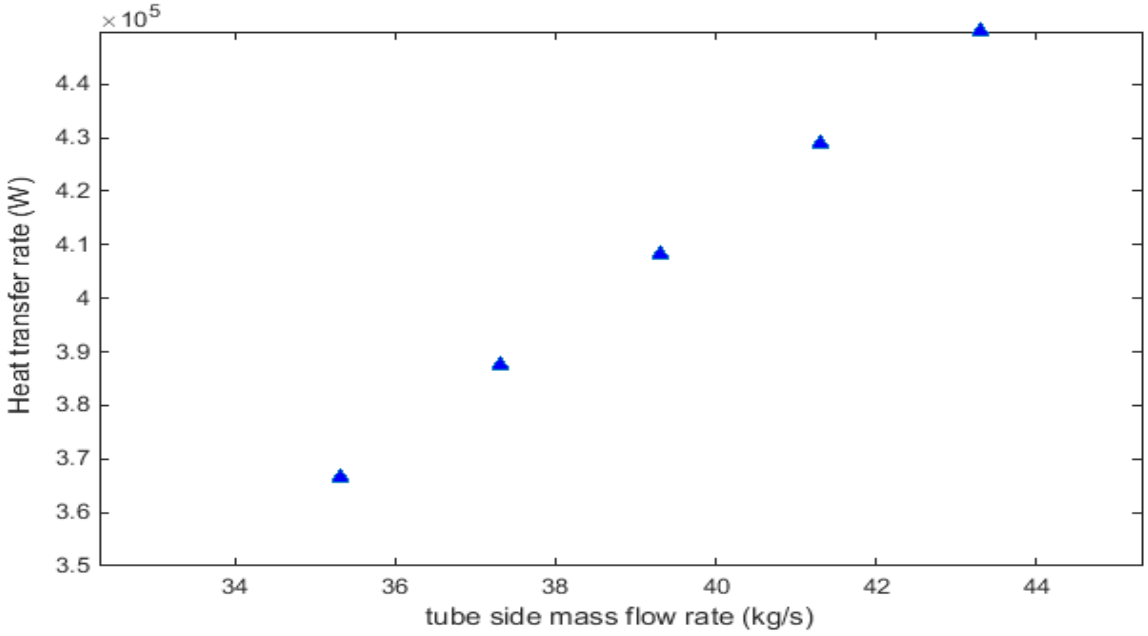


(b)

**Fig 6.1** (a) and (b) Effect of mass flow rate against actual heat transfer (Q) at 0.023 and 0. 043vol.fraction nanofluids concentration for case study 1 and 2**.**

### 6.2 Effect of mass flow rate on capital cost

This part of the analysis describes the effect of mass flow rate on the capital cost as shown Fig 6.2. The capital investment cost is computed as a function of overall heat transfer area. The heat transfer area is a function of heat transfers coefficient. By increasing the flow rate, higher velocity is experienced in the system but at the expense of high pressure drop. Owing to that, the annual operating cost and total discounted cost are both functions of the operating parameters (pressure drop and velocity), the annual operating cost becomes higher which leads to increase in overall capital cost. Fig 6.2 show the effect of mass flow rate on capital cost which can be seen from the two case studies. It depicts that the capital cost increases with the increase in mass flow rate at constant nanofluids concentration and particle diameter by approximately 1% and 2.5% for both the two case studies respectively.

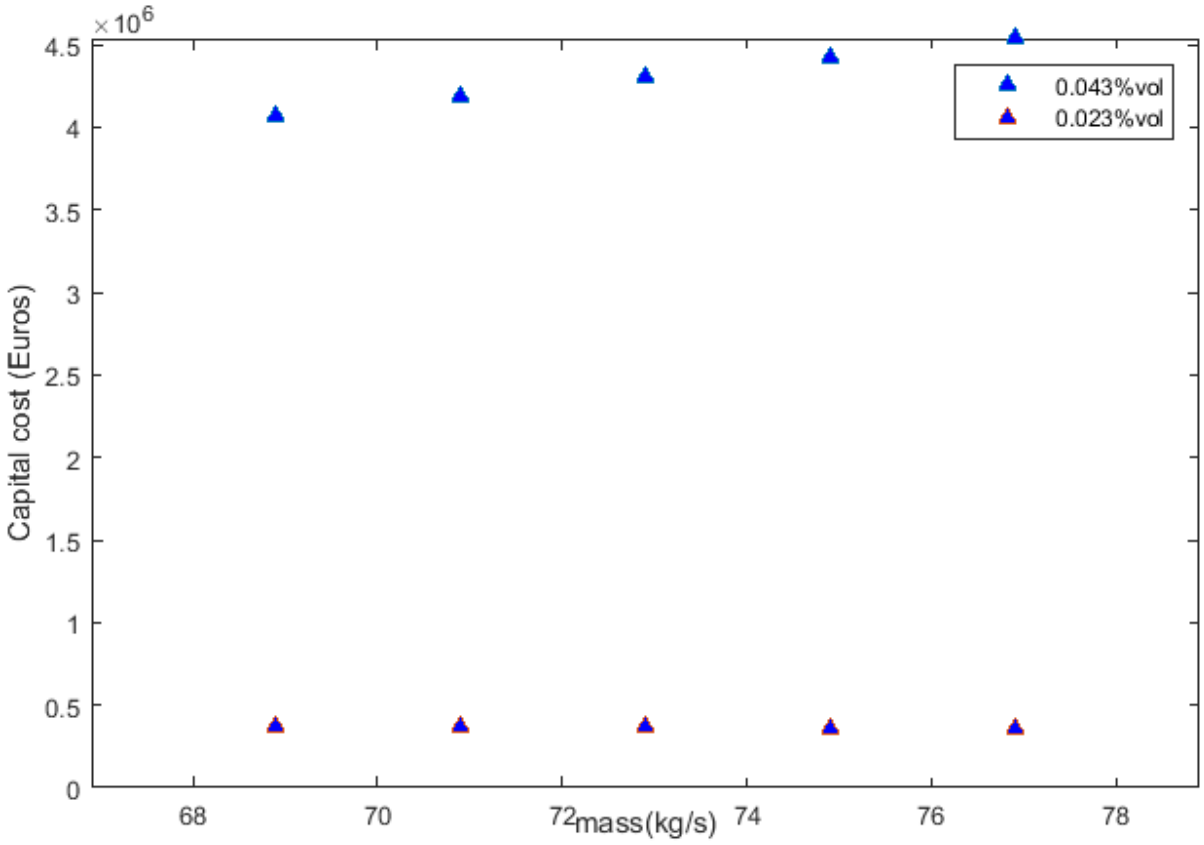


**Fig 6.2** Mass flow rate against total capital cost ($C_{tot}$) at 0.023 and 0.043 vol. fraction nanofluids concentration for case study 1 and 2.

### 6.3 Effect of concentration on pressure drop

The effect of nanofluids concentration on pressure drop was analyzed in this section. To depict that, the nanofluids volume concentration was varied by -5%, -10% and +5%, +10% while the mass flow rate and the particle diameter were held constant. Velocity and pressure drop are of paramount importance in operating process, as such, monitoring these parameters is necessary in heat transfer system as they both function in estimating the annual operating cost. Table 6.1 illustrate volume concentration against pressure drop for case study 1 and 2. It can be seen that presumably, with the increase in volume fraction of nanofluids from +5 to +10%, the value of pressure drop becomes higher by 2.58% and 13% for case 1 and 2 respectively, and these lead to an increase in annual operating cost. Hence, this could be due to the fact that the viscosity of nanofluids also rises as the volume fraction increase. This could be result in influence of pressure drop and velocity. On the other hand, enumerating the reduction of volume concentration from -5% to -10% for both the case studies the pressure drop was reduced by 0.48 and 0.35% respectively. Experimental work from Manetti et al. (2017) also attested to this scenario of internal friction rising with increase in nanofluids volume fraction while the specific heat capacity reduces. This is presumed that at higher volume concentration of nanofluids, there will be reduced specific heat capacity value and high viscosity value which can lead to fouling (deposition of particle) in the surface of heat exchanger. As a result, lower performance of heat exchanger can fall in place and high value of pressure drop is also obtained.

**Table 6.1** Effect nanofluids concentration on pressure drop

| **Percentage (%)** | **Nanofluids vol. fraction** | **Case 1 Pressure drop (kPa)** | **Percentage (%)** | **Nanofluids vol. fraction** | **Case 2 Pressure drop (kPa)** |
|---|---|---|---|---|---|
| -10 | 0.0207 | 1451.72 | -10 | 0.0387 | 3364 |
| -5 | 0.002185 | 1458.72 | -5 | 0.04080 | 3376 |
| 0 | 0.0230 | 1444.53 | 0 | 0.043 | 3335 |
| +5 | 0.02415 | 3864 | +5 | 0.04515 | 6148 |
| +10 | 0.0253 | 3963.88 | +10 | 0.0473 | 7072 |

### 6.4 Effect of nanofluids concentration on actual heat transfer

The volume concentration (vol. fraction) was varied from the base case to 0.0207, 0.02145 0.023, 0.02415 0.0253 for case 1. For case 2 the variation was done from 0.0387, 0.04080, 0.043, 0.04515, and 0.0473. As shown in Fig 6.3 and Table 6.2, it can be seen that for both case studies at the increasing volume fraction of nanofluids from +5% to +10% it shows a negative impact on actual transfer, the actual heat transfer decreased by approximately 0.3%, and 0.5% for both case study 1 and 2 respectively. Meanwhile, as the percentage of the nanofluids' volume concentration was reduced from -5% to -10%, the rate of actual heat transferred result were observed as follows. The actual heat transfer was increased by 0.3% and 0.5% for both the case studies respectively. Thus, it is therefore generally noticed that decrease in nanofluids volume concentration increased the actual heat transfer based on the range of nanofluids volume fraction obtain, while an increase in nanofluids volume concentration decreased the actual heat transfer as illustrated in Fig 6.3 and Table 6.2 for both case studies. This is due to the decrease in specific heat capacity. This attribute is as a result of solid particles having lower specific heat capacity compared to the base fluids. Meanwhile, heat capacity is a function of actual rate of heat transfer, which is directly related to the flow rate. Therefore, the decrease in heat capacity of the nanofluids increased with increase of volume fraction which negatively affects the actual rate of heat transfer in the heat transfer system. Generally, the effect of nanofluids volume concentration induces the increment of heat transfer this is proven and supported by the experimental work done by Abdolbaqi et al. (2017).

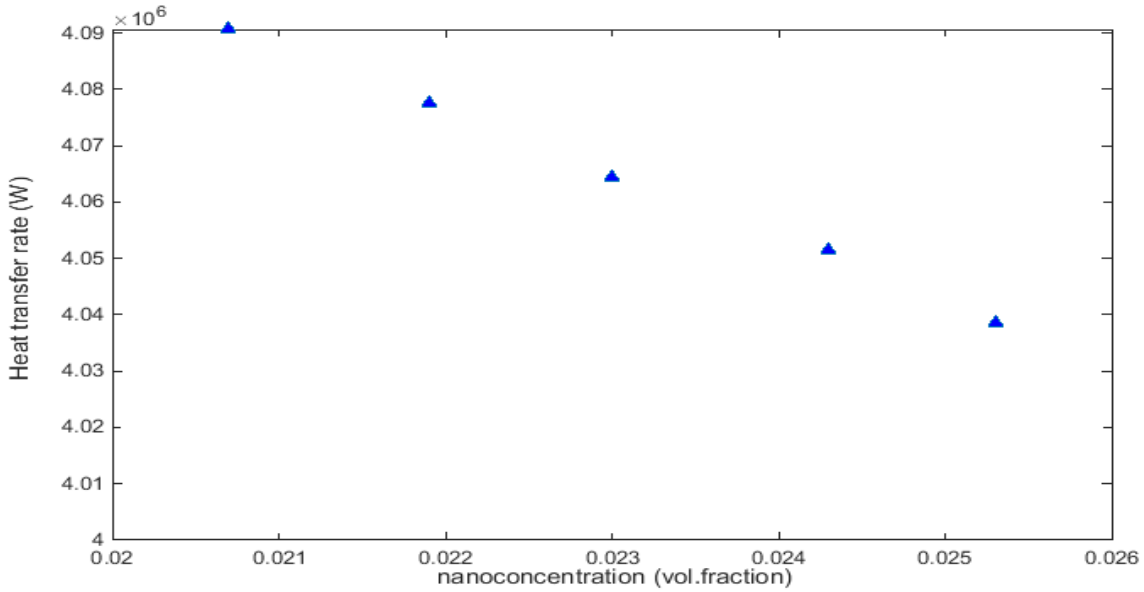


**Fig 6.3** Nanofluids concentration for case study 1 against actual heat transfer (Q)

**Table 6.2** Effect nanofluids concentration on actual heat transfer for case 2

| **Percentage (%)** | **Nanofluids vol. fraction** | **Q (W)** |
|---|---|---|
| -10 | 0.0387 | 370933 |
| -5 | 004080 | 368864 |
| 0 | 0.0430 | 366714 |
| +5 | 0.04515 | 364645 |
| +10 | 0.0473 | 362592 |

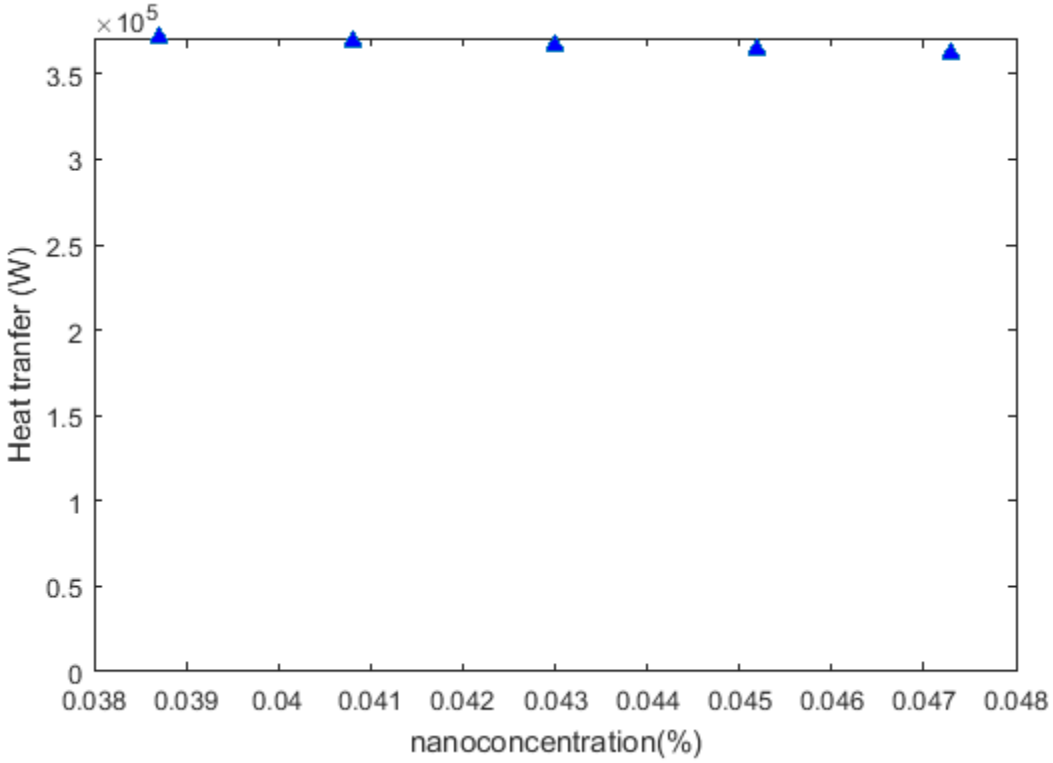


**Fig 6.4** Nanofluids concentration against heat transfer (Q) for case 2

### 6.5 Effect of concentration on capital cost.

This section shows the sensitivity of capital cost against nanofluids volume concentration. To detect that, the nanofluids volume concentration was varied by subtracting and adding a certain percentage of concentration which were -5% and -10% and +5%, +10% from the optimized nanofluids concentration which was found to be 0.023 and 0. 043vol.fraction for both case study 1 and 2 respectively. Looking at the Table 6.3 it is observed that by increasing the volume concentration from 0% that is the base case to +10%, the capital cost is increased to 2.5% and 3.6% for both case study 1 and 2. Thus this scenario was carefully observed to be as a result of influence of annual operating cost being the function of the total cost, which does have negative effect on it. On the other hand, when the volume concentration was compared between -10% and +10% the difference of total annual cost was increased to be about 2.75% and 3.7% for both the two cases respectively. It can be hypothesized base on this observation that, lower concentration of nanofluids have a negligible effect on the capital cost as well as the operating cost, thus the reduction of capital cost found was negligible with increase in volume concentration of

nanofluids base on this range of concentration. Nevertheless, looking at the outcomes of this part, presented in Table 6.3, it can be seen that in both cases, the positive increase in nanofluids volume concentration by up to 10% increases the total capital investment cost, but this is achieved at the expense of annual operating cost.

**Table 6.3** Effect nanofluids concentration on operating cost and total capital cost

| **Percentage (%)** | **Nanofluids vol. fraction** | **Case 1 Operating cost** | **Case1 Total cost** | **Nanofluids vol. fraction** | **Case 2 Operating cost** | **Case 2 Total cost** |
|---|---|---|---|---|---|---|
| -10 | 0.0207 | 726 | 37988 | 0.0387 | 248.644 | 19443 |
| -5 | 0.002185 | 728 | 37960 | 0.04080 | 248.860 | 19425 |
| 0 | 0.0230 | 721 | 38061 | 0.0430 | 245.63 | 19455 |
| +5 | 0.02415 | 718 | 39051 | 0.04515 | 378.31 | 20171 |
| +10 | 0.0253 | 926 | 39064 | 0.0473 | 385.19 | 20190 |

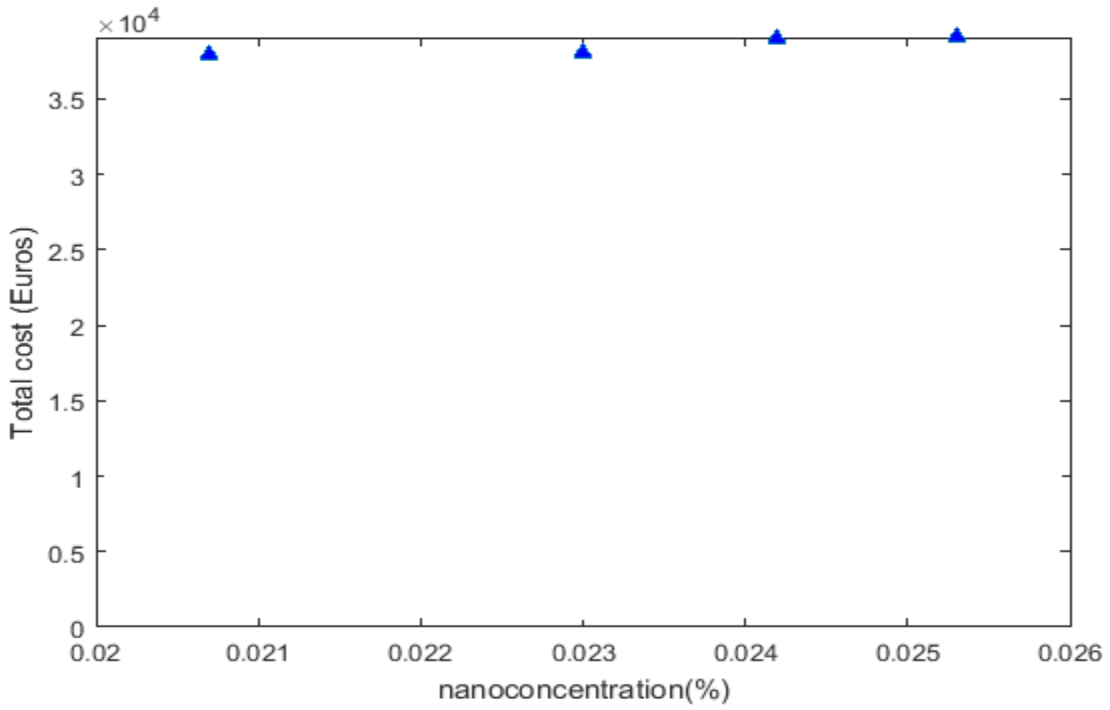


(a)

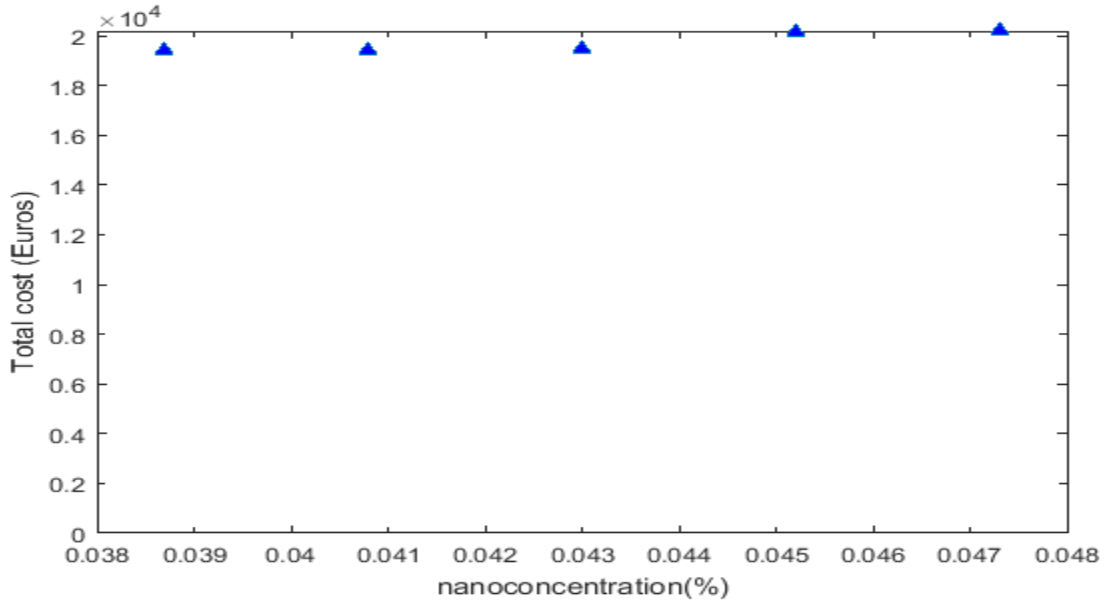


(b)

**Fig 6.5** (a) and (b) Effect of nanofluids concentration on total capital cost for case 1 and 2

However, a higher value of annual operating cost is obtained with a positive increase of nanofluids volume fraction, this due to the increase in the rate of flow velocity and pressure drop. Taking to this account, it can be seen that through increasing the concentration from +5% to +10%, the operating cost increased by approximately 22.5%, and 1.8% for both case study 1 and 2. On the other hand, by reducing the concentration from -5% to -10%, for case study1 it is observed that, the operating cost dropped by approximately 0.27%. This reduction is due to the decrease in both velocity and pressure drop values. In respect to this explanation, it is discovered that at very high concentration of nanofluids, it can affect the total annual cost due to high value of annual operating cost.

However, the sensitivity analysis on nanofluids volume concentration is of very important just as conducted in this work, because the increase in nanofluids concentration increase the overall heat transfer, which then minimized the exchanger area and result in reducing the capital investment. On the other hand, the increase in concentration of nanofluids attend some certain limit which began to rise the operating cost rapidly and with that the annual total capital cost also raises high. This could also be hypothesized that the influence of the operating cost is due to increase in internal friction (viscosity) of the operating fluids which result in high demand the pumping power. Base on the range of nanofluids volume concentration attend in this research, by adding the concentration up to 10% the capital was found to be increased.

## 6.6 GUIDELINES OF THE DESIGNED HEAT EXCHANGER WITH NANOFLUIDS

This chapter provides the summary of guidelines and the frame work of the designed shell and tube heat exchanger operated with nanofluids. Based on the outcome on the optimal design and sensitivity analysis, it is envisaged that for industrial application of the propose design, the nanoparticle diameter that should be taken into consideration is 13nm, meanwhile, the volume concentration should be within the range of 1-6% The heat duty of the exchanger is similar to the value proposed by Kern (1950) and Sinnott et al. (2005)

The design operating constraints (pressure drop and velocity) in this work however are still under the tolerance limit. However, the sensitivity analysis was conducted to monitor the behavior of this constraints, where the volume concentration of the nanofluids was increased by 10% and the mass flow rate was increased by 2kg/s in both the two case studies applied. Presumably, the value of pressure drop and velocity were still within the limit of design constraint. The optimum

point of nanofluids volume concentration obtained was 0.023 and 0. 043vol.fraction, in both cases respectively, it is therefore recommended that the volume concentration of the nanofluids can be increased by 10% and a desirable pressure drop and velocity is still achieved. Finally, the operation of the designed heat exchanger is only applicable for $Al_2O_3$/ water based nanofluids where the volume concentration of the designed heat exchanger operated with nanofluids is ranged between 1-6% and the optimum value was found to be 0. 023vol.fraction for case 1 and 0. 043vol.fraction for case 2, while the particle diameter ranges from 13nm. As such, it is therefore recommended that the heat exchanger should be strictly considered in regards to the design rules as stated.

## 6.7 Summary

This section presents the sensitivity analysis performed to study the effect of nanofluids volume concentration and mass flow rate on total cost, heat transfer and pressure drop. In view of the outcome, it is observed that the increase in nanofluids volume concentration in case study from +5 to +10 increase the annual capital cost for both the two cases applied, and these scenario was carefully observed to be due to the increment in annual operating cost, at the expense of velocity and high pressure drop. However, relationship observed between case 1 and 2 in this research was that, though the optimum concentration differs, but the cases were in good agreement in the sensitivity analyses conducted.

# CHAPTER 7

## 7.1 CONCLUSION

In the present work, a modified Kern's method is used and named as automated Kern's method to obtain an optimal design for shell and tube heat exchanger. The minimization of the total cost (objective function) is considered as the objective in the optimization process which includes both the annual operating cost, total discounted cost and the capital investment cost. The present model is basically applied to two case studies and the design optimization of the proposed method was conducted in three different stages after successfully validating the model. The major conclusions of this project can be drawn according to the following.

- In the first stage the proposed model, a design optimization is conducted with the same number of variables and the system of heat exchanger as proposed by Kern (1950) and Sinnott et al. (2005). The result showed that the reduction of capital cost can be achieved by 25.93% and 52.84%.
- In stage two, more variables were included such as tube diameter, tube length, number of tube pass, baffle cut, type of pitch, tube pitch, head type, ratio of baffle spacing to shell diameter and tube wall thickness for optimizations (multivariable heat exchanger design) for both cases. Hence, the cost is further reduced to 37.85% and 55.18% as compared to the original design.
- However, in stage three, a different design of heat exchanger system was considered. The optimization for this section was performed using $Al_2O_3$ / water nanofluids in the tube side of heat exchanger. Hence, more variables were included for this optimization which includes nanofluids volume concentration. The result showed that the reduction of annual operating cost and total capital cost was further achieved. The total annual capital cost is reduced by 40.97% and 55.77% as compared to the original design for both the case studies applied with heat exchanger of the same heat duty of 4.34MW and 0.46MW in respect to the original design.
- Nevertheless, for the sensitivity analysis conducted, the outcome showed that an increase in nanofluids concentration gave a negative effect on the objective function (total capital cost) in both the two cases applied. The total cost was raised with about 2.7% and 3.6% when nanofluids concentration was increased from 0 to +10, this is due to increase annual

operating cost which was increased by 21% and 36% for both the two cases respectively. Thus, it was observed that the increment of annual operating cost was at the expense of pressure drop, on the other hand the total cost was found to be raising up with increase in mass flow rate. Therefore, the efficiency and effectiveness of the present design will be of significant importance in this area of studies. In view of all the examined cases presented by the proposed model, it is found that the application of automated Kern's method provides the most economical design for a shell and tube heat exchanger with same heat duty application. Nevertheless, the comparison of the present result with other methods found in the literature such as GA, PSO, BBO, I-ITHS, DEACO, FFA GSA showed that the current method, using automated Kern's method operated with nanofluids, is the most effective method of optimization for shell and tube heat exchanger from an economical perspective. Hence, this method can be adopted and recommended as a reliable option for the design of shell and tube heat exchangers in industrial application.

## 7.2 FUTURE WORK

Besides cost reduction and supporting the efforts in energy conservation that this model provides, it is still recommended that more efforts are still required in this area of study. In view of future research, CuO, $TiO_2$ and MWCNT nanoparticles can be put into consideration in the optimization process of shell and tube heat exchanger as the present method is limited on $Al_2O_3$/ water based nanofluids. This is due to insufficient correlations in regards to Nusselt number, Reynold number and frictional factor for CuO, $TiO_2$ and MWCNT nanoparticles respectively.

However, ethylene glycol is one of the base fluids used for nanofluids that can also be considered in the future work, instead of water that is used in this work. Meanwhile plate heat exchanger or air cooled can also be considered in the design optimization using different procedures such as Bale Delaware method.

**REFERENCES**


Abdolbaqi, M Kh, Rizalman Mamat, Nor Azwadi Che Sidik, WH Azmi, and P Selvakumar. 2017. "Experimental investigation and development of new correlations for heat transfer enhancement and friction factor of BioGlycol/water based TiO2 nanofluids in flat tubes." *International Journal of Heat and Mass Transfer* 108:1026-1035.

Agarwar, NK., Vaidya Nathan, A., and Kumar, SS. 2013. "Synthesis and characterization of kerosene -alumina fluids." *Applied Thermal Engineering* 60:275-84.

Agarwar,R., Verma A, Agrawal NK, Duchaniya RK, and Singh RK. 2016. "Synthesis, characterisation, thermal conductivity and sensitivity of CuO nanofluids." *Applied Thermal Engineering* 102:1024-1036.

Anoop, Kanjirakat, Jonathan Cox, and Reza Sadr. 2013. "Thermal evaluation of nanofluids in heat exchangers." *International Communications in Heat and Mass Transfer* 49:5-9.

Anoop, Kanjirakat, Sundararajan, T., and Das, SK. 2009. "Effect of particle size on the convective heat transfer in nanofluids in developing rigion." *International Journal Heat Mass Transfer* 52:2189-95.

Asadi, Masoud, Yidan Song, Bengt Sunden, and Gongnan Xie. 2014. "Economic optimization design of shell-and-tube heat exchangers by a cuckoo-search-algorithm." *Applied Thermal Engineering* 73 (1):1032-1040.

Ayayarkanni, SA, and Philip J. 2014. "Effect of nanofluids aggregation on thermal and electrical conductivity of nanofluids." *Journal Nanofluids* 3:17-25.

Azad, Abazar Vahdat, and Nader Vahdat Azad. 2016. "Application of nanofluids for the optimal design of shell and tube heat exchanger using genetic algorithm." *Case Studies in Thermal Engineering* 8:198-206.

Azmi, WH, NA Usri, Rizalman Mamat, KV Sharma, and MM Noor. 2017. "Force convection heat transfer of $Al_2O_3$ nanofluids for different based ratio of water: Ethylene glycol mixture." *Applied Thermal Engineering* 112:707-719.

Azari, Ahmad, and Masoud Derakhshande. 2015. "An eperimental comparison of convective heat transfer and friction factor of $Al_2O_3$ nanofluids in a tube with and without butterfly tube." *Journal of Taiwan Institute of Chemical Engineers* 52:31-39.

Azmi, WH., Sharma, KV. Sarma, PK., Mamat, R., and Anua, S. 2014. "Comparison of convective heat transfer coefficient and friction factor of $TiO_2$ nanofluids flow in a tube with twisted tape insert." *International Journal Thermal Science* 81 (84-93).

Bott, T.R. 2007. "Fouling control and energy conservation." *Thermal Issues in Emerging Technologies* (1):191-198.

Buongiorno, J. 2005. "Convective transport in nanofluids." *Journal of Heat Transfer* 128 (3):240-250.

Caputo, AC., Pelagage, PM., and Salini, P. 2008. "Economic optimization of heat exchanger design and maintenance policy" *Applied Thermal Engineering* 28:1151-1159

Chavda, NK. 2015. "Effect of nanofluids on heat transfer characteristics of double pipe heat exchanger." *International Journal of Research in Engineering and Techno*logy 4(4):688-696.

Duangthongsuk, W and Wongwises S. 2010. "An experimental study on the heat transfer performance and pressure drop of $TiO_2$-water nanofluids flowing under under a turbulent flow regime." *International Journal Heat Mass Transfer* 53:334-344.

Durga Prasad, PV., and Gupta, A.V.S.S.K.S. 2016. "Experimental investigation on enhancement of heat transfer using $Al_2O_3$/Water nanofluid in a u-tube with twisted tape insert." *International Communications in Heat and Mass Transfer* 70:154-161.

Eastman, JA., Choi US., Li S., Thompson JA., and Lee S. 1997. "Enhanced thermal conductivity through the development of nanofluids, material research society symposium - proceedings " *Material Research Society Pittsburgh , PA, USA, Boston MA, USA* 457:3-11.

Elias, MM., Shahrul, IM., Mahbubul, IM., Saidur, R, and Rahim, NA. 2014. "Effect of different nanoparticle shapes on shell and tube heat exchanger using different baffle angles and operated " *International Communications in Heat and Mass Transfer* 70:289-297.

Esmaeilzadeh, E., Almohammadi H., Nazari Vatan, S., and Omrani AM. 2013. "Experimental investigation of hydrodynamics and heat transfer characteristics of $Al_2O_3$/Water under laminar flow inside a horizontal tube." *International Journal Thermal Science* 63:31-37.

Fesanghary, M., Damangir, E. and Soleimani, 2009. "Design optimization of shell and tube heat exchangers using global sensitivity analysis and ha I. Harmony search algorithm." *Applied Thermal Engineering* 29 (5–6):1026-103

Farajollahi, B., Etemad, GH, S and Hojjat, M. 2010. "Heat transfer of nanofluids in a shell and tube heat exchanger." *International Journal of Heat and Mass Transfer* 53 (1–3):12-17.

Fettaka, S., Jules, T., and Yash, G. 2013. "Design of shell-and-tube heat exchangers using multiobjective optimization." *International Journal of Heat and Mass Transfer* 60:343-354.

Garg, J, B Poudel, M Chiesa, JB Gordon, JJ Ma, JB Wang, ZF Ren, YT Kang, H Ohtani, and J Nanda. 2008. "Enhanced thermal conductivity and viscosity of copper nanoparticles in ethylene glycol nanofluid." *Journal of Applied Physics* 103 (7):074301.

Gupta, Munish, Neeti Arora, Rajesh Kumar, Sandip Kumar, and Neeraj Dilbaghi. 2014. "A comprehensive review of experimental investigations of forced convective heat transfer characteristics for various nanofluds." *International Journal of Mechanical and Material Engineering* no. 9 (11):1-21.

Hwang, Y., Lee, JK. Lee, CH., Jung, YM. Cheong, SI. Lee, CG. Ku, BC. And Jang, SP. 2007. "Stability and thermal conductivity characteristics of nanofluids." *Thermochemica Acta* 455:70-74.

Hadidi, A., and Ali, N. 2013. "Design and economic optimization of shell and tube heat exchanger using biogeography-based (BBO) algorithm." *Applied Thermal Engineering* 51:1263-1272.

Hassan., Hajabdollahi, Mehdi Naderi, and Sima Adimi. 2016. "A comparative study on the shell and tube and gasket-plate heat exchangers: The economic point of view." *Applied Thermal Engineering* 92:271-282.

Heris, SZ., Etemad SG., and Esfahany MN. 2006. "Experimental investigation of oxide nanofluids laminar convective heat transfer." *International Communications in Heat and Mass Transfer* 33:529-535.

Heyhat, MM., Kowsari F., Rashidi AM., Alem Varzane Esfehani S., and Amrollahi A. 2012. "Experimental investigation of turbulent flow and convective heat transfer characteristics of alumina water nanofluids in fully developed flow regime." *International Communications in Heat and Mass Transfer* 39:1272-1278.

Hosseini, Masoud S., Leila Vafajoo, and B.H. Salman. 2016. "Performance of CNT-water nanofluids as coolant fluid in shell and tube intercooler of LPG absorber tower." *International Journal of Heat and Mass Transfer* 102:45-53.

Jeong, J., Li C., Kwon L., Kim SH., and Yun R. 2013. "Particle shape effect on the viscosity and thermal conductivity of ZnO nanofluids." *International Journal of Refrigeration* 36:2233-41.

Jie Yang, and Wei Liu. 2015. "Numerical investigation on a novel shell and tube heat exchanger with plate baffles and experimental validation." *Energy Conversion and Management* 101:689-696.

Kern, D.Q. 1950. *process heat transfer*. international edition 1965 ed. Singapore: M.C. Graw-Hill Company.

Khedar, RS, Shrivastava N, Sonawane SS, and Wasewar KL. 2016. "Experimental investigations and theoretical determination of thermal conductivity and viscosity of TiO2/Ethylene glycol nanofluids." *International Communications in Heat and Mass Transfer* 73:54-61.

Koupaei, J Alikhani, SMM Hosseini, and FM Maalek Ghaini. 2016. "A new optimization algorithm based on chaotic maps and golden section search method." *Engineering Applications of Artificial Intelligence* 50:201-214.

Kulkarni, SY., Jagadish, SB., and M.B Manjurath. 2014. "Analysis comparing performance of conventional shell and tube heat exchanger using Kern, Bell and Bell Delaware method " *International Journal of Research in Eng. and Tech* 3 (3):486-496.

Lahiri, SK., and Khalfe, NM. 2015. "Hybrid particle swarm optimization and ant colony optimisation technique for the optimal design of shell and tube heat exchanger." *Chemical Product and Process Modeling* 10 (2):81-96.

Lahiri, SK., Khalfe, NM. And Wadhwa, SK. 2012. "Particle swarm optimization technique for the optimal design of shell and tube heat exchangers." *Chemical Product and Process Modeling* 7 (1):1-35.

Lahiri, SK., and Khalfe, NM. 2014. "Improve shell and tube heat exchangers design by hybrid deferential evolution and ant colony optimization technique." *Asia- Pacific Journal of Chemical Engineering* 9:431-448.

Lee, S., Choi S.U.S, Li S., and Eastman J.A. 1999. "Measuring thermal conductivity of fluids containing oxide nano particles " *Journal of Heat Transfer* 121:280-289.

Leong, CC., Simon, B., and Christopher, WW. 2015. "Genetic algorithm optimized chemical reactors network. A novel technique for alternative fuels emission production." *Article In Press* 1- 12.

Leong, KY., Saidur, R., Mahlia, T.M.I., and Yau Y.H. 2012. "Modeling of shell and tube heat recovery exchanger operated with nanofluids base coolants." *International Journal of Heat and Mass Transfer* 55:808-816.

Mansour, R Ben ., Galanis, N., and Nguyen CT. 2009. "Experimantal study of mixed convection with water- $Al_2O_3$ nanofluids in inclined tube with uniform wall heat flux " *International Journal Thermal Science* 50:403-410.

Mamourian, Mojtaba, Kamel Melani Shirvan, and Soroush Mirzakhanlari. 2016. "Two phase simulation and sensitivity analysis of effective parameters on turbulent combined heat transfer and pressure drop in a solar heat exchanger filled with nanofluids by response surface methodology." *Energy* 109:49-61.

Mintsa, HA. Gilles, R., Nguyen, CT., and Dominique D. 2009. "New temperature dependent thermal conductivity data for water-based nanofluids." *International Journal of Thermal Sciences* 48(2):363-371.

Manetti, Leonardo Lachi, Mogaji Taye Stephen, Paulo Arthur Beck, and Elaine Maria Cardoso. 2017. "Evaluation of the heat transfer enhancement during pool boiling using low concentrations of $Al_2O_3$-water based nanofluid." *Experimental Thermal and Fluid Science*. 87:191-200

Mohanty, Dillip Kumar. 2016a. "Application of firefly algorithm of design optimization of shell and tube heat exchanger from economic point of view." *International Journal of Thermal Sciences* 102:228-238.

Mohanty, Dillip Kumar. 2016b. "Gravitational search algorithm for economic optimization of shell and tube heat exchanger." *Applied Thermal Engineering* no. 107:184-193.

Mohsen, A., and Bazargan, M. 2014. "Two objective optimization in shell-and-tube heat exchangers using genetic algorithm." *Applied Thermal Engineering* 69 (1–2):278-285.

Mott, JE, WR Brock, and JT pearson. 1972. computerized design of a minimum cost heat-exchanger. *Paper Read at Mechanical Engineering.* 94(55) 347E 47th ST NEW YORK

Namburu, PK., Das, DK., Tanguri, KM., and Vajjha RS. 2009. "Numerical study on turbulent flow and heat transfer characteristics of nanofluids considering variable properties." *International Journal Thermal Science* 48:290-302.

Nazir, A., Sharity, NM. Rashidi, AM., and Khodafarin, R. 2012. "Effect of CNT structures on thermal conductivity and stability of nanofluids." *International Journal Heat Mass Transfer* 55:1529-35.

Pantzali, MN, Mouza, AA, and Paras, SV. 2009. "Investigating the efficacy of nanofluids as coolants in plate heat exchangers (PHE)." *Chemical Engineering Science* 64 (14):3290-3300.

Patel, V. K., and R. V. Rao. 2010. "Design optimization of shell-and-tube heat exchanger using particle swarm optimization technique." *Applied Thermal Engineering* 30 (11–12)1417-1425.

Ponce, O., Jose M., Medardo, SG., and Arturo, JG. 2009. "Use of genetic algorithms for the optimal design of shell-and-tube heat exchangers." *Applied Thermal Engineering* 29(23):203-209.

Ponmanis, S.,Willian, JKM., Samuel R., Nagarajan R., and Sungai JS. 2014. "Formation and characterisation of thermal and electrical properties of CuO and ZnO nanofluids in xantan gum. Colloids surface." *A Physiocochem of Eng Asp* 443:37-43.

Rao, R Venkata, and Ankit Saroj. 2017. "Constrained economic optimization of shell-and-tube heat exchangers using elitist-Jaya algorithm." *Energy*.116:473-487

Rao, Singiresu S, and Singiresu S Rao. 2009. *Engineering optimization: theory and practice*: John Wiley & Sons Ink, Hoboken New Jersy Canada

Ray, Dustin R, and Debendra K Das. 2014. "Superior performance of nanofluids in an automotive radiator." *Journal of Thermal Science and Engineering Applications* 6 (4):041002.

Razi, R., Akhavan-Behabadid MA., and Saeedinia M. 2012. "Pressure drop and thermal characteristics of CuO-base oil nanofluid laminar flow in flettened tubes under constant heat flux." *International Communications in Heat and Mass Transfer* 38:964-971.

Saffar-Avval, M, and E Damangir. 1995. "A general correlation for determining optimum baffle spacing for all types of shell and tube exchangers." *International Journal of Heat and Mass Transfer* 38 (13):2501-2506.

Sarafraz, M.M, and Hormozi, F. 2016. "Comparetively experimental study on the boiling thermal performance of metal oxide and multi-walled carbon nanotube nanofluids." *Power Technology* 287:412-430.

Sahooli, M., Sabbaghi, S., and Niassar, MS. 2012. "Preparation of CuO/water nanofluids using polyvynyl pyrolidine and a survey on its stabibility and thermal conductivity." *International Journal Nanoscience Nanotechnology* 8:27-34.

Sanaye, S., and Hassan, H. 2010. "Multi-objective optimization of shell and tube heat exchangers" *Applied Thermal Engineering* 30:1937-1945.

Serebrayakova, MA., Dimov, SV., and Bardakhanov, SA. 2015. "Thermal conductivity, Viscosity and Rheology of a suspension based on $Al_2O_3$ nanoparticles and mixture of 90% ethylene glycol and 10% water." *International Journal Heat Mass Transfer* 83:187-91. *Thermal Science* 48(2):363-371.

Serna, M., and Jiménez, A. 2005. "A Compact Formulation of the Bell–Delaware Method for Heat Exchanger Design and Optimization." *Chemical Engineering Research and Design* 83 (5):539-550.

Sinnot, RK and Coulson and Rechardson's. 2005. "Chemical Engineering. *Chemical Engineering Design* 6. 566-568, Elsevier Butter Worth Heineman, Oxford.

Sinjari, Sina. 2015. "Performance investigation of baffled shell and tube heat exchanger using different nanofluids." *16th Conference on Fluid Dynamics*. November 17-19, Razi University, Kermanshah, Iran

Shahrul, IM., Mahbubul, IM., saidur, R., and Sabri, M.F.M. 2016. "Experimental investigation on $Al_2O_3$-W, $SiO_2$-W, and ZnO-W nanofluids and their application in a shell and tube heat exchanger " *International Journal Heat and Mass Transfer* 97:547-558.

Shahrul, IM., Mahbubul, IM., saidur, R., and Sabri, M.F.M. 2016. "Performance evaluation of a shell and tube heat exchanger with oxide base nanofluids " *International Journal Heat and Mass Transfer* 52:1425-1433.

Shahmohammadi,P and Beiki H. 2016. "A numerical investigation of Al2O3-water nanofluids heat transfer and pressure drop in a shell and tube heat exchanger." *Trans. Phenom. Nano Micro Scale* 4 (1):29-35.

SOLTEQ. 2014. Expermental manual for heat exchanger training. Edited by Solteq equipment for engineering education and research.

Syam, LS. Ventaka, RE., Singh, MK., and Saosa, ACM. 2014. "Thermal conductivity and viscosity of stablized ethylene glycol and water mixture $Al_2O_3$ nanofluids for heat transfer applications and experimental study." *International Communications in Heat and Mass Transfer* 56:86-95.

Tawfik, Mohamed M. 2016. "Experimental studies of nanofluids thermal conductivity enhancement and applications: review." *Renewable and Sustainable Energy Reviews*: 1-15.

Tiwari, Arun Kumar. 2015. "Thermal performance of shell and tube heat exchanger using nanofluids " *International Journal of Advance in Production and Mechanical Engineering* 1 (1):27-31.

Turget, Oguz Emrah, Mert Sinan Turget, and Mustafa Turhan Coban. 2014. "Design and economic investigation of shell and tube heat exchangers using improved intelligent tuned harmony search algorithm." *Ain Shams Engineering Journal* 5:1215- 1231.

Vajjha, RS., and Debendra, KD. 2012. "A review and analysis on influence of temperature and concentration of nanofluids on thermo physical properties, heat transfer and pumping power." *International Journal of Heat and Mass Transfer* 55 (15–16):4063-4078.

Vajjha, RS., and Debendra, KD. 2010. " Development of new correlations for convective heat transfer and friction factor in turbulent regime fir nanofluids." *International Journal of Heat and Mass Transfer* 53:4607-4018.

Vasu, V., Krishma, KR., and Kumar, A.C.S. 2009. "Heat transfer with nanofluids for electronic cooling." *International Journal and Product Technology* 34:158-171.

Xie, H., and Chen L. 2009. "Adjustable thermal conductivity in carbon nano tube nanofluids " *physics letter* 373:1861-1864.

Xing, Meibo, Jialin Yu, and Ruixiang Wang. 2015. "Thermophysical properties of water-based single-walled carbon nanotube nanofluids as advanced coolant." *Applied Thermal Engineering* 87:344-351.

Xing, M, Yu J, and Wang R. 2016. "Experimental investigationand modelling on the thermal conductivityof CNTs based nanofluid." *International Journal Thermal Science* 104:404-411.

Yang, J., Aiwu F., Wei, L., and Anthony, MJ. 2014a. "Optimization of shell and tube heat exchanger conforming to TEMA standards with design motivated by constructal theory."

Yang, J., Sun, RO., and Wei, L. 2014b. "Optimization of shell and tube heat exchangers using a general design approach motivated by constructal theory." *International Journal Heat Mass Transfer* 77:1144-1154.

Yank, S., Ozge, S., and Basar, O. 2016. "Designing sustainable energy regions using genetic algorithm and location - location approach." *Energy* 97:161-172.

Yousefi, Moslem, Danial Hooshyar, Joong Hoon Kim, and Heuiseok Lim. 2017. "Modeling and thermo-economic optimization of a biomass heat recovery exchanger operating on Al2O3-water nanofluid." *International Communications in Heat and Mass Transfer* 82:63-73

**APPENDICES**

**Code sample (for nanofluids design heat exchanger)**

```
% Q=ms*cps*(Tsi-Tso); % heat duty of the exchanger

x11=[0.00635,0.009525,0.0127,0.01905,0.022225,0.0254,0.03175,0.0381,0.04445,0.0508,0.057
15,0.0635];
 %tube outside diameter (m)
 x22=[1.2192,1.8288,2.4384,3.048,3.6576,4.8768,6.096,6.7056,7.3152]; % tube length (m)

x33=[0.20,0.25,0.30,0.35,0.40,0.45,0.50,0.55,0.60,0.65,0.70,0.75,0.80,0.85,0.90,0.95,1.00];%Rat
io
 %of baffle spacing to shell diameter
 x44=[1,2,4,6,8]; % number of tube pass
 x55=[1,2]; % Pitch type  1: triangular; 2: square
 x66=[1,2,3,4];% type of head  1: fixed tube sheer or U tube; 2: outside packed head;
 %3: split ring floating head; 4: pull through floating head
 x77=[15,25,35,45];% baffle cut
 [mm1,nn1]=size(x11);
 [mm2,nn2]=size(x22);
 [mm3,nn3]=size(x33);
 [mm4,nn4]=size(x44);
 [mm5,nn5]=size(x55);
 [mm6,nn6]=size(x66);
 [mm7,nn7]=size(x77);
 xresult=[];

x5best=0;x4best=0;x6best=0;Dsbest=0;x2best=0;x3best=0;Bbest=0;x7best=0;x1best=0;x8best=
0;clearancebest=0;
```

```
Ntbest=0;vtbest=0;Retbest=0;Prtbest=0;htbest=0;ftbest=0;deltaPtbest=0;Sabest=0;Desbest=0;vs
best=0;Resbest=0;
 Prsbest=0;hsbest=0;fsbest=0;deltaPsbest=0;Uoptbest=0;Soptbest=0;

Cinvbest=0;Cobest=0;Codbest=0;Ctotbest=1000000000000000000000000000000000000;x10b
est=0;x111best=0;Qbest=0;
 deltacon=0.1;deltadp=1;
 nnn1=(6-0.1)/0.1;
 mmm1=13;
 for iii=1:nnn1+1

    x10=  (0.1+((iii-1)*deltacon))*0.01;
 %for jjj=1:mmm1+1
    x111= mmm1; %jjj*deltadp;

%average temperature in the tube side
T=((Tto+273)+(Tti+273))/2;

denst =(densp*(x10))+(densbf*(1-(x10)));                                    %density of
nanofluid(kg/m3)

cpt=((x10*cpp*densp)+((1-(x10))*densbf*cpbf))/(denst);                      %specific heat
capacity of nanofluid(J/kg/K)


vist=(1+39.11*x10+533.9*x10^2)*visbf;          %Azad et al.(2016)          % viscocity
of nanofluid(kg/m/s)

kt=((kp+2*kbf+2*x10*(kp-kbf))/(kp+2*kbf-x10*(kp-kbf)))*kbf; %Minea Alina Adriana
(20017)        %thermal conductivity of nanofluid(W/m/K)
```

```
 for i=1:nn1
    x1=x11(1,i);

    x8=1.25*x1;%tube pitch
    x9=0.8*x1;%tube inner diameter (m)

    for j=1:nn2
       x2=x22(1,j);

       for k=1:nn3
         x3=x33(1,k);

         for l=1:nn4
             x4=x44(1,l);

             for ii=1:nn5
                x5=x55(1,ii);

                for jj=1:nn6
                   x6=x66(1,jj);

                   for kk=1:nn7
                      x7=x77(1,kk);

         % Optimising Uo
Ucalc=600; %initial value of overall heat transfer coefficient

  % Optimising Uo
percenterror=6.5;
while percenterror > 5.5
```

```
Uinit=Ucalc;


  Q=mt*cpt*(Tto-Tti);   % heat duty of the exchanger

  deltaTlm=((Tsi-Tto)-(Tso-Tti))/log((Tsi-Tto)/(Tso-Tti));


%F=correction factor to deltaTlm, depending on number of tube passes
if x4 == 1
    f=1;
    deltaTlm=deltaTlm*f;
 else
    RR=(Tsi-Tso)/(Tto-Tti);
    PP=(Tto-Tti)/(Tsi-Tti);
     f=(sqrt(RR^2+1)/(RR-1))*log((1-PP)/(1-(PP*RR)))/log((2-PP*(RR+1-sqrt(RR^2+1)))/(2-
PP*(RR+1+sqrt(RR^2+1))));
    deltaTlm=deltaTlm*f;
 end

 Strial=Q/(Uinit*deltaTlm);% heat transfer area

 %Tube side calculation
 Nttrial=Strial/(pi*x1*x2);  % Number of tubes
 vt=mt*x4/Nttrial/(pi*0.25*x9^2*denst);
 Ret=denst*vt*x9/vist;
 Prt=vist*cpt/kt;

  %estimation of local HT coefficient in the tube side
if Ret <=2300
```

```
  ft=64/Ret;                              %R.Sajedi et al.(2016)
    Nu=0.021*(Ret^0.8)*Prt^0.5;                % J. Boungiorno (2005)
    ht=(kt*Nu)/(x9);                         %Azad et al.(2016)
    deltaPt=0.5*(denst*vt^2)*((x2*ft/x9)+2.5)*x4;
elseif Ret >2300 && Ret <=10000
     ft=(1.82*log(Ret)-1.64)^-2;               %R.Sajedi et al.(2016)
    Nu=0.021*(Ret^0.8)*Prt^0.5;
    ht=(kt*Nu)/(x9);
    deltaPt=0.5*(denst*vt^2)*((x2*ft/x9)+2.5)*x4;

  elseif Ret>=10000
    ft=0.3164*Ret^-0.25;
    Nu=0.021*(Ret^0.8)*Prt^0.5;
    ht=(kt*Nu)/(x9);
    deltaPt=0.5*(denst*vt^2)*((x2*ft/x9)+2.5)*x4;
end
 %Shell side calculation
 %bundle diameter
 if x4 == 1
     if x5 == 1
     K1=0.319;n1=2.142;
     Dbtr=x1*(Nttrial/K1)^(1/n1);
     else
     K1=0.215;n1=2.207;
     Dbtr=x1*(Nttrial/K1)^(1/n1);
     end
 elseif x4==2
     if x5 == 1
     K1=0.249;n1=2.207;
     Dbtr=x1*(Nttrial/K1)^(1/n1);
     else
```

```
    K1=0.156;n1=2.291;
    Dbtr=x1*(Nttrial/K1)^(1/n1);
    end
elseif x4==4
    if x5 == 1
    K1=0.175;n1=2.285;
    Dbtr=x1*(Nttrial/K1)^(1/n1);
    else
    K1=0.158;n1=2.263;
    Dbtr=x1*(Nttrial/K1)^(1/n1);
    end
elseif x4==6
    if x5 == 1
    K1=0.0743;n1=2.499;
    Dbtr=x1*(Nttrial/K1)^(1/n1);
    else
    K1=0.04028;n1=2.617;
    Dbtr=x1*(Nttrial/K1)^(1/n1);
    end
else
    if x5 == 1
    K1=0.0365;n1=2.675;
    Dbtr=x1*(Nttrial/K1)^(1/n1);
    else
    K1=0.0331;n1=2.643;
    Dbtr=x1*(Nttrial/K1)^(1/n1);
    end
end

%clearance values were taken from Chemical Eng Design Vol. 6
```

```
if x6==1  % Fixed and U-tube
   clearancetr=(1.0182*Dbtr+9.0273)/1000;  % clearance (m)

   Dstr=Dbtr+clearancetr;  % shell diameter (m)
elseif x6==2    % Outside packed head
   clearancetr=38/1000;

   Dstr=Dbtr+clearancetr;  % shell diameter (m)
elseif x6 == 3  % Split-ring floating head
   clearancetr=(27.818*Dbtr+44.391)/1000;  % clearance (m)

   Dstr=Dbtr+clearancetr;  % shell diameter (m)
else  %pull through floating head
   clearancetr=(10.045*Dbtr+85.65)/1000;  % clearance (m)

   Dstr=Dbtr+clearancetr;  % shell diameter (m)
end

Btr=x3*Dstr;  % baffle spacing (m)

Satr=Dstr*Btr*(1-(x1/x8));  % cross sectional area normal to flow direction

vstr=ms/(denss*Satr);
if x5 == 1   % triangular pitch
   Destr=4*(0.43*x8^2-((0.5*pi*x1^2)/4))/(0.5*pi*x1);
else  % square pitch
   Destr=4*(x8^2-(pi*x1^2/4))/pi/x1;
end

Res=ms*Destr/viss/Satr;
Prs=viss*cps/ks;
```

```
fstr=2*0.72*Res^(-0.15);
deltaPstr=fstr*denss*vstr^2*x2*Dstr/2/Destr/Btr;
if x7==15
   jh=10^(-0.4786*log10(Res)-0.2434);
elseif x7==25
   jh=10^(-0.4767*log10(Res)-0.3143);
elseif x7==35
   jh=10^(-0.4834*log10(Res)-0.3426);
else %x7=45
   jh=10^(-0.4904*log10(Res)-0.3556);
end
hs=jh*ks*Res*Prs^0.333/Destr;  % local HT coefficient in shell side
denoU=(1/hs)+Rfouls+(x1*Rfoult/x9)+(x1/ht/x9);
Ucalc=1/denoU;
percenterror=100*abs(Uinit-Ucalc)/Uinit;
end


Uopt=Ucalc;


deltaTlm=((Tsi-Tto)-(Tso-Tti))/log((Tsi-Tto)/(Tso-Tti));


%F=correction factor to deltaTlm, depending on number of tube passes
if x4 == 1
    f=1;
    deltaTlm=deltaTlm*f;
 else
    RR=(Tsi-Tso)/(Tto-Tti);
    PP=(Tto-Tti)/(Tsi-Tti);
```

```
    f=(sqrt(RR^2+1)/(RR-1))*log((1-PP)/(1-(PP*RR)))/log((2-PP*(RR+1-sqrt(RR^2+1)))/(2-
PP*(RR+1+sqrt(RR^2+1))));
    deltaTlm=deltaTlm*f;
 end

 Sopt=Q/(Uopt*deltaTlm);% heat transfer area

 %Tube side calculation
 Nt=Sopt/(pi*x1*x2);  % Number of tubes
 vt=mt*x4/Nt/(pi*0.25*x9^2*denst);
 Ret=denst*vt*x9/vist;
 Prt=vist*cpt/kt;
 %ft=(1.82*log10(Ret)-1.64)^-2;
 % deltaPt=0.5*(denst*vt^2)*((x2*ft/x9)+2.5)*x4;

  %estimation of local HT coefficient in the tube side
  if Ret <=2300
  ft=64/Ret;                              %R.Sajedi et al.(2016)
    Nu=0.021*(Ret^0.8)*Prt^0.5;                %Azad et al.(2016)
    ht=(kt*Nu)/(x9);                         %Azad et al.(2016)
    deltaPt=0.5*(denst*vt^2)*((x2*ft/x9)+2.5)*x4;
elseif Ret >2300 && Ret <=10000
     ft=(1.82*log(Ret)-1.64)^-2;                %R.Sajedi et al.(2016)
    Nu=0.021*(Ret^0.8)*Prt^0.5;
    ht=(kt*Nu)/(x9);
    deltaPt=0.5*(denst*vt^2)*((x2*ft/x9)+2.5)*x4;

  elseif Ret>=10000
    ft=0.3164*Ret^-0.25;
    Nu=0.021*(Ret^0.8)*Prt^0.5;
    ht=(kt*Nu)/(x9);
```

```
  deltaPt=0.5*(denst*vt^2)*((x2*ft/x9)+2.5)*x4;
 end

%Shell side calculation
%bundle diameter
if x4 == 1
   if x5 == 1
   K1=0.319;n1=2.142;
   Db=x1*(Nt/K1)^(1/n1);
   else
   K1=0.215;n1=2.207;
   Db=x1*(Nt/K1)^(1/n1);
   end
elseif x4==2
   if x5 == 1
   K1=0.249;n1=2.207;
   Db=x1*(Nt/K1)^(1/n1);
   else
   K1=0.156;n1=2.291;
   Db=x1*(Nt/K1)^(1/n1);
   end
elseif x4==4
   if x5 == 1
   K1=0.175;n1=2.285;
   Db=x1*(Nt/K1)^(1/n1);
   else
   K1=0.158;n1=2.263;
   Db=x1*(Nt/K1)^(1/n1);
   end
elseif x4==6
   if x5 == 1
```

```
    K1=0.0743;n1=2.499;
    Db=x1*(Nt/K1)^(1/n1);
    else
    K1=0.04028;n1=2.617;
    Db=x1*(Nt/K1)^(1/n1);
    end
 else
    if x5 == 1
    K1=0.0365;n1=2.675;
    Db=x1*(Nt/K1)^(1/n1);
    else
    K1=0.0331;n1=2.643;
    Db=x1*(Nt/K1)^(1/n1);
    end
 end

 %clearance values were taken from Chemical Eng Design Vol. 6

if x6==1  % Fixed and U-tube
   clearance=(1.0182*Db+9.0273)/1000;  % clearance (m)

   Ds=Db+clearance;  % shell diameter (m)
elseif x6==2    % Outside packed head
   clearance=38/1000;

   Ds=Db+clearance;  % shell diameter (m)
elseif x6 == 3  % Split-ring floating head
   clearance=(27.818*Db+44.391)/1000;  % clearance (m)

   Ds=Db+clearance;  % shell diameter (m)
else  %pull through floating head
```

```
   clearance=(10.045*Db+85.65)/1000;  % clearance (m)

   Ds=Db+clearance;  % shell diameter (m)
end

B=x3*Ds;  % baffle spacing (m)

Sa=Ds*B*(1-x1/x8);  % cross sectional area normal to flow direction

vs=ms/(denss*Sa);

if x5 == 1   % triangular pitch
   Des=4*(0.43*x8^2-((0.5*pi*x1^2)/4))/(0.5*pi*x1);
else  % square pitch
   Des=4*(x8^2-(pi*x1^2/4))/pi/x1;
end

Res=ms*Des/viss/Sa;

fs=2*0.72*Res^(-0.15);
deltaPs=fs*denss*vs^2*x2*Ds/2/Des/B;


%Objective function

 Cinv=8000+259.2*Sopt^0.91;  % Capital investment

 P=(1/0.7)*((mt*deltaPt/denst)+(ms*deltaPs/denss))/1000;  % pump power (KW), efficiency=0.7

 H=7000;  %working hours/year
 Ce=0.12;% electricity rate, Euro/kWh
```

```
Co=P*Ce*H;

ny=10;% lifetime of the heat exchanger

gg=0.1;%annual discount rate
Cod=0;
for cc=1:ny
   Cod=Cod+Co/(1+gg)^cc;
end

Ctot=Cinv+Cod;
  if Ctot<Ctotbest


                if vist < 0.001 && viss <0.001
                   if deltaPt<=35000 && deltaPs<=35000

x5best=x5;x4best=x4;x6best=x6;Dsbest=Ds;x2best=x2;x3best=x3;Bbest=B;x7best=x7;x1best=x
1;x8best=x8;clearancebest=clearance;

Ntbest=Nt;vtbest=vt;Retbest=Ret;Prtbest=Prt;htbest=ht;ftbest=ft;deltaPtbest=deltaPt;Sabest=Sa;
Desbest=Des;vsbest=vs;Resbest=Res;

Prsbest=Prs;hsbest=hs;fsbest=fs;deltaPsbest=deltaPs;Uoptbest=Uopt;Soptbest=Sopt;

Cinvbest=Cinv;Cobest=Co;Codbest=Cod;x10best=x10;x111best=x111;Qbest=Q;
                   Ctotbest=Ctot;
                   xresult=[x5best x4best x6best Dsbest x2best x3best Bbest x7best x1best x8best
clearancebest Ntbest vtbest Retbest Prtbest htbest ftbest deltaPtbest Sabest Desbest vsbest
```

```
Resbest Prsbest hsbest fsbest deltaPsbest Uoptbest Soptbest Cinvbest Cobest Codbest Ctotbest
x10best x111best Qbest];
                    else


x5best=x5best;x4best=x4best;x6best=x6best;Dsbest=Dsbest;x2best=x2best;x3best=x3best;Bbest
=Bbest;x7best=x7best;x1best=x1best;x8best=x8best;clearancebest=clearancebest;

Ntbest=Ntbest;vtbest=vtbest;Retbest=Retbest;Prtbest=Prtbest;htbest=htbest;ftbest=ftbest;deltaPt
best=deltaPtbest;Sabest=Sabest;Desbest=Desbest;vsbest=vsbest;Resbest=Resbest;

Prsbest=Prsbest;hsbest=hsbest;fsbest=fsbest;deltaPsbest=deltaPsbest;Uoptbest=Uoptbest;Soptbe
st=Soptbest;

Cinvbest=Cinvbest;Cobest=Cobest;Codbest=Codbest;x10best=x10best;x111best=x111best;Qbes
t=Qbest;
                    Ctotbest=Ctotbest;
                    xresult=[x5best x4best x6best Dsbest x2best x3best Bbest x7best x1best x8best
clearancebest Ntbest vtbest Retbest Prtbest htbest ftbest deltaPtbest Sabest Desbest vsbest
Resbest Prsbest hsbest fsbest deltaPsbest Uoptbest Soptbest Cinvbest Cobest Codbest Ctotbest
x10best x111best Qbest];

                    end
                else
                    if deltaPt<=50000 && deltaPs<=50000

x5best=x5;x4best=x4;x6best=x6;Dsbest=Ds;x2best=x2;x3best=x3;Bbest=B;x7best=x7;x1best=x
1;x8best=x8;clearancebest=clearance;

Ntbest=Nt;vtbest=vt;Retbest=Ret;Prtbest=Prt;htbest=ht;ftbest=ft;deltaPtbest=deltaPt;Sabest=Sa;
Desbest=Des;vsbest=vs;Resbest=Res;
```

```
Prsbest=Prs;hsbest=hs;fsbest=fs;deltaPsbest=deltaPs;Uoptbest=Uopt;Soptbest=Sopt;

Cinvbest=Cinv;Cobest=Co;Codbest=Cod;x10best=x10;x111best=x111;Qbest=Q;
                    Ctotbest=Ctot;
                    xresult=[x5best x4best x6best Dsbest x2best x3best Bbest x7best x1best x8best
clearancebest Ntbest vtbest Retbest Prtbest htbest ftbest deltaPtbest Sabest Desbest vsbest
Resbest Prsbest hsbest fsbest deltaPsbest Uoptbest Soptbest Cinvbest Cobest Codbest Ctotbest
x10best x111best Qbest];
                else

x5best=x5best;x4best=x4best;x6best=x6best;Dsbest=Dsbest;x2best=x2best;x3best=x3best;Bbest
=Bbest;x7best=x7best;x1best=x1best;x8best=x8best;clearancebest=clearancebest;

Ntbest=Ntbest;vtbest=vtbest;Retbest=Retbest;Prtbest=Prtbest;htbest=htbest;ftbest=ftbest;deltaPt
best=deltaPtbest;Sabest=Sabest;Desbest=Desbest;vsbest=vsbest;Resbest=Resbest;

Prsbest=Prsbest;hsbest=hsbest;fsbest=fsbest;deltaPsbest=deltaPsbest;Uoptbest=Uoptbest;Soptbe
st=Soptbest;

Cinvbest=Cinvbest;Cobest=Cobest;Codbest=Codbest;x10best=x10best;x111best=x111best;Qbes
t=Qbest;
                    Ctotbest=Ctotbest;
                    xresult=[x5best x4best x6best Dsbest x2best x3best Bbest x7best x1best x8best
clearancebest Ntbest vtbest Retbest Prtbest htbest ftbest deltaPtbest Sabest Desbest vsbest
Resbest Prsbest hsbest fsbest deltaPsbest Uoptbest Soptbest Cinvbest Cobest Codbest Ctotbest
x10best x111best Qbest];
                end
            end
```

```
        else

x5best=x5best;x4best=x4best;x6best=x6best;Dsbest=Dsbest;x2best=x2best;x3best=x3best;Bbest
=Bbest;x7best=x7best;x1best=x1best;x8best=x8best;clearancebest=clearancebest;

Ntbest=Ntbest;vtbest=vtbest;Retbest=Retbest;Prtbest=Prtbest;htbest=htbest;ftbest=ftbest;deltaPt
best=deltaPtbest;Sabest=Sabest;Desbest=Desbest;vsbest=vsbest;Resbest=Resbest;

Prsbest=Prsbest;hsbest=hsbest;fsbest=fsbest;deltaPsbest=deltaPsbest;Uoptbest=Uoptbest;Soptbe
st=Soptbest;

Cinvbest=Cinvbest;Cobest=Cobest;Codbest=Codbest;x10best=x10best;x111best=x111best;Qbes
t=Qbest;
                Ctotbest=Ctotbest;
                xresult=[x5best x4best x6best Dsbest x2best x3best Bbest x7best x1best x8best
clearancebest Ntbest vtbest Retbest Prtbest htbest ftbest deltaPtbest Sabest Desbest vsbest
Resbest Prsbest hsbest fsbest deltaPsbest Uoptbest Soptbest Cinvbest Cobest Codbest Ctotbest
x10best x111best Qbest];
            end



                end
              end

            end
         end
       end
    end
 end
 end
```

```
xresult=xresult';
```

**Code sample (for multivariable conventional fluids designed heat exchanger)**

```
x11=[0.00635,0.009525,0.0127,0.01905,0.022225,0.0254,0.03175,0.0381,0.04445,0.0508,0.057
15,0.0635];
 %tube outside diameter(m)
 x22=[1.2192,1.8288,2.4384,3.048,3.6576,4.8768,6.096,6.7056,7.3152]; % tube length (m)

x33=[0.20,0.25,0.30,0.35,0.40,0.45,0.50,0.55,0.60,0.65,0.70,0.75,0.80,0.85,0.90,0.95,1.00];%Rat
io
 %of baffle spacing to shell diameter
 x44=[1,2,4,6,8]; % number of tube pass
 x55=[1,2]; % Pitch type  1: triangular; 2: square
 x66=[1,2,3,4];% type of head  1: fixed tube sheer or U tube; 2: outside packed head;
 %3: split ring floating head; 4: pull through floating head
 x77=[15,25,35,45];% baffle cut
 [mm1,nn1]=size(x11);
 [mm2,nn2]=size(x22);
 [mm3,nn3]=size(x33);
 [mm4,nn4]=size(x44);
 [mm5,nn5]=size(x55);
 [mm6,nn6]=size(x66);
 [mm7,nn7]=size(x77);
 xresult=[];
 Ctotbest=10000000000000000000000000000000000000;
 for i=1:nn1
```

```
    x1=x11(1,i);
    x8=1.25*x1;%tube pitch
    x9=0.8*x1;%tube inner diameter (m)



    for j=1:nn2
       x2=x22(1,j);



    for k=1:nn3
         x3=x33(1,k);

         for l=1:nn4
             x4=x44(1,l);

             for ii=1:nn5
                x5=x55(1,ii);

                for jj=1:nn6
                   x6=x66(1,jj);

                   for kk=1:nn7
                      x7=x77(1,kk);

         % Optimising Uo
Ucalc=600;  %initial value of overall heat transfer coefficient

  % Optimising Uo
percenterror=11;
while percenterror > 10
```

```
Uinit=Ucalc;


 Q=ms*cps*(Tsi-Tso);   % heat duty of the exchanger

 deltaTlm=((Tsi-Tto)-(Tso-Tti))/log((Tsi-Tto)/(Tso-Tti));


%F=correction factor to deltaTlm, depending on number of tube passes
if x4 == 1
    F=1;
    deltaTlm=deltaTlm*F;
 else
    RR=(Tsi-Tso)/(Tto-Tti);
    PP=(Tto-Tti)/(Tsi-Tti);
     F=(sqrt(RR^2+1)/(RR-1))*log((1-PP)/(1-(PP*RR)))/log((2-PP*(RR+1-sqrt(RR^2+1)))/(2-
PP*(RR+1+sqrt(RR^2+1))));
    deltaTlm=deltaTlm*F;
 end

 Strial=Q/(Uinit*deltaTlm);% heat transfer area

 %Tube side calculation
 Nttrial=Strial/(pi*x1*x2);  % Number of tubes

 vt=mt*x4/Nttrial/(pi*0.25*x9^2*denst);
 Ret=denst*vt*x9/vist;
 Prt=vist*cpt/kt;
 ft=(1.82*log10(Ret)-1.64)^-2;  %Caputo et al.
```

```
deltaPt=0.5*(denst*vt^2)*((x2*ft/x9)+2.5)*x4;

 %estimation of local HT coefficient in the tube side (Caputo et al.,
 %2008)
if Ret < 2300
   ht=(kt/x9)*(3.657+(0.0677*(Ret*Prt*x9/x2)^1.33)/(1+(0.1*Prt*(Ret*x9/x2)*0.3)));


elseif Ret > 2300 && Ret < 10000
   nume=(ft/8)*(Ret-1000)*Prt*(1+(x9/x2)^0.67);
   deno=(1+12.7*sqrt((ft/8)*(Prt^(0.67)-1)));
   ht=(kt/x9)* nume/deno;
else  % Ret>10000
    ht=0.027*(kt/x9)*Ret^0.8*Prt^(1/3); % did not include the effect of wall T on viscosity
end


%Shell side calculation
%bundle diameter
if x4 == 1
    if x5 == 1
    K1=0.319;n1=2.142;
    Dbtr=x1*(Nttrial/K1)^(1/n1);
    else
    K1=0.215;n1=2.207;
    Dbtr=x1*(Nttrial/K1)^(1/n1);
    end
elseif x4==2
    if x5 == 1
    K1=0.249;n1=2.207;
    Dbtr=x1*(Nttrial/K1)^(1/n1);
```

```
    else
    K1=0.156;n1=2.291;
    Dbtr=x1*(Nttrial/K1)^(1/n1);
    end
elseif x4==4
    if x5 == 1
    K1=0.175;n1=2.285;
    Dbtr=x1*(Nttrial/K1)^(1/n1);
    else
    K1=0.158;n1=2.263;
    Dbtr=x1*(Nttrial/K1)^(1/n1);
    end
elseif x4==6
    if x5 == 1
    K1=0.0743;n1=2.499;
    Dbtr=x1*(Nttrial/K1)^(1/n1);
    else
    K1=0.04028;n1=2.617;
    Dbtr=x1*(Nttrial/K1)^(1/n1);
    end
else
    if x5 == 1
    K1=0.0365;n1=2.675;
    Dbtr=x1*(Nttrial/K1)^(1/n1);
    else
    K1=0.0331;n1=2.643;
    Dbtr=x1*(Nttrial/K1)^(1/n1);
    end
end

%clearance values were taken from Chemical Eng Design Vol. 6
```

```
if x6==1  % Fixed and U-tube
   clearancetr=(1.0182*Dbtr+9.0273)/1000;  % clearance (m)

   Dstr=Dbtr+clearancetr;  % shell diameter (m)
elseif x6==2    % Outside packed head
   clearancetr=38/1000;

   Dstr=Dbtr+clearancetr;  % shell diameter (m)
elseif x6 == 3  % Split-ring floating head
   clearancetr=(27.818*Dbtr+44.391)/1000;  % clearance (m)

   Dstr=Dbtr+clearancetr;  % shell diameter (m)
else  %pull through floating head
   clearancetr=(10.045*Dbtr+85.65)/1000;  % clearance (m)

   Dstr=Dbtr+clearancetr;  % shell diameter (m)
end

Btr=x3*Dstr;  % baffle spacing (m)

Satr=Dstr*Btr*(1-(x1/x8));  % cross sectional area normal to flow direction

vstr=ms/(denss*Satr);

if x5 == 1   % triangular pitch
   Destr=4*(0.43*x8^2-(0.5*0.25*pi*x1^2))/(0.5*pi*x1);
else  % square pitch
   Destr=4*(x8^2-(pi*x1^2/4))/pi/x1;
end
```

```
Res=ms*Destr/viss/Satr;
Prs=viss*cps/ks;
fstr=2*0.72*Res^(-0.15);
deltaPstr=fstr*denss*vstr^2*x2*Dstr/2/Destr/Btr;
if x7==15
   jh=10^(-0.4786*log10(Res)-0.2434);
elseif x7==25
   jh=10^(-0.4767*log10(Res)-0.3143);
elseif x7==35
   jh=10^(-0.4834*log10(Res)-0.3426);
else %x7=45
   jh=10^(-0.4904*log10(Res)-0.3556);
end

hs=jh*ks*Res*Prs^0.333/Destr;  % local HT coefficient in shell side

denoU=(1/hs)+Rfouls+(x1*Rfoult/x9)+(x1/ht/x9);
Ucalc=1/denoU;

percenterror=100*abs(Uinit-Ucalc)/Uinit;


end


Uopt=Ucalc;


deltaTlm=((Tsi-Tto)-(Tso-Tti))/log((Tsi-Tto)/(Tso-Tti));
```

```
%F=correction factor to deltaTlm, depending on number of tube passes
if x4 == 1
    F=1;
    deltaTlm=deltaTlm*F;
 else
    RR=(Tsi-Tso)/(Tto-Tti);
    PP=(Tto-Tti)/(Tsi-Tti);
     F=(sqrt(RR^2+1)/(RR-1))*log((1-PP)/(1-(PP*RR)))/log((2-PP*(RR+1-sqrt(RR^2+1)))/(2-
PP*(RR+1+sqrt(RR^2+1))));
    deltaTlm=deltaTlm*F;
 end

 Sopt=Q/(Uopt*deltaTlm);% heat transfer area

 %Tube side calculation
 Nt=Sopt/(pi*x1*x2);  % Number of tubes

 vt=mt*x4/Nt/(pi*0.25*x9^2*denst);
 Ret=denst*vt*x9/vist;
 Prt=vist*cpt/kt;
 ft=(1.82*log10(Ret)-1.64)^-2;

 deltaPt=0.5*(denst*vt^2)*((x2*ft/x9)+2.5)*x4;

  %estimation of local HT coefficient in the tube side (Caputo et al.,
  %2008)
 if Ret < 2300
   ht=(kt/x9)*(3.657+(0.0677*(Ret*Prt*x9/x2)^1.33)/(1+(0.1*Prt*(Ret*x9/x2)*0.3)));

 elseif Ret > 2300 && Ret < 10000
   nume=(ft/8)*(Ret-1000)*Prt*(1+(x9/x2)^0.67);
```

```
  deno=(1+12.7*sqrt((ft/8)*(Prt^(0.67)-1)));
  ht=(kt/x9)* nume/deno;
else  % Ret>10000
   ht=0.027*(kt/x9)*Ret^0.8*Prt^(1/3); % did not include the effect of wall T on viscosity
end



%Shell side calculation
%bundle diameter
if x4 == 1
   if x5 == 1
   K1=0.319;n1=2.142;
   Db=x1*(Nt/K1)^(1/n1);
   else
   K1=0.215;n1=2.207;
   Db=x1*(Nt/K1)^(1/n1);
   end
elseif x4==2
   if x5 == 1
   K1=0.249;n1=2.207;
   Db=x1*(Nt/K1)^(1/n1);
   else
   K1=0.156;n1=2.291;
   Db=x1*(Nt/K1)^(1/n1);
   end
elseif x4==4
   if x5 == 1
   K1=0.175;n1=2.285;
   Db=x1*(Nt/K1)^(1/n1);
   else
```

```
    K1=0.158;n1=2.263;
    Db=x1*(Nt/K1)^(1/n1);
    end
 elseif x4==6
    if x5 == 1
    K1=0.0743;n1=2.499;
    Db=x1*(Nt/K1)^(1/n1);
    else
    K1=0.04028;n1=2.617;
    Db=x1*(Nt/K1)^(1/n1);
    end
 else
    if x5 == 1
    K1=0.0365;n1=2.675;
    Db=x1*(Nt/K1)^(1/n1);
    else
    K1=0.0331;n1=2.643;
    Db=x1*(Nt/K1)^(1/n1);
    end
 end

 %clearance values were taken from Chemical Eng Design Vol. 6

   clearance=(1.0182*Db+9.0273)/1000;  % clearance (m)
if x6==1  % Fixed and U-tube

   Ds=Db+clearance;  % shell diameter (m)
elseif x6==2    % Outside packed head
   clearance=38/1000;

   Ds=Db+clearance;  % shell diameter (m)
```

```
elseif x6 == 3  % Split-ring floating head
   clearance=(27.818*Db+44.391)/1000;  % clearance (m)

   Ds=Db+clearance;  % shell diameter (m)
else  %pull through floating head
   clearance=(10.045*Db+85.65)/1000;  % clearance (m)

   Ds=Db+clearance;  % shell diameter (m)
end

B=x3*Ds;  % baffle spacing (m)

Sa=Ds*B*(1-x1/x8);  % cross sectional area normal to flow direction

vs=ms/(denss*Sa);

if x5 == 1   % triangular pitch
   Des=4*(0.43*x8^2-(0.5*0.25*pi*x1^2))/(0.5*pi*x1);
else  % square pitch
   Des=4*(x8^2-(pi*x1^2/4))/pi/x1;
end

Res=ms*Des/viss/Sa;

fs=2*0.72*Res^(-0.15);
deltaPs=fs*denss*vs^2*x2*Ds/2/Des/B;


%Objective function

 Cinv=8000+259.2*Sopt^0.91;  % Capital investment
```

```
P=(1/0.7)*((mt*deltaPt/denst)+(ms*deltaPs/denss))/1000;  % pump power (KW), efficiency=0.7

H=7000;  %working hours/year
Ce=0.12;% electricity rate, Euro/kWh

Co=P*Ce*H;

ny=10;% lifetime of the heat exchanger

i=0.1;%annual discount rate
Cod=0;
for ii=1:ny
   Cod=Cod+Co/(1+i)^ii;
end

Ctot=Cinv+Cod;

if Ctot<Ctotbest

            if vist < 0.001 && viss <0.001
               if deltaPt<=35000 && deltaPs<=35000
                 Ctotbest=Ctot;
                 xresult=[x5 x4 x6 Ds x2 x3 B x7 x1 x8 clearance Nt vt Ret Prt ht ft deltaPt Sa
Des vs Res Prs hs fs deltaPs Uopt Sopt Cinv Co Cod Ctot];
               else
                 Ctotbest=Ctot
               end
            else
               if deltaPt<=50000 && deltaPs<=50000
                Ctotbest=Ctot;
```

```
                    xresult=[x5 x4 x6 Ds x2 x3 B x7 x1 x8 clearance Nt vt Ret Prt ht ft deltaPt Sa
Des vs Res Prs hs fs deltaPs Uopt Sopt Cinv Co Cod Ctot];
                  else
                    Ctotbest=Ctot
                  end
                end



          else
             Ctotbest=Ctotbest
            end




   end
end
            end
         end
   end
   end
end

xresult=xresult';
```

**codes sample (for model validations analysis)**

```
%TUBE (Single pass, Rotated square)
l=1.220;       %tube length(m)
do=0.007;      %tube outer diameter(m)
di=0.0064;     %tube inner diameter(m)
```

```
Nt=20;        %total number of tubes
Th=0.0009525;  %tube thickness(m)

%SHELL
Ds=0.0890;     %shell inner diameter(m)
Do=0.1150;     %shell outer diameter(m)

%BAFFLES
 Bc= 0.25;      %baffle cut
 b=0.0555;      %baffle spacing(m)
 Pt=0.0088;     %tube pitch(m)

 %FLOWRATE IN SHELL (HOT FLUID STREAM (WATER))
 Vs=4;          %volumetry flowrate in the shell side (L/min)
 Tsi=70;       %inlet temperature in the shell side(degC)
 Tso=41.40;       %outlet temperature in the shell side(degC)
 cps= 4179;       %heat capacity of water(J/kgk)
 denss=993;       %density of water(kg/m^3)
 viss=7.7733e-4;  %viscosity of water(kg/m/s)
 ks = 0.61;       %thermal conductivity of water(W/m/K)
 vs=0.45;         %shell side velosity(m/s)
 ms=Vs/(1000*60)*denss; %mass flowrate in shell side(kg/s)

 %FLOWRATE IN THE TUBE (COLD FLUID IS NANOFLUID,WITH VARRYING VT
FROM 2-8
  %L/min)
 Tti=20.00;                %inlet temperature in the tube side(degC)

 %NANOFLUID(NANOPARTICLES:Al2O3; BASE FLUUID:WATER)
 cn= (0.5);      %volumetric concentration of nanofluids
 dn= (10);       %nanoparticle size (nm)
```

```
%BASE FLUID
densbf=995.18;      %density of water (kg/m^3)
visbf=7.7733e-4;    %viscosity of water(kg/m/s)
cpbf= 4070.20;      %specific heat capacity of water(J/kg/K)
kbf = 0.61941;      %thermal conductivity of water(W/m/K)

%NANOPARTICLE(Al2O3)
densp=2200; %density of SiO2
cpp= 703;   %specific heat capacity of Al2O3(J/kgk)
kp = 1.2;    %thermal conductivity of Al2O3 (W/m/K)



%CONSTANT FACTORS
Rs=0.15;       %fouling factor in shell side(m^2K/W)
Rt=0.15;       %fouling factor in tube side (m^2K/W)
T1=304;        %average tube wall temperature(degC)
bo=0.72;
T = 296;       % nanofluid average temperature (k)
f=0.9;         %correction factor
vt=1.01;       %tube side velosity(m/s)

%COST CRITERIA
h=7000;          %annual amount of working per hour(h/year)
CE=0.12;         %energy cost(euros/kWh

%EXPERIMENTAL DATA
 qexp=[5650,6700,7100,7200,7900];
 qsimul=[4277,5702,7128,8554,9849]; %al2o3data
 Tto=[52,48,42,39,36.5,35];  %outlet temperature in the shell side(degC)
```

```
 Vt=[2,3,4,5,6,7,8];        %volumetriic flow rate in tube side (L/min)


%CODING ON NANOFLUIDS THERMOPHYSICAL PROPERTIES

 index=1;

for i = 1:size(cn,2);
    for j = 1:size(dn,2);

        for to=1:size(Tto,2);
            for k=1:size(Vt,2)
   output(index,1) = cn(i);
   output(index,2) = dn(j);
   output(index,3) =(densp*(cn(i)))+(densbf*(1-(cn(i)))); %density of nanofluid(kg/m3)



   %output 1: concentration;
   %output 2: particle diameter;
   %output 3: temprature;
   %output 4: density;
   %output 5: specific heat capacity;
   %output 6: viscosity;
   %output 7: thermal conductivity;

   %CORRELATIONS
denst =(densp*(x10))+(densbf*(1-(x10)));                    %density of
nanofluid(kg/m3)

cpt=((x10*cpp*densp)+((1-(x10))*densbf*cpbf))/(denst);                    %specific heat
capacity of nanofluid(J/kg/K)
```

```
vist=(1+39.11*x10+533.9*x10^2)*visbf;          %Azad et al.(2016)          % viscocity
of nanofluid(kg/m/s)

kt=((kp+2*kbf+2*x10*(kp-kbf))/(kp+2*kbf-x10*(kp-kbf)))*kbf; %Minea Alina Adriana
(20017)        %thermal conductivity of nanofluid(W/m/K)



%HEAT EXCHANGER THERMAL MODELING
output(index,8)= mt(r);                                          %mass flowrate in (kg/sec)
output(index,9)= mt(r)*output(index,5)* (Tto(to) - Tti);                    %rate of heat
transfer(q)
output(index,10)=((Tsi-Tto(to))-(Tso-Tti))/(log((Tsi-Tto(to))/(Tso-Tti)));          %logarithm
mean temperature difference(Tlm)
output(index,11)=(Nt*pi*do*l);                                   %surface area(S)
output(index,12)=4*((Pt^2)/(2*0.87*Pt)-(0.5*pi*do^2)/(4))/(pi*do);          %shell
hydraulic diameter(De)
output(index,13)= (4* (Vt(k)))/((pi)*(di)*(output(index,6)));               %tube side
Reynold's number(Ret)
output(index,14)=((output(index,6))*(output(index,5)))/(output(index,7));          %tube side
Prandtl number(Prt)
output(index,15)=3.66+((0.0668*0.0057*output(index,13)*output(index,14))/(1.004*(((0.0057*
output(index,13)*output(index,14)))^(2/3))));   %Nusselt number(Nu)
output(index,16)=(Ds*b*(Pt-do))/(Pt);                            %cross-sectional
area(As)
output(index,17)=(ms*output(index,12))/(viss*output(index,16));             %shell side
Reynold's number(Res)
output(index,18)=(viss*cps)/(ks);                                %shell side Prandtl
number(Prs)
```

```
output(index,19)=((output(index,7))*(output(index,15)))/(di);                    %convective
coefficient heat transfer in tube side (ht)
output(index,20)=(((0.36*ks)/(output(index,12)))*((output(index,17)^0.55)*(output(index,18)^(1
/3))*(viss)))^(0.14);       %convective coefficient heat transfer in shell side(hs)
output(index,21)= (output(index,9))/ ((output(index,10))*(output(index,11)));          %overall
heat transfer(Uo)
output(index,22)=((output(index,21))*(output(index,10))*(output(index,11)*f));          %heat
dity(Q)
output(index,23)=T1- output(index,21)*(T1 - Tsi)/(output(index,20));                %wall
temperature in shell side (Tsw)
output(index,24)=((output(index,21)*(T1-Tsi))/(output(index,19)))+ Tsi;              %wall
temperature in tube side(Ttw)

%HYDRAULLIC MODELLING

output(index,25)= 0.316*(output(index,13)^-0.25);
%friction fractor in tube side(ft)
output(index,26)= 4*(output(index,25))*(((l)/(di)) + 2.5)*((output(index,3)*(vt^2))/(2));
%pressure drop in tube side   (dPt)
output(index,27)= 2*(bo)*(output(index,17)^-0.15);
%friction fractor in shell side(fs)
output(index,28)= (output(index,27))*(((denss)*(vs^2))/(2))*((l)/(b))*((Ds)/(output(index,12)));
%pressure drop in shell side  (dPs)
output(index,29)= ((1.4286* ms)/(denss*output(index,28))) +
((mt(r))/(output(index,3)*output(index,26)));        %pump efficiency(P)



%ECONOMIC MODELING(OBJECTIVE FUNCTION)
output(index,30)=a1*a2*(output(index,10)^a3);
%capital investment(Cinv)
```

```
output(index,31)=(output(index,29))*CE*h;
%operating cost(Co)

%KEY IN THE FOLLOWING FOR THE SUMMATION OF CAOP
ny=(1:1:10);

Co = output(index,31);
Caop = 0;
      for x = 1:size(ny,2);

      Caop= Caop + (Co)/((1+0.1)^x);
      end

      output(index,32) = Caop;
output(index,33) =(output(index,30)+ output(index,32));
%total cost(Ctot)
output(index,34)=Tto(to);
output(index,35)= Vt(k);
output(index,36)= mt(r);

index = index + 1;
        end
      end
  end
end
end
%PLOTING SIMULATED VS EXPERIMENTAL DATA
 figure;
Vtflow=[3,4,5,6,7];
plot(Vtflow,qexp,'s','MarkerFaceColor','b');
hold on;
```

```
plot(Vtflow,qsimul,'o','MarkerFaceColor','g');
xlabel('Tube side volumetry flow rate in L/min');
ylabel('Actual  heat transfer qft (W)');
legend('experiment', 'simulation');
title('qt against Vt at constant Vs (4)');
axis([2 8 0 inf])
Q=[5650,6700,7100,7200,7900];
  qsimul=[4277,5702,7128,8554,9849]; %al2o3data
  Tto=[52,48,42,39,36.5,35];  %outlet temperature in the shell side(degC)
  Vt=[2,3,4,5,6,7,8];         %volumetriic flow rate in tube side (L/min)
```

**Code sample (for sensitivity analysis)**

```
%Q=ms*cps*(Tsi-Tso);   % heat duty of the exchanger


x11=[0.00635];%tube outside diameter(m)

%[0.00635,0.009525,0.0127,0.01905,0.022225,0.0254,0.03175,0.0381,0.04445,0.0508,0.05715,
0.0635];
 x22=[1.8288];   % tube length (m)
 %[1.2192,1.8288,2.4384,3.048,3.6576,4.8768,6.096,6.7056,7.3152];
 x33=[1];  %Ratio of baffle spacing to shell diameter
 %[0.20,0.25,0.30,0.35,0.40,0.45,0.50,0.55,0.60,0.65,0.70,0.75,0.80,0.85,0.90,0.95,1.00];
 x44=[1];% number of tube pass
 %[1,2,4,6,8];
 x55=[1]; % Pitch type  1: triangular
 %2: square
 %[1,2];
```

```
x66=[4];
%[1,2,3,4];% type of head   pull through floating head
%1: fixed tube sheer or U tube; 2: outside packed head;
%3: split ring floating head; 4: pull through floating head
x77=[15];% baffle cut
%[15,25,35,45];
[mm1,nn1]=size(x11);
[mm2,nn2]=size(x22);
[mm3,nn3]=size(x33);
[mm4,nn4]=size(x44);
[mm5,nn5]=size(x55);
[mm6,nn6]=size(x66);
[mm7,nn7]=size(x77);
xresult=[];

x5best=0;x4best=0;x6best=0;Dsbest=0;x2best=0;x3best=0;Bbest=0;x7best=0;x1best=0;x8best=
0;clearancebest=0;

Ntbest=0;vtbest=0;Retbest=0;Prtbest=0;htbest=0;ftbest=0;deltaPtbest=0;Sabest=0;Desbest=0;vs
best=0;Resbest=0;
Prsbest=0;hsbest=0;fsbest=0;deltaPsbest=0;Uoptbest=0;Soptbest=0;

Cinvbest=0;Cobest=0;Codbest=0;Ctotbest=1000000000000000000000000000000000000;x10b
est=0;x111best=0;Qbest=0;
Ctotbest=100000000000000000000000000000000000;
%deltacon=0.1;deltadp=1;
%nnn1=(6-0.1)/0.1;
mmm1=13;


   x10=0.02415;
```

```
    x111= mmm1; %jjj*deltadp;

%average temperature in the tube side
T=((Tto+273)+(Tti+273))/2;

denst =(densp*(x10))+(densbf*(1-(x10)));                    %density of
nanofluid(kg/m3)

cpt=((x10*cpp*densp)+((1-(x10))*densbf*cpbf))/(denst);      %specific heat
capacity of nanofluid(J/kg/K)


vist=(1+39.11*x10+533.9*x10^2)*visbf;      %Azad et al.(2016)      % viscocity
of nanofluid(kg/m/s)

kt=((kp+2*kbf+2*x10*(kp-kbf))/(kp+2*kbf-x10*(kp-kbf)))*kbf; %Minea Alina Adriana
(20017)      %thermal conductivity of nanofluid(W/m/K)

 for i=1:nn1
    x1=x11(1,i);

    x8=1.25*x1;%tube pitch
    x9=0.8*x1;%tube inner diameter (m)

    for j=1:nn2
       x2=x22(1,j);

       for k=1:nn3
         x3=x33(1,k);

         for l=1:nn4
```

```
            x4=x44(1,l);

            for ii=1:nn5
               x5=x55(1,ii);

               for jj=1:nn6
                  x6=x66(1,jj);

                  for kk=1:nn7
                     x7=x77(1,kk);

         % Optimising Uo
Ucalc=847.57;  %initial value of overall heat transfer coefficient
%Optimising Uo
%percenterror=6.5;
%while percenterror > 5.5

Uinit=Ucalc;


  Q=mt*cpt*(Tto-Tti);   % heat duty of the exchanger

  deltaTlm=((Tsi-Tto)-(Tso-Tti))/log((Tsi-Tto)/(Tso-Tti));


%F=correction factor to deltaTlm, depending on number of tube passes
if x4 == 1
    f=1;
    deltaTlm=deltaTlm*f;
 else
    RR=(Tsi-Tso)/(Tto-Tti);
```

```
    PP=(Tto-Tti)/(Tsi-Tti);
     f=(sqrt(RR^2+1)/(RR-1))*log((1-PP)/(1-(PP*RR)))/log((2-PP*(RR+1-sqrt(RR^2+1)))/(2-
PP*(RR+1+sqrt(RR^2+1))));
    deltaTlm=deltaTlm*f;
 end

 Strial=Q/(Uinit*deltaTlm);% heat transfer area

 %Tube side calculation
 Nttrial=Strial/(pi*x1*x2);  % Number of tubes
 vt=mt*x4/Nttrial/(pi*0.25*x9^2*denst);
 Ret=denst*vt*x9/vist;
 Prt=vist*cpt/kt;

  %estimation of local HT coefficient in the tube side
if Ret <=2300
  ft=64/Ret;                              %R.Sajedi et al.(2016)
    Nu=0.021*(Ret^0.8)*Prt^0.5;                %Azad et al.(2016)
    ht=(kt*Nu)/(x9);                         %Azad et al.(2016)
    deltaPt=0.5*(denst*vt^2)*((x2*ft/x9)+2.5)*x4;
elseif Ret >2300 && Ret <=10000
     ft=(1.82*log(Ret)-1.64)^-2;                %R.Sajedi et al.(2016)
    Nu=0.021*(Ret^0.8)*Prt^0.5;
    ht=(kt*Nu)/(x9);
    deltaPt=0.5*(denst*vt^2)*((x2*ft/x9)+2.5)*x4;

  elseif Ret>=10000
    ft=0.3164*Ret^-0.25;
    Nu=0.021*(Ret^0.8)*Prt^0.5;
    ht=(kt*Nu)/(x9);
    deltaPt=0.5*(denst*vt^2)*((x2*ft/x9)+2.5)*x4;
```

```
end
 %Shell side calculation
 %bundle diameter
 if x4 == 1
    if x5 == 1
    K1=0.319;n1=2.142;
    Dbtr=x1*(Nttrial/K1)^(1/n1);
    else
    K1=0.215;n1=2.207;
    Dbtr=x1*(Nttrial/K1)^(1/n1);
    end
 elseif x4==2
    if x5 == 1
    K1=0.249;n1=2.207;
    Dbtr=x1*(Nttrial/K1)^(1/n1);
    else
    K1=0.156;n1=2.291;
    Dbtr=x1*(Nttrial/K1)^(1/n1);
    end
 elseif x4==4
    if x5 == 1
    K1=0.175;n1=2.285;
    Dbtr=x1*(Nttrial/K1)^(1/n1);
    else
    K1=0.158;n1=2.263;
    Dbtr=x1*(Nttrial/K1)^(1/n1);
    end
 elseif x4==6
    if x5 == 1
    K1=0.0743;n1=2.499;
    Dbtr=x1*(Nttrial/K1)^(1/n1);
```

```
    else
    K1=0.04028;n1=2.617;
    Dbtr=x1*(Nttrial/K1)^(1/n1);
    end
 else
    if x5 == 1
    K1=0.0365;n1=2.675;
    Dbtr=x1*(Nttrial/K1)^(1/n1);
    else
    K1=0.0331;n1=2.643;
    Dbtr=x1*(Nttrial/K1)^(1/n1);
    end
 end

 %clearance values were taken from Chemical Eng Design Vol. 6

if x6==1  % Fixed and U-tube
   clearancetr=(1.0182*Dbtr+9.0273)/1000;  % clearance (m)
   Dstr=Dbtr+clearancetr;  % shell diameter (m)
elseif x6==2    % Outside packed head
   clearancetr=38/1000;

   Dstr=Dbtr+clearancetr;  % shell diameter (m)
elseif x6 == 3  % Split-ring floating head
   clearancetr=(27.818*Dbtr+44.391)/1000;  % clearance (m)

   Dstr=Dbtr+clearancetr;  % shell diameter (m)
else  %pull through floating head
   clearancetr=(10.045*Dbtr+85.65)/1000;  % clearance (m)

   Dstr=Dbtr+clearancetr;  % shell diameter (m)
```

```
end

Btr=x3*Dstr;  % baffle spacing (m)

Satr=Dstr*Btr*(1-(x1/x8));  % cross sectional area normal to flow direction

vstr=ms/(denss*Satr);
if x5 == 1   % triangular pitch
   Destr=4*(0.43*x8^2-((0.5*pi*x1^2)/4))/(0.5*pi*x1);
else  % square pitch
   Destr=4*(x8^2-(pi*x1^2/4))/pi/x1;
end
Res=ms*Destr/viss/Satr;
Prs=viss*cps/ks;
fstr=2*0.72*Res^(-0.15);
deltaPstr=fstr*denss*vstr^2*x2*Dstr/2/Destr/Btr;
if x7==15
   jh=10^(-0.4786*log10(Res)-0.2434);
elseif x7==25
   jh=10^(-0.4767*log10(Res)-0.3143);
elseif x7==35
   jh=10^(-0.4834*log10(Res)-0.3426);
else %x7=45
   jh=10^(-0.4904*log10(Res)-0.3556);
end
hs=jh*ks*Res*Prs^0.333/Destr;  % local HT coefficient in shell side
denoU=(1/hs)+Rfouls+(x1*Rfoult/x9)+(x1/ht/x9);
Ucalc=1/denoU;
percenterror=100*abs(Uinit-Ucalc)/Uinit;

                    end
```

```
Uopt=Ucalc;
deltaTlm=((Tsi-Tto)-(Tso-Tti))/log((Tsi-Tto)/(Tso-Tti));
%F=correction factor to deltaTlm, depending on number of tube passes
if x4 == 1
    f=1;
    deltaTlm=deltaTlm*f;
 else
    RR=(Tsi-Tso)/(Tto-Tti);
    PP=(Tto-Tti)/(Tsi-Tti);
     f=(sqrt(RR^2+1)/(RR-1))*log((1-PP)/(1-(PP*RR)))/log((2-PP*(RR+1-sqrt(RR^2+1)))/(2-
PP*(RR+1+sqrt(RR^2+1))));
    deltaTlm=deltaTlm*f;
 end
 Sopt=Q/(Uopt*deltaTlm);% heat transfer area

 %Tube side calculation
 Nt=Sopt/(pi*x1*x2);  % Number of tubes
 vt=mt*x4/Nt/(pi*0.25*x9^2*denst);
 Ret=denst*vt*x9/vist;
 Prt=vist*cpt/kt;
 %ft=(1.82*log10(Ret)-1.64)^-2;
 % deltaPt=0.5*(denst*vt^2)*((x2*ft/x9)+2.5)*x4;

  %estimation of local HT coefficient in the tube side
  if Ret <=2300
  ft=64/Ret;                              %R.Sajedi et al.(2016)
    Nu=0.021*(Ret^0.8)*Prt^0.5;                %Azad et al.(2016)
    ht=(kt*Nu)/(x9);                         %Azad et al.(2016)
    deltaPt=0.5*(denst*vt^2)*((x2*ft/x9)+2.5)*x4;
elseif Ret >2300 && Ret <=10000
     ft=(1.82*log(Ret)-1.64)^-2;                %R.Sajedi et al.(2016)
```

```
   Nu=0.021*(Ret^0.8)*Prt^0.5;
   ht=(kt*Nu)/(x9);
   deltaPt=0.5*(denst*vt^2)*((x2*ft/x9)+2.5)*x4;

 elseif Ret>=10000
   ft=0.3164*Ret^-0.25;
   Nu=0.021*(Ret^0.8)*Prt^0.5;
   ht=(kt*Nu)/(x9);
   deltaPt=0.5*(denst*vt^2)*((x2*ft/x9)+2.5)*x4;
 end

%Shell side calculation
%bundle diameter
if x4 == 1
    if x5 == 1
    K1=0.319;n1=2.142;
    Db=x1*(Nt/K1)^(1/n1);
    else
    K1=0.215;n1=2.207;
    Db=x1*(Nt/K1)^(1/n1);
    end
elseif x4==2
    if x5 == 1
    K1=0.249;n1=2.207;
    Db=x1*(Nt/K1)^(1/n1);
    else
    K1=0.156;n1=2.291;
    Db=x1*(Nt/K1)^(1/n1);
    end
elseif x4==4
    if x5 == 1
```

```
    K1=0.175;n1=2.285;
    Db=x1*(Nt/K1)^(1/n1);
    else
    K1=0.158;n1=2.263;
    Db=x1*(Nt/K1)^(1/n1);
    end
 elseif x4==6
    if x5 == 1
    K1=0.0743;n1=2.499;
    Db=x1*(Nt/K1)^(1/n1);
    else
    K1=0.04028;n1=2.617;
    Db=x1*(Nt/K1)^(1/n1);
    end
 else
    if x5 == 1
    K1=0.0365;n1=2.675;
    Db=x1*(Nt/K1)^(1/n1);
    else
    K1=0.0331;n1=2.643;
    Db=x1*(Nt/K1)^(1/n1);
    end
 end

 %clearance values were taken from Chemical Eng Design Vol. 6

if x6==1  % Fixed and U-tube
   clearance=(1.0182*Db+9.0273)/1000;  % clearance (m)

   Ds=Db+clearance;  % shell diameter (m)
elseif x6==2    % Outside packed head
```

```
    clearance=38/1000;

    Ds=Db+clearance;  % shell diameter (m)
elseif x6 == 3  % Split-ring floating head
    clearance=(27.818*Db+44.391)/1000;  % clearance (m)

    Ds=Db+clearance;  % shell diameter (m)
else  %pull through floating head
    clearance=(10.045*Db+85.65)/1000;  % clearance (m)

    Ds=Db+clearance;  % shell diameter (m)
end

B=x3*Ds;  % baffle spacing (m)

Sa=Ds*B*(1-x1/x8);  % cross sectional area normal to flow direction

vs=ms/(denss*Sa);

if x5 == 1   % triangular pitch
    Des=4*(0.43*x8^2-((0.5*pi*x1^2)/4))/(0.5*pi*x1);
else  % square pitch
    Des=4*(x8^2-(pi*x1^2/4))/pi/x1;
end

Res=ms*Des/viss/Sa;

fs=2*0.72*Res^(-0.15);
deltaPs=fs*denss*vs^2*x2*Ds/2/Des/B;
```

```
%Objective function

 Cinv=8000+259.2*Sopt^0.91;  % Capital investment

 P=(1/0.7)*((mt*deltaPt/denst)+(ms*deltaPs/denss))/1000;  % pump power (KW), efficiency=0.7

 H=7000;  %working hours/year
 Ce=0.12;% electricity rate, Euro/kWh

 Co=P*Ce*H;

 ny=10;% lifetime of the heat exchanger

 gg=0.1;%annual discount rate
 Cod=0;
 for cc=1:ny
    Cod=Cod+Co/(1+gg)^cc;
 end

 Ctot=Cinv+Cod;
  if Ctot<Ctotbest

                if vist < 0.001 && viss <0.001
                   if deltaPt<=35000 && deltaPs<=35000

x5best=x5;x4best=x4;x6best=x6;Dsbest=Ds;x2best=x2;x3best=x3;Bbest=B;x7best=x7;x1best=x
1;x8best=x8;clearancebest=clearance;

Ntbest=Nt;vtbest=vt;Retbest=Ret;Prtbest=Prt;htbest=ht;ftbest=ft;deltaPtbest=deltaPt;Sabest=Sa;
Desbest=Des;vsbest=vs;Resbest=Res;
```

```
Prsbest=Prs;hsbest=hs;fsbest=fs;deltaPsbest=deltaPs;Uoptbest=Uopt;Soptbest=Sopt;

Cinvbest=Cinv;Cobest=Co;Codbest=Cod;x10best=x10;x111best=x111;Qbest=Q;
                    Ctotbest=Ctot;
                    xresult=[x5best x4best x6best Dsbest x2best x3best Bbest x7best x1best x8best
clearancebest Ntbest vtbest Retbest Prtbest htbest ftbest deltaPtbest Sabest Desbest vsbest
Resbest Prsbest hsbest fsbest deltaPsbest Uoptbest Soptbest Cinvbest Cobest Codbest Ctotbest
x10best x111best Qbest];
                  else


x5best=x5best;x4best=x4best;x6best=x6best;Dsbest=Dsbest;x2best=x2best;x3best=x3best;Bbest
=Bbest;x7best=x7best;x1best=x1best;x8best=x8best;clearancebest=clearancebest;

Ntbest=Ntbest;vtbest=vtbest;Retbest=Retbest;Prtbest=Prtbest;htbest=htbest;ftbest=ftbest;deltaPt
best=deltaPtbest;Sabest=Sabest;Desbest=Desbest;vsbest=vsbest;Resbest=Resbest;

Prsbest=Prsbest;hsbest=hsbest;fsbest=fsbest;deltaPsbest=deltaPsbest;Uoptbest=Uoptbest;Soptbe
st=Soptbest;

Cinvbest=Cinvbest;Cobest=Cobest;Codbest=Codbest;x10best=x10best;x111best=x111best;Qbes
t=Qbest;
                    Ctotbest=Ctotbest;
                    xresult=[x5best x4best x6best Dsbest x2best x3best Bbest x7best x1best x8best
clearancebest Ntbest vtbest Retbest Prtbest htbest ftbest deltaPtbest Sabest Desbest vsbest
Resbest Prsbest hsbest fsbest deltaPsbest Uoptbest Soptbest Cinvbest Cobest Codbest Ctotbest
x10best x111best Qbest];

                  end
                else
```

```
            if deltaPt<=50000 && deltaPs<=50000

x5best=x5;x4best=x4;x6best=x6;Dsbest=Ds;x2best=x2;x3best=x3;Bbest=B;x7best=x7;x1best=x
1;x8best=x8;clearancebest=clearance;

Ntbest=Nt;vtbest=vt;Retbest=Ret;Prtbest=Prt;htbest=ht;ftbest=ft;deltaPtbest=deltaPt;Sabest=Sa;
Desbest=Des;vsbest=vs;Resbest=Res;

Prsbest=Prs;hsbest=hs;fsbest=fs;deltaPsbest=deltaPs;Uoptbest=Uopt;Soptbest=Sopt;

Cinvbest=Cinv;Cobest=Co;Codbest=Cod;x10best=x10;x111best=x111;Qbest=Q;
                Ctotbest=Ctot;
                xresult=[x5best x4best x6best Dsbest x2best x3best Bbest x7best x1best x8best
clearancebest Ntbest vtbest Retbest Prtbest htbest ftbest deltaPtbest Sabest Desbest vsbest
Resbest Prsbest hsbest fsbest deltaPsbest Uoptbest Soptbest Cinvbest Cobest Codbest Ctotbest
x10best x111best Qbest];
            else

x5best=x5best;x4best=x4best;x6best=x6best;Dsbest=Dsbest;x2best=x2best;x3best=x3best;Bbest
=Bbest;x7best=x7best;x1best=x1best;x8best=x8best;clearancebest=clearancebest;

Ntbest=Ntbest;vtbest=vtbest;Retbest=Retbest;Prtbest=Prtbest;htbest=htbest;ftbest=ftbest;deltaPt
best=deltaPtbest;Sabest=Sabest;Desbest=Desbest;vsbest=vsbest;Resbest=Resbest;

Prsbest=Prsbest;hsbest=hsbest;fsbest=fsbest;deltaPsbest=deltaPsbest;Uoptbest=Uoptbest;Soptbe
st=Soptbest;

Cinvbest=Cinvbest;Cobest=Cobest;Codbest=Codbest;x10best=x10best;x111best=x111best;Qbes
t=Qbest;
                Ctotbest=Ctotbest;
```

```
                xresult=[x5best x4best x6best Dsbest x2best x3best Bbest x7best x1best x8best
clearancebest Ntbest vtbest Retbest Prtbest htbest ftbest deltaPtbest Sabest Desbest vsbest
Resbest Prsbest hsbest fsbest deltaPsbest Uoptbest Soptbest Cinvbest Cobest Codbest Ctotbest
x10best x111best Qbest];
                  end
               end


          else

x5best=x5best;x4best=x4best;x6best=x6best;Dsbest=Dsbest;x2best=x2best;x3best=x3best;Bbest
=Bbest;x7best=x7best;x1best=x1best;x8best=x8best;clearancebest=clearancebest;

Ntbest=Ntbest;vtbest=vtbest;Retbest=Retbest;Prtbest=Prtbest;htbest=htbest;ftbest=ftbest;deltaPt
best=deltaPtbest;Sabest=Sabest;Desbest=Desbest;vsbest=vsbest;Resbest=Resbest;

Prsbest=Prsbest;hsbest=hsbest;fsbest=fsbest;deltaPsbest=deltaPsbest;Uoptbest=Uoptbest;Soptbe
st=Soptbest;

Cinvbest=Cinvbest;Cobest=Cobest;Codbest=Codbest;x10best=x10best;x111best=x111best;Qbes
t=Qbest;
                Ctotbest=Ctotbest;
                xresult=[x5best x4best x6best Dsbest x2best x3best Bbest x7best x1best x8best
clearancebest Ntbest vtbest Retbest Prtbest htbest ftbest deltaPtbest Sabest Desbest vsbest
Resbest Prsbest hsbest fsbest deltaPsbest Uoptbest Soptbest Cinvbest Cobest Codbest Ctotbest
x10best x111best Qbest];
  end
```

```
 end
             end
         end

       end
    end
end


xresult=xresult';
```